Priority areas assessment for soil erosion control in watershed using geospatial technology in Shivalik foothills (Haryana)

BY

SUNDEEP KUMAR ANTIL

(2017AE4D)

Thesis submitted to Chaudhary Charan Singh Haryana Agricultural University, Hisar in partial fulfillment of the requirements for the degree of

DOCTORATE OF PHILOSOPHY

(AGRICULTURAL ENGINEERING)

IN

SOIL AND WATER ENGINEERING

Department of Soil and Water Engineering

College of Agricultural Engineering and Technology

CCS Haryana Agricultural University

Hisar-125004, Haryana, India

2022

CERTIFICATE-I

This is to certify that this thesis entitled "**Priority areas assessment for soil erosion control in watershed using geospatial technology in Shivalik foothills (Haryana)**" submitted for the degree of **Doctorate of Philosophy** in the subject of **Agricultural Engineering (Soil and Water Engineering)** to the **Chaudhary Charan Singh Haryana Agricultural University, Hisar,** is a bonafide research work carried out by **Sundeep Kumar Antil** Admission No. **2017AE4D** under my supervision and that no part of the thesis has been submitted by him for any other degree. The assistance and help received during the course of investigation have been duly acknowledged.

Dr. M. S. Sidhpuria
(Major Advisor)
Professor
Department of Soil & Water Engineering
CCS Haryana Agricultural University
Hisar - 125004, Haryana

CERTIFICATE-II

This is to certify that this thesis entitled "**Priority areas assessment for soil erosion control in watershed using geospatial technology in Shivalik foothills (Haryana)**" submitted by **Sundeep Kumar Antil** Admission No. **2017AE4D** to the Chaudhary Charan Singh Haryana Agricultural University, Hisar in partial fulfillment of the requirements for the degree of **Doctorate of Philosophy** in the subject of **Agricultural Engineering (Soil and Water Engineering)** has been approved by the Student's Advisory Committee after an oral examination on the same, in collaboration with an External Examiner.

(Dr. M. S. Sidhpuria)
MAJOR ADVISOR

(Dr. Rakesh Sharda)
EXTERNAL EXAMINER

(Dr. R. K. Jhorar)
HEAD OF DEPARTMENT

DEAN, POSTGRADUATE STUDIES

CERTIFICATE-III

FORMAT FOR P.G. THESIS

This is to certify that this thesis submitted by **Sundeep Kumar Antil** Admission No. **2017AE4D** a Ph.D. student of Department of Soil and Water Engineering has been checked and found as per specifications of the format circulated by the Dean, PGS vide Memo No. PGS/A-1/09/6926-90 dated 26.08.09.

(Dr. M. S. Sidhpuria)
MAJOR ADVISOR

(Dr. R. K. Jhorar)
HEAD OF THE DEPARTMENT

ACKNOWLEDGEMENTS

A precious debt such as that of learning is the only debt that is not only difficult but also impossible to repay, except perhaps through gratitude. At the very outset, I bow my head with reverence and dedicatedly accord my recondite gratitude to the "Almighty", the merciful and compassionate, whose grace, glory, and blessings allowed me to complete this endeavour. Without the blessing of the "Almighty God", these efforts would have remained a far-fetched dream and a sheath of notes.

I feel immense pleasure in expressing my deep sense of gratitude with reverence to my major advisor, Dr. M. S. Sidhpuria, Professor, Department of Soil and Water Engineering & Estate Officer cum Chief Engineer, CCSHAU, Hisar. The research work undertaken would have remained unaccomplished without his valuable guidance, keen interest, continuous persuasion, and remarkable patience during the entire course of study. His affection and sincerity towards work has been much beyond his formal obligation as a major advisor, for which I shall ever be indebted to him.

I feel profoundly delighted and prerogative to express my deep sense of gratitude to my co-major advisor, Dr. V. S. Arya, Director (Retd.), Haryana Space Application Centre, Haryana and advisory committee members, Dr. Sanjay Kumar, Professor, Department of Soil and Water Engineering and ADSW, CCS HAU, Hisar, Dr. P.S. Sangwan, Associate Professor (Retd.), Soil Science, Dr. Nitin Bhardwaj, Asstt. Scientist (Statistics), Math. & Stat., COBS&IH and Dean PGS Nominee, Dr. S. K. Pahuja, Professor, Genetics & Plant Breeding and Dean, COA, CCSHAU, Hisar for their valuable suggestions and everlasting help.

I express my sincere thanks to Dr. R.K. Jhorar, Professor and Head, Department of Soil and Water Engineering, for valuable suggestions and co-operation in completing this research work.

I am extremely thankful to Dr. Baldev Dogra, Dean, COAE&T, Dr. Balwan Singh Mandal, Director, Extension Education, for being an able leader and institutional head. I am thankful to all the faculty & staff members of the College of Agricultural Engineering and Technology, CCS HAU, Hisar and KVK Sonipat for providing necessary facilities and help during the course of the experimental work.

I'm grateful to my father Sh. Jai Bhagwan Antil, my mother Smt. Sarla Devi, my uncle Ashok Kumar, my auntie Sunila, my caring brothers Gurdeep Antil and Dr. Parvesh Antil, my sisters-in-law Varsha and Khushi, and my loving sister Dr Sonam Antil. I'm also thankful to my life partner Er. Babita Antil, who has spared me and owned all responsibilities of the family during my engagements, I express my love to sweet children Sejal, Angel, Karan, Arjun, Noor, Raavi and Vedant. Without their love, care, and encouragement, I would not have come to this level. Their blessings and love are the source of my spirit every moment.

I would like to extend my heartiest thanks and appreciation to my numerous intimate colleagues, friends, and well-wishers. To name a few of them, Dr. Anil Saroha, Dr. Rakesh Kharb, Dr. Mukesh Dandi, Dr. Kuldeep Dahiya Sushil Goyat, Subodh Aggarwal, and Arvind for the affable assistance, arduous affection, and cheerful company rendered by them during the course of study.

My vocabulary falls short of acknowledging with veneration the help, love, and best wishes rendered to me by my friends and seniors, who were always helpful and cooperative and their kind encouragement during this study.

I wish to extend my gratitude to any person whom my memory has failed to recall who has rendered their support and services in various capacities throughout the tenure of the studies.

I proudly take this opportunity to thank CCS Haryana Agricultural University for providing me facilities from time to time during my studies.

Hisar ***(Sundeep Kumar Antil)***

December, 2022

CONTENTS

LIST OF TABLES

LIST OF FIGURES

ABBREVIATIONS

CCS	Chaudhary Charan Singh
ARS, SCS	Agricultural research service, soil conservation service
DEM	Digital elevation model
E	East
N	North
GIS	Geographical information system
RUSLE	Revised universal soil loss equation
HARSAC	Haryana space applications centre
HSG	Hydrological soil group
LISS	Linear imaging self scanning sensor
LULC	Land use land cover
ROI	Region of interest
m	Meter
mm	Millimeter
km^2	Square kilometer
SRTM	Shuttle radar topography mission
UTM	Universal traverse mercator
WGS	World geodetic system

CHAPTER–I

INTRODUCTION

1.1 General background

Land and water are the most essential natural resources for the survival of living beings on the earth, and these resources always interact with each other in a cyclic manner. Soil erosion by water is a critical environmental hazard worldwide. It erodes the nutritive soil and promotes sedimentation in reservoirs and rivers, which ultimately reduces the storage capacity of the system. The erosion of soil from catchment regions, agricultural fields and the continued silting of rivers, reservoirs, and lakes are reasons of great concern. The deposition of eroded soil not only reduces the capacity of the reservoir but also causes flood hazards and ultimately degrades the quality of water downstream. Exploitation of land due to crop production, population stress, abnormal rainfall events, shifting cultivation on hill slopes, reduction in the capacity of lakes, rivers and reservoirs beyond a certain limit encourage the soil erosion and creates various threats to the society. The sustainable development of any country largely depends upon the proper utilization, efficient management, and sustainable development of natural resources in an integrated manner.

It is estimated that approximately 80% of the world's agricultural land suffers from moderate to severe erosion (Ritchie *et al*., 2003). About 29% of soil being eroded is taken to sea by rivers, 10% gets deposited in reservoirs and storage facilities and remaining 61% get displaced from its place, for a variety of reasons (Narayan and Babu, 1983). The Indo-Gangetic plains, including salt affected lands of Haryana, Punjab, Uttar Pradesh, West Bengal and Bihar, have moderate erosion rates i.e. 5-10 Mg ha^{-1} yr^{-1}, while the north-western Himalayan regions, shifting cultivation regions, ravines, black cotton soils and Western Coastal Ghats of India have severe erosion of more than 20 Mg ha^{-1} yr^{-1} (Singh *et al*., 1992).

The development of erosion prediction began with identification and analysis of three major factors i.e., rainfall and runoff erosivity potential, soil susceptibility to erosion, and soil protection afforded by plant canopy. The first erosion prediction equation described mathematically the effect of slope steepness and slope length on erosion (Renard *et al*., 1997). Erosion issues and their assessment are always dependent and based on spatial, economic, agricultural and environmental criteria. Therefore, efficient soil loss practices and their management are required to minimise degradation of natural resources and to ensure the good quality of water for the flora and fauna. The estimation of soil loss through conventional techniques is expensive, exhaustive, time consuming and labour intensive. Different parametric models such as empirical models, physical models, a mix of empirical and

physical models, physical and raster-based models, and process-based models are available for prediction of runoff and soil loss. Many of these models required basic information related to land use and landform, soil type, climatic condition and topographic situation to estimate runoff and soil losses. These models are designed for a specific set of conditions in a particular area. The various empirical soil loss models are Universal Soil Loss Equation (USLE), Revised Universal Soil Loss Equation (RUSLE), Revised Universal Soil Loss Equation version 2 (RUSLE2), and the Modified Universal Soil Loss Equation (MUSLE) which are being used. The USLE was introduced through a series of regional workshops on the soil loss prediction and later on, in 1987, ARS, SCS, and several cooperators initiated a project to revise the USLE and its documentation (Wischmeier & Smith, 1965, 1978, Renard *et al*., 1991). Originally, USLE was developed for use on cropland, its further improvements expanded its usefulness wide enough and later on it was applied to urban construction locations, highway embankments, recreational sites, prioritization of the watersheds, etc. Such widespread applicability of USLE was a result of technical soundness and the lack of alternative erosion models for planning of conservation programs to control soil erosion by water (Renard *et al*., 1991).

1.2 Most relevant review of literature

The USLE predicts the average rate of soil erosion (tons per unit area) from sheet and rill erosion under specific conditions of agricultural fields. This model can analyze soil loss by using factors, R (erosivity by rainfall), K (soil erodibility), L (slope length (m)), S (% of slope), C (parameter for cover management), and P (parameter for support practice) (Wischmeier and Smith, 1978). Later, the USLE was updated through an extensive review of its database, analysis, and inclusion of previous data which was not included in the USLE earlier. The theory described the fundamental hydrologic and erosion processes and maintained the originality with an improved method of calculation of the different USLE factors. This update of the USLE was so meaningful that the result was known as the RUSLE (Renard *et al*., 1991, 1997). The RUSLE2 is fundamentally different from the USLE and RUSLE1 erosion prediction models. It is a computer-based interface program, and it uses basic variables rather than RKLSCP factors to compute erosion. It does not use RKLSCP factors to compute erosion; rather, it computes values for them and demonstrates their interaction (Foster *et al*., 2003). The MUSLE (Williams, 1975) was developed as a watershed-based model to estimate the sediment yield using runoff and peak flow produced by each storm event individually (Pongsai *et al*., 2010). The upgraded models from USLE like MUSLE (Williams, 1975), and RUSLE (Renard *et al*., 1991) are often used for the assessment of surface erosion and sediment yield from catchment areas (Kothyari and Jain, 1997). These erosion prediction models have wide acceptability all over the world due to their simplicity and low input data requirements.

Delineation of eroded areas in a watershed through study of toposheets and reconnaissance surveys is tiring and at times, not very accurate. The development of information technologies has resolved this issue to some extent and significantly changed the approach to spatial planning, management of natural resources, and watershed prioritization based on erosion risk analysis. The development of Remote Sensing (RS) technology has opened new doors for the study of the hydrologic cycle and its components. This provides an opportunity to study and obtain solutions for more complex problems in hydrology, which are back-breaking when attained by the conventional methods. The Geographical Information System (GIS) platform provides a faster and better method for the manipulation and analysis of spatial information and for assessing various morphometric parameters of watersheds. A morphometric analysis is a necessary aspect of watershed characterization which quantitatively describes the drainage system of a watershed (Strahler, 1964). GIS can also be used as an ideal tool for developing land use management strategies to reduce soil loss (Jain *et al*., 2001). Also, it is necessary to use USLE on a physical basis rather than use it over the entire watershed. The GIS allows accurate and effective use of USLE for small watersheds. Most of the GIS-based model applications are subjected to data limitation (Fistikoglu and Harmancioglu, 2002). Other researchers concluded that the watershed could be subdivided into cells in which different runoff directions are present (Wu *et al*., 2005).

Prediction of magnitude and spatial distribution of erosion using GIS, Agricultural Non-Point Source Pollution Model (AgNPS) and the RUSLE could be more thoughtful analysis through regionalized topographic input parameters and hydrological models at different spatial resolutions (Renschler *et al*., 1997).The RUSLE is widely used to estimate soil erosion due to the ease of use in computational parameters by GIS (Wischmeier and Smith, 1978). The RUSLE model coupled with GIS and RS, has become a useful and vital approach to identify, delineate, and analyse the soil loss rate over the areas. The parameter values of the factors must be calibrated prior to the prediction of soil loss rate for that location so that better soil loss values can be achieved for effective and appropriate land management planning in watersheds (Tiruneh and Ayalew, 2015, Khassaf and Rammahi, 2018, Yesuph and Dagnew, 2019). The application of the RUSLE depends on the kind of data available and the adaption or change of information from other studies to suit our own area's climate, land cover, particular soil type, topography, and support practices (Benavidez *et al*., 2018).

1.3 Significance of study

A watershed is an appropriate hydrological unit and is considered primarily for the preservation of land, water, and other crucial resources. Each watershed has unique properties like physiography, climate, ecology, water quality, land use, and human culture. A generalised watershed management approach should be customised before being put into practice. It is, however, realised that due to financial and organisational constraints, it is not feasible to treat the entire watershed within a short span of time, so watersheds should be

prioritized on the basis of micro-units to evolve an appropriate conservation management strategy so that maximum benefit can be derived out of such money-time-effort-making scheme. Every micro-watershed has distinct characteristics which can affect its functioning with respect to receiving and disposing water. Implementing soil conservation programmes in many areas of the watershed to reduce soil erosion and increase reproductive efficiency is a problematic assignment, mostly due to financial and reserve deficiencies. To understand the problems and to suggest local conservation strategies, it is necessary to adopt a holistic approach to enhance the productivity of all components of watershed. On the basis of watershed prioritization and appropriate analysis, the conservation measures structure can be proposed in the prioritized sub-watershed at the possible locations. (Choudhari *et al*., 2018).

The Shivalik region falls between the Himalayan ecosystem and the Indo-Gangetic plains on the north-western side of India. Degradation of Shivalik foot hills not only affects piedmont plains but it damaged the hills too and the combined action of rain and surface runoff can readily remove the unprotected soil from the land surface in fragile Shivalik. (Kothyari, 1996). So it is very important to assess, analyze, and prioritize the probabilistic erosion hazards so that suitable control measures may be applied to stabilise the degradation of natural resources in this region. The present study pertains to watershed delineation, recent Land use Land cover (LULC) status, and estimation of soil loss on a watershed basis with the integration of the RUSLE parameters and geospatial techniques. This study could be helpful for policymakers, extension workers, and NGOs working in the field of watershed management in this region.

1.4 Objectives

The present study, "Priority areas assessment for soil erosion control in a watershed using geospatial technology in the Shivalik foothills (Haryana)", was conducted in watersheds of the Shivalik foothills falling in Panchkula, Ambala, and Yamunanagar districts of Haryana with the following objectives:

- Thematic mapping related to land use and land cover classification of the study area
- Soil loss estimation using RUSLE on watershed basis
- Priority areas assessment for efficient implementation of soil erosion control programmes

CHAPTER–II

REVIEW AND PATENT SEARCH

A brief account of work carried out at different locations in India and abroad pertaining to the problem under study has been presented in this chapter under different heads:

2.1 Land use and land cover classification

Helmer *et al*. (2000) used multi-date, Landsat Thematic Mapper (TM) imagery to map secondary forests, agricultural lands, and old-growth forests in the Talamanca Mountain Range in southern Costa Rica. They concluded that digital maps of ecological zones should be useful for large-scale mapping of land use and forest succession stages in complex mountain regions such as those in Central America.

Guler *et al*. (2007) observed the necessity of quick preparation of the land use and land cover maps to detect and avoid overuse and damage of the landscape beyond sustainable development limits due to rapid industrialization and urbanisation in Samsun, Turkey. They used three Landsat images from 1980, 1987, and 1999 to determine changes and used a post-classification technique based on a hybrid classification approach (unsupervised and supervised). They classified the image into six LULC types; urban, agriculture, dense forest, open forest-hazelnut, barren land, and water area. They noticed the increased in urban, open forest/hazelnut, barren land and water area and a decrease in agriculture and dense forest in between 1980 and 1999.

Alaguraja *et al*. (2010) created a LULC map using supervised classification from Landsat satellite images for Madurai district, Tamilnadu. The LULC maps clearly showed that the area of crop land was higher than others. The area occupied by the land with or without scrub, plantation and fallow land was 605 km^2, 309 km^2 and 227 km^2 respectively. Dense forest had occupied 160 km^2, while the rest of other had occupied less than 100 km^2 area in the district.

Mallupattu and Reddy (2013) determined the LULC change in an urban area, Tirupati, India from 1976 to 2003, through GIS and RS technology. They used the Survey of India topographic map and the RS data of LISS III and Pan of IRS ID of 2003 and classified the study region into eight categories based on field study, geographical conditions, and RS data. They observed the significant impact of population and development activities on LULC and concluded that integration of GIS and RS technologies was an effective tool for urban

planning and management and useful for various environmental management groups, policymakers, and the public to well understand the environment.

Beniwal *et al*. (2014) carried out LULC mapping for the Adalpur Micro watershed using IRS P-6 LISS-IV satellite images for the *rabi* and *kharif* seasons during the year 2007. They delineated micro-watersheds on the basis of *rabi* and *kharif* seasons and generated LULC classes and found that 64% of the area was cropped and 23% of the area was under wasteland out of the total geographic area of the watershed.

Priyanka (2017) made an attempt to study the LULC of Ambala district, having a total geographic area of 1574 km^2. She used Survey of India toposheets, satellite data IRS-P6 and LISS-III, year 2011 and prepared the thematic map of the district. LULC categories identified in the district were agricultural land, plantations, wastelands, built-up areas and water bodies. She observed the drastic changes in LULC of Ambala district since 2001, and the scrub land, wetlands, and river were severely affected.

Sarkar (2018) analysed the change detection for the period from 1973 to 2015 of the Raniganj open coalfield. Ten LULC classes were characterized on the basis of ground truth geographic coordinates, LULC attributes, species information of different landscapes by stratified random sampling method through Google Earth and GPS device. The change detection of classified images was done using Erdas Imagine software and the 'Before image-after image' algorithm was used to extract the changes considering 10% increase or decrease rules. He noticed that about 30% of forest land was changed to other land use within 10 years in the Sonepur, Satgram, Sripur and Khottadih areas. Contrary to fallow land, agriculture, urban and quarry land retained and gained their original land use.

Choudhary *et al*. (2019) studied the LULC changes and their impact on urban heat island effects due to urban expansion in the Asansol-Durgapur Development Region of West Bengal in Kolkata using multi-temporal satellite data. The speedy transformation in LULC has significantly affected the land surface temperature. They studied the land surface temperature in three seasonal categories i.e. winter, summer and post monsoon periods using Landsat 4-5 TM and Landsat 8 OLI over the period of year 1993, 2009 and 2015 and observed that land surface temperature increased 0.06 °C per year in winter and 0.43 °C per year in summer periods, respectively.

Panaskar *et al*. (2019) analysed the change in land and water bodies of the Western Ghats of India using the Normalized Difference Vegetation Index (NDVI) and the Normalized Difference Water Index (NDWI). They compared the changes in land and water bodies by using Landsat satellite series for the years 1988, 1998, 2008, and 2018, and observed the differences in forest and water resources. The overall percent change in vegetation was found to be 14.19%, with the majority of change being observed in Tamil Nadu state by 21.90%. The overall change in the water bodies was observed to be 3.36%.

They concluded that the time series changes in land use can be used to predict the futuristic changes in land and water bodies and their impact over surroundings.

Chowdhary *et al*. (2020) studied the LULC changes of the Halda watershed of Bangladesh for a period of 40 years using multispectral satellite data obtained from Landsat 2, Landsat 5, and Landsat 8 OLI for April 1978, February 1999, and May 2017, respectively. Furthermore, they determined land cover in three different time frames 1978–1999, 1999–2017, and 1978–2017 and cross tabulated pixel-by-pixel using QGIS 2.18.9 with GRASS 7.2.1 and Semi-Automatic Classification Plugin (SCP). They classified watersheds into agriculture, settlements, bare soil, water bodies, and vegetation, and observed the significant shift from vegetation (35.1%) and water class (85.47%) to agriculture, bare soil, and settlements. They expected that this study would be helpful to policymakers, planners, and other associated development workers to adopt the best suitable land-use management option for the Halda watershed.

Mishra *et al*. (2020) mapped and monitored the change patterns in LULC of Rani Khola watershed in Sikkim in the Himalayas using techniques of RS and GIS for the periods 1988–1996, 1996–2008 and 2008–2017. They used Landsat-5 Thematic Mapper and Sentinel 2A MSI data and applied Maximum Likelihood Classifier (MLC) of supervised classification to prepare LULC maps of the watershed. They assessed the accuracy of the classified map through a high resolution planet scope image and ground truth verification, along with site-specific interviews. They observed the series of changes and impacts of adopted policies in LULC over the past three decades in the watershed and found that the major land use was forestry in the watershed. The dense forest, built-up area, and water bodies were increased by 16.40%, 2.13%, and 0.11%, while open forest, agriculture, and barren land were decreased by 13.98%, 2.83%, and 1.82%, respectively.

Kumar *et al*. (2021b) analysed LULC in three districts of Haryana (viz. Panchkula, Ambala, and Yamunanagar) in the Shivalik region to obtain the possibility and potential for sericulture practices and the selection of suitable seasons in the wasteland. They concluded that RS and GIS technology are capable of finding a suitable site for mulberry sericulture in the study area.

2.2 Soil loss estimation

Renard and Foster (1985) studied USLE and the problems encountered during extrapolating it from cropland to rangeland areas. They concluded that the USLE is a useful tool for estimating erosion, assessment of the impact of erosion on productivity, and for use as a guide to select the erosion control measures in different land uses.

Pandey *et al*. (2007) used GIS as a tool to generate, manipulate, and spatially organized the disparate data for sediment yield modelling. The USLE was used to predict the spatial distribution of the sediment yield on a grid basis. The deviation of estimated sediment

yield from the observed values in the range of 1.37 to 13.85% indicated the accurate estimation of sediment yield from the watershed.

Yadav and Sachdev (2008) calculated soil loss in Haryana using the USLE equation and concluded that soil loss greater than the tolerance limit occurred in less than 6% of the total geographical area but had a contribution of 25% of total soil loss from the Haryana state.

Dabral *et al.* (2008) assessed the soil erosion loss in the Dikrong river basin of Arunachal Pradesh. They observed that the average annual soil loss of the Dikrong river basin was 51 t ha^{-1} yr^{-1}. About 25.61% of the watershed area was observed to be under slight erosion class. Areas covered under moderate, high, very high, severe and very severe erosion potential zones were 26.51%, 17.87%, 13.74%, 2.39%, and 13.88%, respectively. They stressed the need to have immediate attention from a soil conservation point of view in the suggested areas.

Prasannakumar *et al.* (2011) analysed the RUSLE parameters using RS and GIS in the Siruvani river watershed in the Attapady valley, Kerala, India. They used three years of 2005–2008 monthly rainfall data to quantify the R factor using only one available rain gauge station. Based on the results, 42 soil samples were collected from the study area and their textural analysis was carried out. The soil was classified into 11 textural classes based on the results. The LS, C, and P factors were also computed in the GIS environment. The C factor ranged from 0.009 to 1.501 and they divided the area into three zones on the basis of land use, land cover practices, and support factors. The values of the P factor ranged from 0.25 to 1 by assigning the highest values to the areas with no conservation practises and like forest and natural vegetation and minimum values to the crop land with strip and contour cropping systems.

Sheikh *et al*. (2011) integrated USLE with GIS to assess soil erosion in the Lidder catchment in the Himalayan region. They observed that the factors of topography, vegetation type, soil properties, and land use and cover influence soil erosion. The predicted annual soil loss ranged between 0 and 61 t ha^{-1} yr^{-1} and the average soil loss was highest (26 t ha^{-1} yr^{-1}) in the agriculture area and lowest in the forest area (0.99 t ha^{-1} yr^{-1}). For horticulture, plantation, pasture, fallow, and scrub, the soil loss rates were 1.47, 5.39, 25.47, 28.39, and 35.76 t ha^{-1} yr^{-1}, respectively.

Prasannakumar *et al*. (2012) integrated the RUSLE model and GIS techniques and determined the vulnerability of a forested mountainous sub-watershed to soil erosion in Kerala, India. The spatial pattern of annual soil erosion rate was obtained by integrating geo-environmental variables in a raster based GIS method, GIS data layers including USLE parameters, and determining their effects on average annual soil loss in the study area. They suggested that spatial erosion maps generated with RUSLE and GIS integration may serve as an effective input in deriving strategies for land planning and management in environmentally sensitive mountainous areas.

Ashiagbor *et al*. (2013) used RUSLE and GIS tools to model the spatial distribution of soil erosion in the Densu River Basin of Ghana and identified the relationship between erosion susceptibility, slope and LULC, then assigned four different erosion risk classes. This model predicted that 88% of the basin was under low erosion risk, 6% under moderate erosion risk, 3% under high erosion risk, and 3% was under severe erosion risk. The high and severe erosion risk areas were distributed in the region with high slope gradients and moderate forest LULC class sections.

Ghosh *et al*. (2013) estimated the potential and actual soil loss and identified the major erosion prone sub-watersheds in the hilly region of Tripura, India through integration of USLE and GIS. They divided the whole area into 23 sub-watersheds on the basis of intensity of soil erosion and estimated that the average annual predicted soil loss ranged from 11 to 836 t ha^{-1} yr^{-1} and less erosion was noticed in forest areas.

Kamaludin *et al*. (2013) integrated RS, RUSLE and GIS to model potential soil loss and sediment yield within selected sub-catchments of the Pahang River Basin and obtained results with a high correlation (r = 0.99) between soil loss potential and sediment delivery in the catchment of the study area.

Naqvi *et al*. (2013) used the RS, GIS and RUSLE to model the soil loss estimation for soil conservation and vegetation rehabilitation in the Nun Nadi watershed for the years 2000 and 2009. The estimated mean soil loss for the years 2000 and 2009 was 3,283.11 and 1,419.39 Mg ha^{-1} yr^{-1}, respectively. The study found that about 80% of area had a low or least risk of erosion and about 7% were exposed to a high or very high risk, which indicated the improvement in terms of soil loss as compared to the data of both the time periods.

Panagos *et al*. (2016) assessed the rainfall erosivity factor of RUSLE on a monthly basis using 30 min data of precipitation for about 30 years from 80 recording stations located in Greece. They applied a generalised additive model for spatial interpolation and observed that intra-annual variability of rainfall erosivity was high, and the warm season was found to be three times less erosive than the cold season. The rainfall erosivity and precipitation proportion, which was expressed as erosivity density, were variable throughout the year and were observed as low in the first five months (January-May) and relatively high in the remaining seven months (June–December). They had drawn the rainfall erosivity factor (R) maps and revealed a high spatial variability with an average value of R factor of 807 MJ mm ha^{-1} h^{-1} yr^{-1} ranging from 84 to 2825 MJ mm ha^{-1} h^{-1} yr^{-1}. They suggested that combined maps of monthly rainfall erosivity factor (R), vegetation coverage, and tillage maps are useful for monitoring soil erosion risk at a national level.

Tiruneh and Ayalew (2015) predicted the soil loss rate of the watershed with a GIS and RS. The RUSLE adapted to Ethiopian conditions was used to estimate potential soil losses and utilised information on rainfall erosivity (R) by interpolation of rainfall data, soil

erodibility (K) using soil map, vegetation cover (C) using satellite images, topography (LS) using Digital Elevation Model (DEM), and conservation practices (P) using satellite images. The total and average amount of soil loss estimated by RUSLE from the watershed was 30,836.41t yr^{-1} and 4.81t ha^{-1} yr^{-1}, respectively.

Ganasri and Ramesh (2016) integrated the RUSLE with GIS and estimated soil loss in the Nethravathi Basin, located in the south-western part of India. They observed that the estimated total annual potential soil loss of about 473,339 t yr^{-1} was comparable with the measured sediment of 441,870 t yr^{-1} during the water year 2002-2003. The predicted soil erosion rate due to an increase in agricultural area was about 14,673.5 t yr^{-1}. They derived a probability zone map by the weighted overlay index method, which indicated that the major portion of the study area comes under the low probability zone and only a small portion falls under the high and very high probability zone. They expect that the results will be helpful in further implementation of soil management and conservation practices to reduce soil erosion in the Nethravathi Basin.

Gaubi *et al*. (2017) combined the GIS and RUSLE models and predicted the soil erosion for the Lebna watershed, Cap Bon, Tunisia. Monthly rainfall data from five stations for about nine years was used to analyse the R factor. The K factor was analysed by digitizing the soil map of the watershed and then assigning the soil erosivity factor index to each soil unit. The LS factor was estimated by creating a DEM in ArcGIS software by digitizing contour lines from topographic maps. On the basis of the LS distribution map, they distinguished and confirmed the reliability of the results.

Jazouli *et al*. (2017) suggested that the combination of USLE and spectral indexes approaches could be an important tool for integrated soil management, especially with the perspective of evaluating and mapping the soil erosion risk and reducing the soil erosion rate.

Bera (2017) integrated the USLE model with GIS and RS and quantified the soil loss in the Muhuri river basin, Tripura. The daily rainfall data (2001–2010) of 6 rain gauge stations was used to predict the R factor. The K factors in the basin area ranged from 0.15 to 0.36. The spatially distributed soil loss map of the Muhuri river basin was generated and classified into six categories on the basis of the intensity level of soil loss. The average annual predicted soil loss ranges between 0 to 650 t ha^{-1} yr^{-1}. Low soil loss areas were observed under very densely forested areas and intensely planted (mainly rubber plantation) areas, while the high rate of soil erosion was noticed along the main course of the Muhuri river.

Mahala (2018) analysed the erosion characteristics in a river basin that originated from a plateau top region and flows through the plateau fringe region of the eastern Chotanagpur plateau region of India using the RUSLE. The study region was a gently sloped undulated plateau fringe landform which dissected plateau topography. The RUSLE parameters were enumerated using field data and RS data and were verified with past

literature. He observed that soil erosion was dominated by land degradation processes in the upper areas of the watershed, while successful land management activities reduced soil loss in the lower reaches of the watershed. He concluded that soil loss estimation is an important input for LULC management in watershed areas and also inferred that the RUSLE model could be effectively used in the tropical plateau fringe.

Benavidez *et al*. (2018) reviewed the USLE, RUSLE, and their parameters and analysed the adoptability of these equations around the world with local conditions. They discussed the strength, limitation, recommendation of future application and potential of a combination of these equations with the Compound Topographic Index (CTI) and Sediment Delivery Ratio (SDR) for estimating gully erosion and sediment yield. They expected that their recommendations would be helpful to the researchers to use RUSLE in different geo-climatic regions with variable availability of data and modelling the spatial and temporal land cover scenarios at a finer scale.

Bouhadeb *et al*. (2018) estimated the annual soil erosion rate and its spatial distribution in the Bounamoussa watershed in the north-east of Algeria using the RUSLE and GIS. Due to the non-availability of rainfall intensity data in and near the watershed region, they used only available monthly and annual rainfall data sets to calculate the R factor through an alternative equation. The spatial distribution of K factor was extracted from soil type data taken from the soil map and 13 soil samples (0–25 cm deep) collected from all over the watershed area in such a manner that each soil type was represented by 2 or 3 samples, and then the required characteristics of soil were determined in the laboratory. They developed soil loss map indicating an average erosion rate of 7.8 t ha^{-1} yr^{-1}. The four erosion severity classes were assigned and it was suggested to consider these severity areas as priority areas for futuristic erosion control programmes to decrease the siltation rate in the Cheffia reservoir.

Pham *et al*. (2018) quantified soil erosion in the A Sap river basin in the ALuoi district, ThuaThien Hue Province, Vietnam, using the USLE and GIS. They resulted in 34% of land area lost accumulating to 10 t ha^{-1} yr^{-1} while 47% of the total area lost was less than 1 t ha^{-1} yr^{-1}. Natural forestland lost the most, with an average of about 19 t ha^{-1} yr^{-1}, followed by plantation forest with 7 t ha^{-1} yr^{-1} approximately and other agricultural lands at 3.70 and 1.45 t ha^{-1} yr^{-1} for yearly crops and paddy rice, respectively. Soil erosion was most sensitive to the topographic factor (LS), followed by the P factor, K factor, C factor, and the R factor. The changes to the cultivated calendar and intercropping were found to be effective ways to prevent soil erosion in cultivated lands. Furthermore, the introduction of broadleaf trees for mountainous areas in the A Sap basin was the most effective practice in reducing soil erosion. The study also pointed out that the combination of available data sources used with

the USLE and GIS technology is a viable option to calculate soil erosion in central Vietnam, which would allow targeted attention toward a solution to reduce future soil erosion.

Saha *et al*. (2018) carried out soil erosion analysis in the sloping terrain of the upper Kangsabati watershed, having an area of 276.19 km^2 in the district of Puruliya, West Bengal. Average annual soil erosion was estimated through the RUSLE and GIS. The potential average annual soil erosion of the watershed was classified into low, moderate, high, and very high categories. The highest rate of soil erosion was greater than 13.42 t ha^{-1} yr^{-1} and was found along the north-eastern part of the watershed. The lowest amount of soil erosion was less than 1 t ha^{-1} yr^{-1} and was found along the hilly tract of dense forest cover and plantation areas.

Wijesundara *et al*. (2018) assessed the soil erosion using the RUSLE model and GIS environment and developed erosion maps of the important Kirindi Oya river basin in Sri Lanka, which fulfilled irrigation demand for the downstream dry zone of the country. The river basin was categorised into low, moderate, high, very high, and extremely high erosion hazard classes. The predicted soil erosion rates in the entire river basin ranged from 19 to 184 t ha^{-1} yr^{-1} with an average of 33 t ha^{-1} yr^{-1}. They observed that predicted soil loss rates were above the critical soil loss rates (6.7 t ha^{-1} yr^{-1}) stipulated to dry zone of Sri Lanka and this must be helpful to stakeholders to implement various soil conservation measures in the Kirindi Oya basin.

Koirala *et al*. (2019) estimated the soil loss of Nepal using the RUSLE and GIS and also analysed the effect of land use, land cover, and slope exposition on soil erosion. Nepal's mean annual soil loss was estimated at 25 t ha^{-1} yr^{-1}, with a total potential soil loss of 369 million tonnes. The mean soil erosion rate was significantly high for steep slopes and low for gentle slopes. The mean erosion rate based on LULC was observed to be highest (40 t ha^{-1} yr^{-1}) for barren land, followed by agricultural land (29 t ha^{-1} yr^{-1}), shrubland (25 t ha^{-1} yr^{-1}), grassland (23 t ha^{-1} yr^{-1}), and forests (22 t ha^{-1} yr^{-1}). Based on erosion severity, the entire study region was classified into 6 erosion classes, and it was found that 11% of the area was under very severe erosion risk (> 80 t ha^{-1} yr^{-1}) and required urgent measures to reduce the risk of erosion.

Yesuph and Dagnew (2019) used the RUSLE and local perception in the GIS framework and analysed the soil erosion and severity of erosion in the Beshillo catchment of the Blue Nile basin, Ethiopia. They prepared the LULC map based on the landsat 2017 image for the watershed and categorised the watershed into required classes, then assigned corresponding C factor values to each LULC class based on available literature and recommendations in the Highlands of Ethiopia.

2.3 Morphometric analysis

Singh and Sarangi (2008) carried out the hypsometric analysis of two watersheds, Sainj and Tirthan, along with their sub-basins in the Kullu district of Himachal Pradesh. They delineated the watershed through a DEM and GIS and obtained the hypsormetric values of the Sainj and Tirthan watersheds as 0.51 and 0.44, respectively. This analysis indicated that 51% and 44% of the original rock masses still exist in these watersheds. The Sainj watershed and its ten sub basins were more prone to erosion in comparison to the Tirthan watershed and its five sub basins. They expected that this study would help in the construction of soil and water conservation measures in the Sainj watershed and its sub basins at suitable locations for controlling soil erosion, water conservation, and reduction of sediment outflows.

Vittala *et al*. (2008) prioritized the sub-watersheds through an integrated approach with the objective of selecting sub-watersheds to undertake soil and water conservation measures in 67 villages in the Pavagada area, Tumkur district, Karnataka and a small portion in Ananthpur district, Andhra Pradesh, India, using RS inputs and socio-economic data for the purpose of better implementation of development and management programmes in the study area. They adopted a knowledge-based weightage system fully dependent on local terrain and the field situations. Based on relative importance to each parameter in the study area, they further grouped the villages/sub-watersheds into three categories, having high, medium, and low priority, and gave priority to villages/sub-watersheds having large economically weaker populations.

Shinde *et al*. (2010) prioritized the micro watersheds on the basis of soil erosion hazard using RS and GIS systems at the micro watershed level in the Konar basin of the upper Damodar Valley catchment of India. They used USLE with a raster-based geographic information system to calculate potential soil loss in the study area and reported that GIS methodology quickly provides the information on the estimated value of soil loss for any part of the investigated area. They further suggested various management practises in micro-watersheds for the reduction of soil erosion in the Konar basin.

Pandey *et al*. (2011) prioritized the subwatersheds of the Ret watershed of the Mahanadi river basin through morphometric parameters and identified suitable sites for soil and water conservation measures. They divided the Ret watershed into 26 subwatersheds and derived morphometric parameters for each of the subwatersheds independently and achieved the water resource management plan through integration of morphological parameters with land use, land cover, soil and slope information. The four drainage parameters (i.e., bifurcation ratio, drainage density, stream frequency, texture ratios), and three basin shape parameters (i.e., form factor, circulatory ratio, and elongation ratio) among 26 subwatersheds were assigned a rating of 1, and the next highest values were assigned a rating of 2, and so on.

In the case of the shape parameters, the lowest value was given a rating of 1, the next lowest value was given a rating of 2, and so on. The subwatershed having the lowest rating value was assigned the highest priority and vice versa. The subwatersheds were classified into the five priority scales, i.e., very high, high, medium, low, and very low, and suitable sites for check dams were suggested in each sub watershed.

Sujatha *et al.* (2013) carried out morphometric analysis to analyse the drainage characteristics of the Palar sub-watershed in the Amaravati sub-catchment using Advanced Space-borne Thermal Emission and Reflection Global Digital Elevation Model (ASTER GDEM) data, topographical maps, and a GIS platform. They extracted morphometric features at the micro-watershed level and divided the sub-watershed into six micro-watersheds, which included a sixth-order stream. They observed that first-order streams dominated the sub-watershed and that slope and local relief influenced the stream segment development and reported their study as a useful tool in strategic planning for erosion control and soil conservation.

Kushwaha *et al.* (2016) studied the hydrologic response of the Takarla-Ballowal watershed based on morphometric analysis of the watershed using RS and GIS. The drainage density of the Takarla-Ballowal watershed (7.02 km/km^2) indicated the closeness of spacing of channels with impermeable sub strata; the drainage texture (30.45 no./km), categorised the watershed as fine drainage texture; and the small length of overland flow (71.23m) indicated the generation of high peaked storm hydrographs with a short time base, resulting in moderate quantity of runoff generation but high soil erosion rates in the watershed. The slope of around 46.17% of the watershed area is less than 10%, 54.60% and 26.64% of the watershed area have been categorised as forest land and agricultural land, respectively. The runoff potential of the watershed might be moderate, with the possibility of high siltation rates in the downstream water harvesting structures, which would require conservation treatment planning in these catchments.

Meshram and Sharma (2017) carried out morphometric analysis and prioritized the subwatersheds of the Shakkar River Catchment, Narsinghpur district in Madhya Pradesh, India, using RS, GIS, and Principal Component Analysis (PCA) techniques. They concluded that prioritization based on morphometric parameters is time-consuming, while a PCA based approach to watershed prioritization can identify new meaningful underlying variables. They demonstrated the utility of RS, GIS, and PCA techniques in prioritizing sub-watersheds based on morphometric analysis.

Thapliyal *et al.* (2017) prioritized the 22 sub-watersheds of the Alaknanda basin based on morphological analysis using linear, areal, and dimensionless aspects. They delineated subwatersheds using GIS and DEM. The parameters like stream order, stream length ratio, stream frequency, form factor, drainage texture, drainage density, elongation

ratio, circulatory ratio, compactness constant and bifurcation ratio were independently calculated for each sub-watershed. The stream orders up to the 7^{th} order were analyzed and divided the study area into 22 subwatersheds, namely SW1, SW2, and so on till SW22. Based on the analysis, watersheds were divided into nine priority classes, namely Extremely Very High, Extremely High, Very High, High, Medium, Low, Very Low, Extremely Low, and Extremely Very Low for natural resource management.

Puno and Puno (2019) analyzed the different geomorphometric features and existing LULC using the Arc Hydro Tool of ArcGIS version 10.2 in the Muleta watershed, Philippines. They delineated fourteen subwatersheds as SW1 to SW14 using DEM and GIS tools. The ranking was given on the basis of parameters which had direct and inverse effects on erosion risk. Compound values for final prioritization were obtained by adding LULC to geomorphometric parameters. The SW13, SW14, and SW4 were classified under the very high priority class and advised appropriate management actions, while the SW10, SW6, and SW7 were classified under very low priority. They expect that information will be significantly helpful to watershed planners and managers, especially in prioritization of watershed management programmes and their implementation.

Ahirwar *et al*. (2019) prioritized the four subwatersheds of Hoshangabad and Budhni, Madhya Pradesh, India based on geomorphologic analysis through GIS and described the importance of morphometric parameters. They used LISS-III data for LULC assessment, NBSS & LUP soil maps, topographic maps on scale 1:50,000, SRTM DEM data, and analysed various morphometric parameters in each subwatershed, like drainage geometry and texture analysis, drainage network and relief parameters. They compounded each parameter of the subwatershed, assigned rank and prioritized them, and proposed suitable soil and water conservation structures at appropriate places, suggesting that the proposed soil and water conservation structures would reduce soil erosion and increase the surface and groundwater availability in the study area.

Ghosh and Gope (2021) carried out morphological characterization by measuring linear, relief and areal aspects to analyze hydrological behavior of watersheds. The results revealed that SW2 and SW6 were under high priority which indicated that these watersheds were under high risk of erosion and groundwater deficit. The subwatersheds SW3, SW4, SW7 are under category of moderate soil erosion and ground water recharge. The subwatersheds SW1 and SW5 are good for ground water storage.

2.4 Watershed delineation and prioritization

Khan *et al*. (2001) delineated and prioritized the Guhiya drainage basin, an area of about 1614 km^2 for proper planning and management of soil and water conservation measures and to obtain sustainable crop production through GIS and RS techniques. They assessed 68 watersheds on the basis of their erosivity and sediment yield index values using the terrain

information derived from geocoded satellite data and 1:50,000 topographic maps. Thematic maps of land use, landform, land-cover, and slope were digitized using ARC/INFO. They grouped watersheds into classes of very high, high, moderate, and low priority classes based on sediment yield index (SYI) values. They concluded that high priority watersheds with very high SYI values required immediate attention for soil and water conservation measures, while low priority watersheds had good vegetative cover and low SYI values may not need immediate attention for such measures.

Kumar and Dhiman (2014) carried out automated and manual delineation of watershed boundaries in Kangra district of Himachal Pradesh in the western Himalayas to analyse the feasibility of such a method for watershed boundary delineation. Manual preparation of watershed boundaries is time consuming and needs some basic information and skilled manpower. They observed that the automated approach to watershed delineation is much simpler than the manual method and can be carried out accurately and smoothly using open source software and freely available databases.

Gajbhiye *et al*. (2014) prioritized the watershed through the SYI method using RS and GIS. The study area was divided into 6 classes of slope as suggested by the All India Soil and Land Use Survey (AISLUS) and the watershed area into 15 classes. On the basis of SYI subwatersheds were prioritized providing higher rank to that subwatershed which had higher SYI value. They stated that a watershed is an ideal unit for planning and management of land and water resources.

Balasubramani *et al*. (2019) studied a GIS-based spatial multi criteria approach for prioritization of micro watersheds in the Andipatti watershed using morphometric, soil erosion, and surface runoff parameters and integrated all these parameters through the analytical hierarchy process (AHP) approach, which has strengthened the prioritization process and removed biases. They observed that the results of prioritization could be more appropriate for ungauged watersheds because the index gives importance to the intensity of the problem in each micro watershed on a comparative scale. The GIS based multi-criteria priority index would also help planners adopt sustainable development measures in a phased manner.

Fayas *et al*. (2019) studied and assessed erosion severity in the Kelani river basin in Sri Lanka using the RUSLE model and GIS environment. The severity of erosion was estimated using the RUSLE, Digital Elevation (15x15m), 20 years of rainfall data at 14 raingauge stations across the basin, soil maps, LULC and cropping factors. They observed that about 70% of the Kelani river basin area has low to moderate erosion severity (12 t ha^{-1} yr^{-1}) and urgently needed erosion control measures to ensure a sustainable ecosystem in the basin. They further suggested refining RUSLE results with sub-basin level real-time erosion estimations in the basin.

Singh *et al*. (2021) prioritized the six reservoir located in Shivalik foothills of north-west India using RS, GIS, morphometric component and PCA technique. The catchment areas were delineated by using ALOS PALSAR DEM in ArcGIS 10.4.1 software. They concluded that morphometric analysis followed principal component analysis based prioritization was observed as more consistent and can be useful in identification and managing the critical issues in the reservoir.

The reviews presented in this chapter has provided sufficient evidence that many researchers have made many attempts to integrate the RS, GIS and erosion prediction models to analyse the LULC classification, watershed delineation, morphometric studies of watersheds and to predict the soil erosion remotely. The satellite imaginary, topographic information and GIS application quickly analysed and categorised the LULC classes of the study area and found reliable when coupled with ground truth surveys. Time series comparison of classified LULC was found an effective tool for futuristic prediction in land use change over a period from one land use to another land use. Various researchers have estimated the annual soil erosion rate and its spatial distribution through integration of RUSLE and GIS. They found that integration of RUSLE and GIS even with limited data source is a viable and quick option to identify the erosion prone areas rather than the exhaustive physical surveys. GIS based approach of watershed prioritisation was suggested to be helpful for planner to adopt the sustainable development measure in systematic manner. Lot of work has been carried out in LULC classification, morphometric analysis of watersheds and soil loss estimation through integration of RS, GIS and RUSLE in the India and abroad. But very less work or almost negligible attempt has been carried out in Haryana Shivalik for prioritisation and area assessment for soil erosion control in watersheds using geospatial technology.

CHAPTER–III

MATERIALS AND METHODS

The GIS is well suited for quantification of heterogeneity in the topographic and drainage features of a catchment (Shamsi, 1996). The USLE and RUSLE methods have been found useful for producing realistic estimates of soil loss over areas of small size (Wischmeier & Smith, 1978; Renard *et al*., 1997). As a result, the current study was designed to examine land use and land cover classification, soil loss estimation in the study area using the integration of the quantitative empirical model RUSLE with RS and GIS, and then prioritization of watersheds based on the severity of soil erosion.

3.1 Shivalik hills region

The Shivalik hills region is part of the Sub-Himalayan mountain system and is spread across the states of Jammu and Kashmir, Panjab, Hayana, Himachal Pradesh, and Uttarakahnd. Most of the parts of the Shivalik region fall in Himachal Pradesh and parts of Punjab and Haryana. The Shivalik region in the Sub-Himalyan mountainous region is located between latitudes 28°57'16" to 34°10'48"N and longitudes 73°29'24" to 80°14'23"E in the northwestern part of India and forms a long and narrow stretch from Jammu & Kashmir to Uttarakhand. This stretch passes through Punjab, Chandigarh, Haryana, Himachal Pradesh, and Uttar Pradesh, covering an area of 3.33 mha out of which 1.79 mha is in the hills and 1.54 mha is in the piedmont plains, respectively, in north-western India. The elevation ranged from 217 to 2332 m above mean sea level (MSL); the lowest range passes through Punjab at 283 to 848 m above MSL (Yadav *et al*., 2015).

The Shivalik region is considered the most fragile ecosystem in the country. In past few decades, the increased population of human and livestock pressed hard over the natural resources of Shivaliks and generated threat to the flora and fauna of the Shivalik. Other calamities like frequent forest fires might be due to man-made mistakes or by their own. Improper land use management, construction of new approach roads, and construction of new residential towns along with improper land use management have contributed to the steady degradation of natural resources like land, water, soil, and flora and fauna in the Shivalik region.

3.1.1 Shivalik hills region in Haryana

The Shivalik region in Haryana is spread in districts like Panchkula, Ambala, and Yamunanagar in the north and north-eastern parts of the state and lies in latitude 30°08'36"-30°55'05"N and longitude 76°36'05"-77°34'48"E. Different researchers have reported the Shivalik region in Haryana as 600 km^2 (Kukal *et al*., 1991), 2889 km^2 (Grewal *et al*., 1995)

and 1920 km^2 (Yadav *et al*., 2005). Physiographically, the Shivalik region in Haryana is spread over 3,514 km^2 within the Panchkula, Ambala, and Yamunanagar districts of the state (Yadav *et al*., 2015). The Government of Haryana formed the Shivalik Development Board (SDB) and Shivalik Development Agency (SDA) in the year 1993 for the overall and integrated development of the Shivalik region in Haryana in the fields of agriculture and allied activities, education, public health, bridal paths & roads, irrigation, watershed management, afforestation, animal husbandry and wild life etc. They included entire districts like Panchkula, Ambala and Yamunanagar irrespective of foothills.

3.1.2 Topography and soil

The Shivalik hills in the Haryana region are mainly comprised of alluvium and boulder conglomerate with clay bands. The hilly areas are made up of conglomerates, medium to coarse-grained pale brown sandstones, thin light brown or chocolate-colored sandy clays in the lower part, and highly weathered, closely-joined exposed rock in the form of silt stone clays in some places. The foothill zones comprise boulders, pebbles, gravel, sand, and clay, followed by alluvial deposits of sand, sand with clay. In places, the Shivalik has highly dissected plateau topography formed by ephemeral streams. Weathering and denudation have produced a variety of erosional landform features such as rills, gullies, scarps, and variously shaped ridges and amphitheatrically basins. The drainage channels carry huge amounts of detritus and bed load, creating problems of silting of reservoirs, deposition of sand on agricultural fields and disrupting communication.

3.1.3 Panchkula

The Panchkula district lies between latitudes 30°26'-30°55'N and longitudes76°46'-77°10'E in northern part of Haryana state. The northern side of the district is surrounded by Himachal Pradesh eastern side by Uttar Pradesh, southern and western side by Karnal, Kuruksherta and Ambala district. Total geographical area of the district is 898 km^2. The district is mainly drained by the river Ghaggar and its tributaries. Panchkula district is bestowed with rich water resources, both surface as well as ground water resources. The ground water is major sources of irrigation in the district. Net irrigated area is 80 km^2 whereas, gross irrigated area is 180 km^2.

3.1.3.1. Climate and rainfall

Panchkula district has a subtropical monsoon with mild and dry winter, hot summer and sub-humid which remains dry with very hot summer and cold winter, except in monsoon season. The temperature may rise over 43 °C in summer and may fall down to -1°C in winter season. The normal annual rainfall of the district is 1057 mm, The southwest monsoon sets in from last week of June and withdraws in end of September, contributed about 86% of annual rainfall. July and August are the wettest months. Rest 14% rainfall is received during non-monsoon period in the wake of western disturbances and thunderstorms.

3.1.4 Ambala

Ambala district lies between latitude 30º10'-31°35'N and longitude 76°30'-77°10'E in the northern part of Haryana state. This district is surrounded by Yamunanagar district in the southeast, Kurukshetra district in the south, while district Patiala, Ropar and the union territory of Chandigarh in the west. The Shivalik Range of Solan and Sirmaur districts of Himachal Pradesh bounded the Ambala district in the north and northeast. The total geographical area of the district is 1574 km^2.

3.1.4.1 Climate and rainfall

The climate of Ambala district can be classified as subtropical monsoon with mild and dry winter, hot summer and sub-humid, that is mainly dry with very hot summer and cold winter, except during the monsoon season when moist air of oceanic origin penetrates into the district. In May and June, it can be really hot with the temperature soaring to over 48 ºC, while in winter it can be as low as -1°C. The normal annual rainfall of the district is 1076 mm and is unevenly distributed over the area. The southwest monsoon sets in from the last week of June and withdraws at the end of September, contributing about 81% of normal annual rainfall. July and August are the wettest months. The remaining 19% of rainfall is received during the non-monsoon period in the wake of western disturbances and thunderstorms. The mean maximum temperature is 40.8°C (May and June) and the mean minimum is 6.8°C (January) in the district.

3.1.5 Yamunanagar

Yamunanagar district lies between latitude 29º09'-29º50' N and longitude 76°31'-77°12'E. It is bounded by Himachal Pradesh in north and Uttar Pradesh in the east, by Ambala district in the west, and the Karnal and Kurukshetra district in the south. The geographical area of the district is 1,756 km^2. The Yamuna River flows through the Yamunanagar district.

3.1.5.1 Climate and rainfall

The climate of Yamunanagar district can be classified as subtropical monsoon, mild and dry winter, hot summer and sub-humid, which is mainly dry with hot summer and cold winter except during the monsoon season when moist air of oceanic origin penetrates into the district. The normal annual rainfall for the district is 1107 mm. The southwest monsoon sets in from the last week of June and withdraws at the end of September, contributing about 81% of the annual rainfall. The remaining 19% of rainfall is received during the non-monsoon period in the wake of western disturbances and thunderstorms. Most of the monsoonal rainfall dominated in the month of July and August.

3.2 Data used

The study required the satellite imaginary, topographical data, ArcGIS and window based software, information on rainfall and soil classification and other necessary auxiliary data related to study area. The data used in the study is described as follows.

3.2.1 Satellite data

The DEM and satellite imaginary data are freely available to the researchers and users on Unites States Geological Survey (USGS) portal in GeoTiff format. The Shuttle Radar Topography Mission (SRTM), DEM data posted at every 1 arc-second (approximately 30 m) and Sentinel-2A (10 m resolution, Path-147 Row-39) cloud free imaginaries of April 29th, 2021 were downloaded from USGS, Earth Explorer for the delineation of watersheds and further analysis of the study area (Table 3.1).

3.2.2 Topographical data

The Shivalik region in Haryana comes under Survey of India (SOI) toposheets no. H43K13/53B/13, H43K14/53B/14, H43K15/53B/15, H43L1/53F/1, H43L2/53F/2, H43L3/53F/3, H43K11/53B/11, H43K12/53B/12, H43K16/53B/16, H43L4/53F/4, H43I12/44J/12, H43L11/53F/11, H43L12/53F/12, H43L7/53F/7, H43L8/53F/8, H43R1/53G/1, H43R5/53G/5 on 1:50,000 scale. These toposheets were used for identification of district boundaries of Panchkula, Ambala and Yamunanagar and geo-referencing and delineation of watersheds and extraction of other features of the study area.

3.2.3 Software used

The ArcGIS 10.7.1, Erdas Imagine 2015 and other window based software were used for the purpose of analysis in this study.

3.2.4 Rainfall data

Daily rainfall data was not available at many locations, so 22 years of monthly rainfall data ranging from the year 1999 to 2020 was collected for 14 raingauge stations located within and outside the study area from the block and district offices of the Department of Agriculture and Farmer Welfare and the Department of Revenue, Govt. of Haryana (Fig. 3.2). The data was analysed and tabulated as mean annual rainfall data (Table 3.2). The study area wholly and partially includes the districts of Panchkula, Ambala, and Yamunanagar of Haryana.

3.2.5 Soil classification data

The information on soil classification of the study area was obtained from FAO digital soil map of the world (DSMW, 2003).

3.2.6 Auxiliary data

The ground reference data obtained from field surveys and Google Earth was used in the analysis and for ground truth verification of the results.

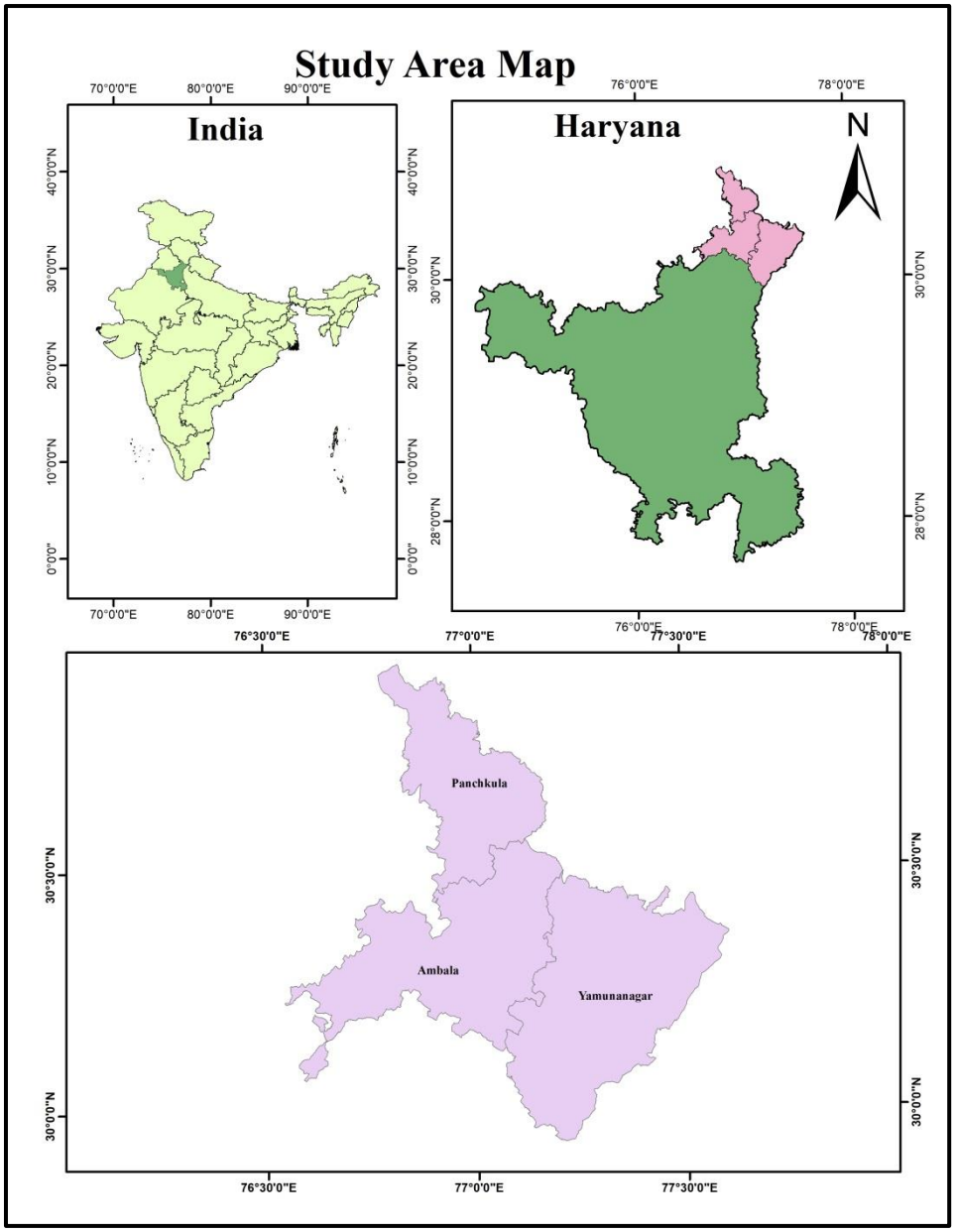

Fig. 3.1: Location map of study area in (Panchkula, Ambala and Yamunanagar) Shivalik region of Haryana

3.2.7 Geo-referencing, mosaicing and subsetting

All the toposheets were first geo-referenced, removing the excess portion, and then mosaicing of all toposheets was performed in a GIS environment. The district boundary of Panchkula, Ambala, and Yamunanagar was digitized and a vector image or shape file was created, which was further used for the delineation of watersheds and extraction of other features of the study area (Fig. 3.1). The mosaicing and geo-referencing of all satellite imagery was also performed. The district shapefile was overlaid over DEM and satellite imagery. DEM and satellite imaginary were masked with shapefile and subsetted individually for further analysis in the study.

Table 3.1: Details of satellite data

Satellite	Sensor	Projection	Year of Acquisition	Resolution (M)
Sentinel-2A	MSI	WGS_1984_UTM_Zone_43N	April, 2021	10
SRTM	Shuttle Radar Topography Mission (SRTM)	n29_e077_1arc_v3 n29_e077_1arc_v3	2000	30

3.2.8 Delineation of watershed

A depression-less DEM is required for the process of watershed delineation. The SRTM DEM of 30 m resolution was used as the basis for delineating the study area. Data extraction and analysis were carried out. The area of interest was extracted from the SRTM raster by masking the shape file of ROI. The terrain elevation of the study area ranged from 238 m to 1541 m. SRTM DEM is processed by filling the sinks. The flow direction and flow accumulation were generated. The stream orders were extracted using Strahler's (1964) method. For each watershed, the length and number of streams of various orders were obtained. The spatial analysis tool was used to delineate the watershed. Regardless of size or shape, ten watersheds adjacent to the Shivalik foothills were selected from delineated watershed and designated as WS1, WS2, WS3, WS4, WS5, WS6, WS7, WS8, WS9, and WS10. The spatial coordinate system of the World Geodetic System (WGS) 1984 UTM 43N was used for the entire study. The LULC assessment was done to classify the various classes in selected watershed using Erdas Imagine software (Table 3.3).

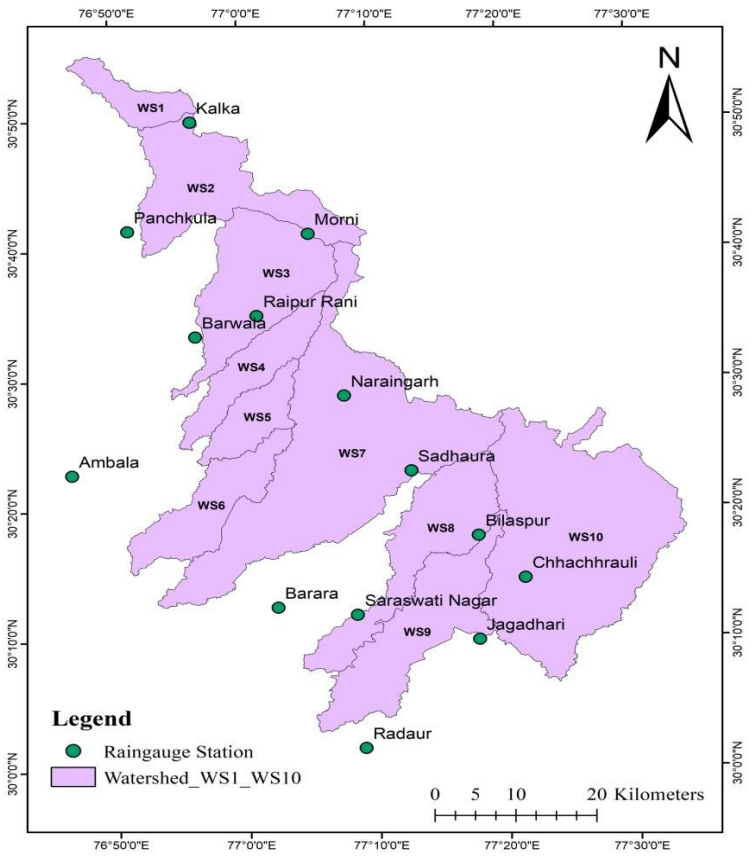

Fig. 3.2: Rain gauge stations in study area

Table 3.2: Information on rainfall data within and outside study area (1999-2020)

District	Station	Elevation (m)	Mean Annual Rainfall (mm)
Panchkula	Panchkula	353	457.45
	Kalka	659	950.58
	Barwala	319	253.72
	Raipurani	340	351.28
	Morni	1074	621.11
Ambala	Ambala	273	535.21
	Naraingarh	328	1482.21
	Barara	281	398.00
Yamunanagar	Jagadhari	286	1004.79
	Chhichhroli	296	965.33
	Radaur	269	768.64
	Saraswati Nagar	279	696.93
	Sadhaura	313	1177.93
	Bilaspur	307	1011.71

Table 3.3: Land use land cover classification of study area

Class	Description
Barren land	Exposed soil, barren land and similar
Waterbody	River, Lakes, Ponds, Water logged area and similar
Plantation	Include all types of Forest, Agro-forestry
Built up	Residential, industrial zone, scattered rural settlements roads and similar
Agriculture	Agricultural fields

3.2.9 Accuracy assessment

Accuracy assessment is the most important step in the LULC classification process. The main aim is to put to test the accuracy of classified images using a reliable statistical approach. In the present study, accuracy assessment of raster layer was assessed through the development of an error matrix to get the user's and producer's accuracy. A random sampling technique was adopted for locating the 153 points (locations) by both the field survey and Google Earth and matched them with the LULC map and obtained the user's accuracy, producer's accuracy, and overall accuracy. Photographs taken during the field survey are shown in Fig. 3.3.

Fig. 3.3: Field survey

The accuracy assessment was carried out using the following equation (Jothimani, *et al*., 2021)

User accuracy = (number of correctly classified pixel in each category /total number of classified pixel in that category)×100 (1)

Producer Accuracy = (number of correctly classified pixel in each category / total number of reference pixel in that category)×100 (2)

Overall Accuracy = total number of classified pixels / total number of reference pixels) ×100 (3)

Kappa coefficient = ((Total sample × Total corrected sample) - Sum (column total × row total) / (Total sample)^2 – Sum (column total × row total)) × 100 (4)

3.3 Morphometric analysis

The hydrological behaviour of watersheds was studied by analysing the morphometric parameters. The drainage network of all the watersheds WS1 to WS10 was extracted by series of geo-processing tools in ArcGIS 10.7.1 The morphometric parameters namely linear, areal and relief aspects were computed using formula as depicted in Table 3.4 for all the watersheds.

Table 3.4: Formulae used for computation of morphometric parameters

Sr. No.	Morphometric parameters	Formula/Definition	References
Estimation of linear parameters			
1	Stream order (μ)	Ranking hierarchically	Strahler (1964)
2	Stream Number (N_u)	Stream segment of various order	Horton (1945)
3	Stream length (L_μ)	Total Length of the stream segments of that particular order	Horton(1945)
4	Mean stream length (L_{sm})	$L = L_\mu/N_\mu$	Strahler (1964)
5	Stream length ratio (R_L)	$R_l = L_\mu / L_{(\mu-1)}$ Where L_μ = mean length of all stream segments of a given order (μ) $L_{(u-1)}$ = The mean length of all stream segments of one order less to given order (u)	Horton(1945)
6	Bifurcation ratio(R_b)	$R_b = N_u/N_{u+1}$ Where N_u = Total Number of stream segments of the order "u" $N_{(u+1)}$ = Number of stream segments of the next higher order	Schumm (1956)
7	Drainage density (D_d)	$D_d = L_\mu/A$ Where, L_μ = Total Length of the stream segments of all order A = Area of the river basin or grid (km^2)	Horton (1932)
8	Texture ratio	Number of stream segments of all order present in per perimeter of that area	Horton (1945)
9	Length of overland flow (L_o)	$L_o = 1/2D_d$ Where D_d= Drainage density of basin	Horton(1945)
Estimation of areal parameters			
1	Circularity ratio (R_c)	$R_c = 4\pi A/P^2$ Where A = Area of the basin (km^2), P = Perimeter (km)	Miller (1953) Strahler (1964)
2	Elongation ratio (R_e)	$R_e = 1.128 \sqrt{A} / L$ A = Area of the basin (km^2), L = Basin length (Km)	Schumm (1956)
3	Form Factor (F_f)	$F_f = A/L^2$ Where A = Area of the basin (km^2), L = Basin length (km)	Horton (1932, 1945)
4	Compactness constant (C_c)	$C_c = 0.2821 \times P/A^{0.5}$ A = Area of the basin (km^2), P = Perimeter (km)	Horton (1945)
5	Drainage texture (T_s)	$T = D_d \times F_s$ Where D_d = Drainage density, F_s = Stream frequency	Horton(1945)
6	Shape factor(B_S)	$B_S = L^2 /A$ Where L = Basin length (Km), A = Area of the Basin (km^2)	Horton(1932)
7	Constant of channel maintenance (R)	$C = 1/D_d$ Where D_d= Drainage density of basin	Schumm (1956)
8.	Stream frequency (F_s)	$Fs = N_\mu/A$ N_u = Total Number of stream segments of the order "μ", A = Area of the Basin (km^2)	Horton (1945)
Estimation of relief aspects			
1	Basin relief (R)	R = H – h Where H = maximum elevation (m), h = minimum elevation (m)	Hadley and Schumm (1961)
2	Relief ratio (R_r)	$R_r = R/L$ Where R = Basin relief, L = longest axis of major river (Basin length) in km	Schumm (1956)
3.	Ruggedness No. (R_n)	$R_n = (Dd \times R)/1000$	Schumm (1956)

The flow chart for the Morphometric analysis methodology is shown in Fig. 3.4.

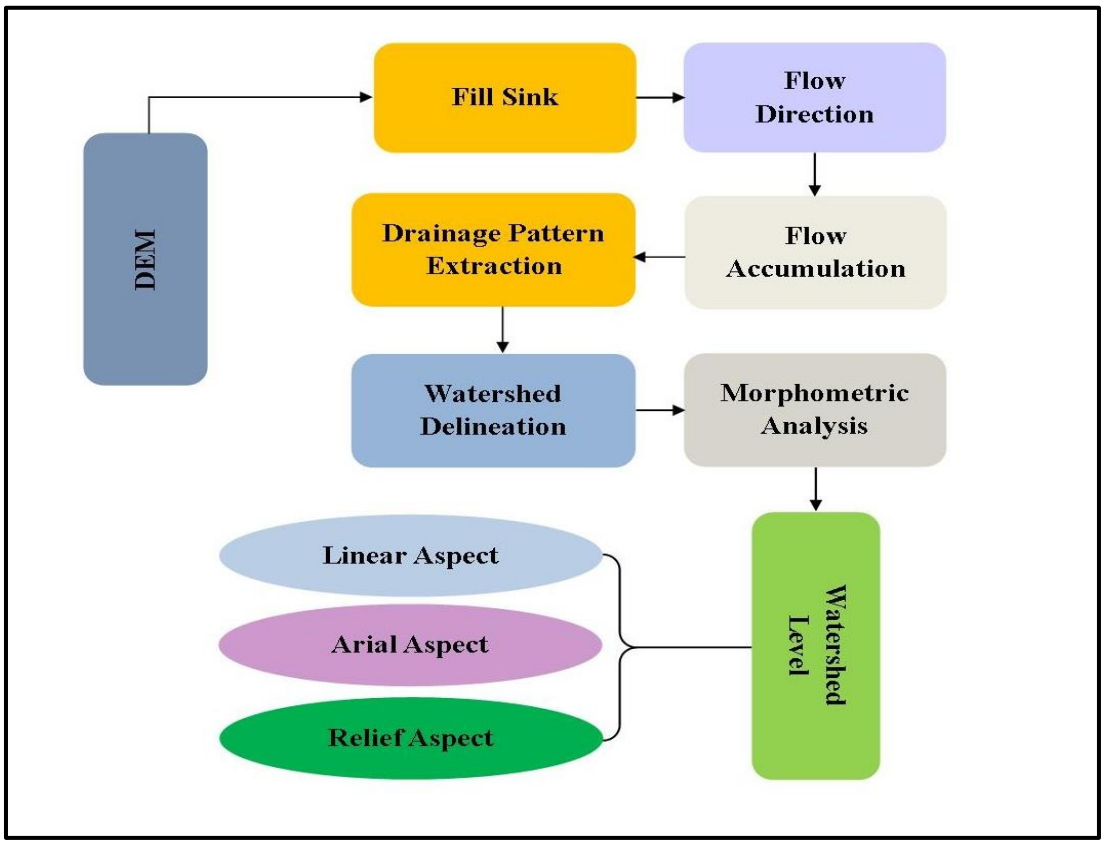

Fig. 3.4: Flow chart of morphometric analysis

3.4 Revised universal soil loss equation (RUSLE)

The USLE determines soil loss at any given point as a function of rainfall energy and intensity, soil erodibility, slope length, slope gradient, soil cover, and conservation practices (Wischmeier and Smith, 1978). The originality of USLE was retained in RUSLE while technology was altered for evaluation of the factors and introduced new data to evaluate the terms for specified conditions. The RUSLE can predict the long term average annual average soil loss from rill and interill erosion caused by rainfall splash and overland flow, but not from gully and channel erosion (Renard *et al*., 1997). Therefore, GIS methods are used to partition the areas into overland and channel types to estimate the soil loss in individual grid cells of overland areas. The flow chart for the RUSLE methodology is shown in Fig. 3.5.

$$A = R \times K \times LS \times C \times P \quad (5)$$

Where

A= average annual soil loss per unit area (t ha^{-1} yr^{-1}),

R = rainfall-runoff erosivity factor (MJ mm ha^{-1} h^{-1} yr^{-1}),

K = soil erodibility factor (t ha h $ha^{-1}MJ^{-1}$ mm^{-1})

LS = slope length steepness factor (dimensionless)

C = cover management factor (dimensionless, ranging between 0 and 1.5)

P= support and conservation practices factor (dimensionless, ranging between 0 and 1).

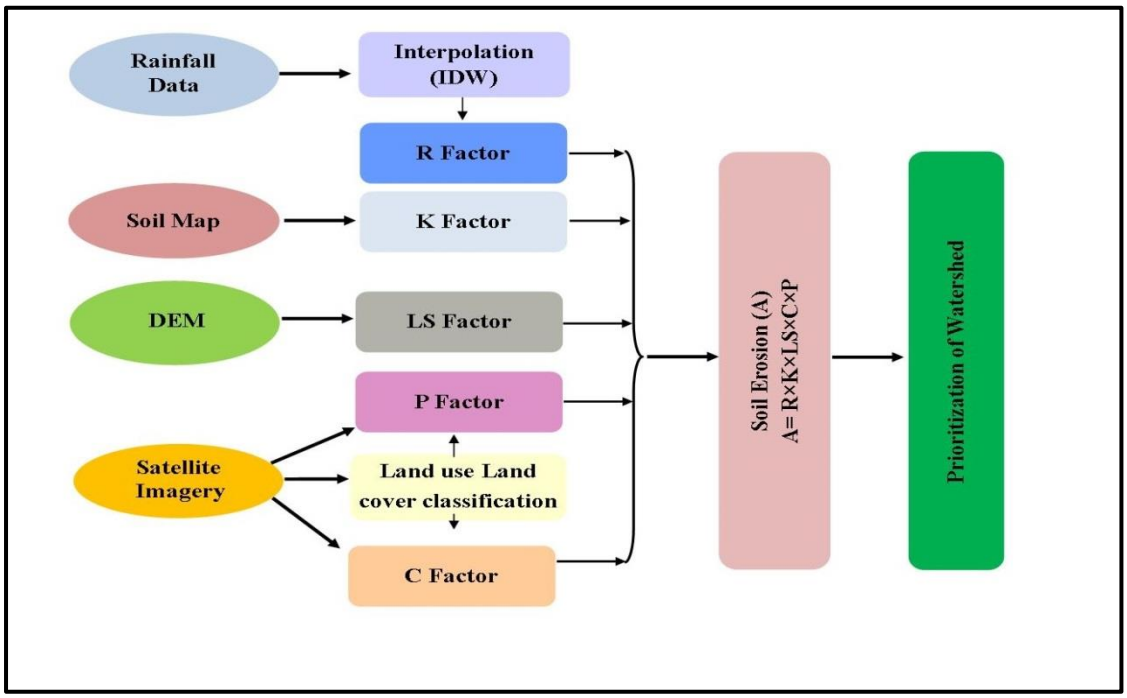

Fig. 3.5: Flow chart of soil loss estimation methodology

3.4.1 Rainfall erosivity factor (R)

The R factor is a key input for the RUSLE and is a climatic factor that reveals the influence of rainfall intensity on soil erosion and its calculation required detailed and continuous precipitation data (Wischmeier and Smith, 1978). The annual R factor is a function of the mean annual EI_{30} that is calculated from detailed and long-term records of storm kinetic energy (E) and maximum 30 minute intensity (I_{30}) (Renard *et al*., 1997). The aforementioned long term data is not available in the study area. In fact, only monthly and annual rainfall data sets are available. To overcome the lack of detailed rainfall data, the monthly rainfall was collected, tabulated, and analysed in an excel file, which was then converted into a .csv file and imported into an ArcGIS environment. For better accuracy, all these rainfall stations were marked as point layers and subsequently interpolated with the Inverse distance weighted method (IDW) for assessing the spatial variability in the rainfall in the study area. The rainfall erosivity values for the different stations were used to interpolate a rainfall erosivity surface. The equation given below is used in the computation (Singh *et al*., 1981).

$$R = 79 + 0.363 \times P \quad (6)$$

Where,

R is the rainfall erosivity factor (MJ mm ha^{-1} h^{-1} yr^{-1}), P is the annual rainfall (mm).

3.4.2 Soil erodibility factor (K)

The K factor represents the influence of different soil properties on the slope's susceptibility to erosion (Renard et al., 1997). The erodibility of soil is its resistance against detachment and transport. The flow chart of analysing the K factor is presented as Fig. 3.6. The soil data of the

study area was extracted from the DSMW global map in a GIS environment. The percentage of silt, clay, very fine sand, and organic matter for each soil group was calculated. Soil textural class, structure code (b), and permeability (c) were calculated using the USDA soil texture triangle. The K factor was calculated in the raster calculator using the equation (7). The equation effectively described the soil erodibility as a function of the complex interaction between sand, silt, and clay fractions in the soil and other factors such as organic matter, soil structure, and profile permeability class. The K factor was calculated by using the following relationship (Foster *et al*., 1991).

$$K=2.8 \times 10^{-7} \times M^{1.14} \times (12-a) + 4.3 \times 10^{-3} \times (b-2) + 3.3 \times (c-3) \quad (7)$$

Where,

K=soil erodibility factor in t ha h $ha^{-1}MJ^{-1}$ mm^{-1}

M= Particle size parameter (silt (%) + very fine sand (%)) × (100 – clay (%))

a= organic matter (%), b= soil structure code, c= soil permeability class

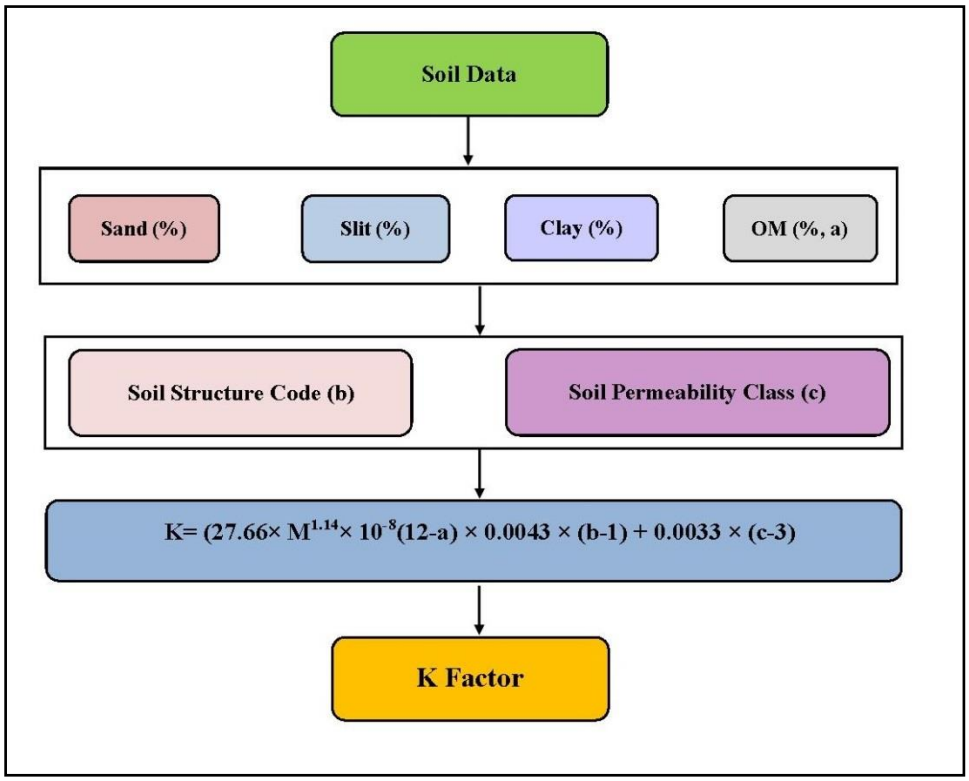

Fig: 3.6: Flow chart of soil erodibility factor (K)

3.4.3 Slope-length (L) and slope steepness (S)

This is a topological factor having two sub-factors: slope gradient (S) and slope length (L) factor. These two L and S factors together form the LS factor that is determined from DEM. These factors affect soil erosion by surface water movement.

The combined LS factor was estimated using the flow accumulation theme. The flow accumulation, which denotes the accumulated upslope contributing area for a given cell, performs a cumulative count of the number of pixels that naturally drain into outlets. The

operation can be used to find the drainage pattern of a terrain. The flow direction operation determines the natural drainage direction for every pixel in a DEM. Based on the output flow direction map, the flow accumulation operation counts the total number of pixels that will drain into outlets. Taking the slope layer and flow accumulation layer and applying the formula below, in the raster calculator, the LS factor was calculated.

$$\mathrm{LS} = \left(\text{Flow accumulation} * \frac{\text{Cell size}}{22.13}\right)^{0.2} * (0.065 + 0.045 * slope\ degree + 0.0065 * (slope)^2) \quad (8)$$

Where,

Flow accumulation denotes the accumulated up slope contributing area for a given cell

LS = combined slope length and slope steepness factor, Cell size = size of grid cell (for this study 30 m), Slope = Slope in degree

3.4.4 Crop management factor (C)

It is the ratio of soil loss from cropped land with specific conditions to the identical tilled continuous fallow (Wischmeier and Smith, 1978). The LULC types and their management are prime aspects for evaluating the sediment yield from a watershed. The crop management factor represents the effect of plants, soil cover, biomass, and activities on the soil surface on soil erosion. The land use type is considered when crop management factors are considered. The C factor ranges from 0 to 1. In the present study, the value of the C factor was assigned according to land use type as depicted in Table 3.5.

Table 3.5: C and P factor values of different land use land cover classes (Ganasari and Ramesh 2016)

Class Name	C- value	P- value
Barren Land	0.500	1.00
Built up	0.090	1.00
Agriculture	0.630	0.50
Waterbody	0	1.00
Plantation	0.003	0.80

3.4.5 Practice factor (P)

The conservation or support factor (P) is basically the ratio of soil loss from a land having specified conservation practices to that from a land ploughed in a direction parallel to the slope if all other conditions remain unchanged (Wischmeier and Smith, 1978).

The support practice factor indicates the rate of soil loss according to the various cultivated lands on the earth. There are contour, cropping, and terrace as its methods, and it is an important factor that can control erosion (Shin, 1999). The P values range from 0 to 1, where the value 0 represents a very good manmade erosion resistance facility and the value 1 represents no manmade erosion resistance facility (Sheikh *et al*., 2011).

In the present study, the value of the P factor was assigned according to land use type as depicted in Table 3.5. The LULC map was also used for the preparation of the P values and P factor map. The raster map of the P factor was prepared by using ArcGIS (Naqvi *et al*., 2013).

3.4.6 Average soil loss

The RUSLE parameters were analyzed using ArcGIS 10.7.1 software and the annual average rate of soil loss (A) of the selected watersheds was calculated for the study area. The calculated RUSLE factors, i.e. the R, K, LS, C& P factors, were imported as raster layers in the GIS environment and multiplied in the raster calculator as per Eq. 5 and the final value of the spatial average of soil loss (A) over a period was obtained. This combination computes the simulated spatial distribution of soil erosion potential for the entire study area.

3.5 Prioritization of watersheds

In order to identify the most erosion prone watersheds, all watersheds were classified into slight, moderate, high, very high, and severe soil erosion classes, with soil loss ranging from 0-5, 5-10, 10-20, 20-40, and >40 t ha^{-1} yr^{-1}, respectively. On the basis of severity, the selected watersheds of the Shivalik foothills in Haryana were prioritized accordingly.

CHAPTER–IV

RESULTS

This chapter includes the presentation of results obtained from the analysis of the assessment of the potential soil loss by RS and GIS techniques to accomplish "Priority areas assessment for soil erosion control in a watershed using geospatial technology in the Shivalik foothills (Haryana)". This methodology is capable in mapping the LULC, morphometric parameters of watersheds, assessment of annual soil loss of the study area. The data obtained through RS acts as a key factor in the delineation of the land cover, having superior accuracy of category and range to estimate the suitable annual cover factors. The integration of the RUSLE with RS and GIS methodology supported the prediction of soil loss at the watershed level. The results are presented under the following heads in this chapter.

4.1 Thematic mapping related to LULC classification of the study area

4.2 Morphometric analysis of study area

4.3 Soil loss estimation using RUSLE on watershed basis

4.4 Priority areas assessment for efficient implementation of soil erosion control program

4.1 Thematic mapping related to LULC classification of the study area

The thematic layers like LULC, slope of land, soil characteristics and RUSLE parameters etc. are important factors in the assessment of spatially changing soil losses. The thematic map displays the relationship of a single component with several other variables and also depicts the range of varied attributes. The thematic map may be either qualitative or quantitative. In a qualitative thematic map, the spatial co-ordinates and distribution of specific features are shown, whereas in a quantitative thematic map, the dimension related numeric information is represented. The common variables which can be mapped thematically could be land use, land cover, elevation, slope, RUSLE parameters etc. were presented in this chapter.

4.1.1 Area distribution of watersheds

The study area in the Shivalik foothills in Haryana was delineated using the globally popular SRTM DEM having with 30 m resolution and ArcGIS 10.7.1 software. The 10 watersheds adjoining the Shivalik foothills and located in three districts (Panchkula, Ambala, and Yamunanagar) irrespective of district administrative boundaries were selected from delineated watershed and designated as study area (WS1 to WS10) and shown in Fig. 4.1. The elevation in all the watersheds varied from 264 to 1541 m. The higher elevated points were observed in WS1, WS2 and WS3 as compared to the remaining watersheds. The elevation map of the study area is presented in Fig 4.2.

WS1 was found to be the smallest watershed, having an area of 65.12 km^2, and WS7 was the largest watershed, having an area of 616.53 km^2. The WS1 and WS7 shared the 2.57% and 24.29% area out of the total area of the selected watersheds respectively. The area occupied by individual watershed was found in the order of WS1<WS5<WS4 <WS6<WS8<WS9<WS2<WS3<WS10<WS7 out of the total area of the selected watersheds. The area distribution of the selected watersheds (WS1 to WS10) in the Shivalik foothills is presented in Table 4.1. The corresponding area (%) covered under selected watersheds is shown in Fig. 4.3.

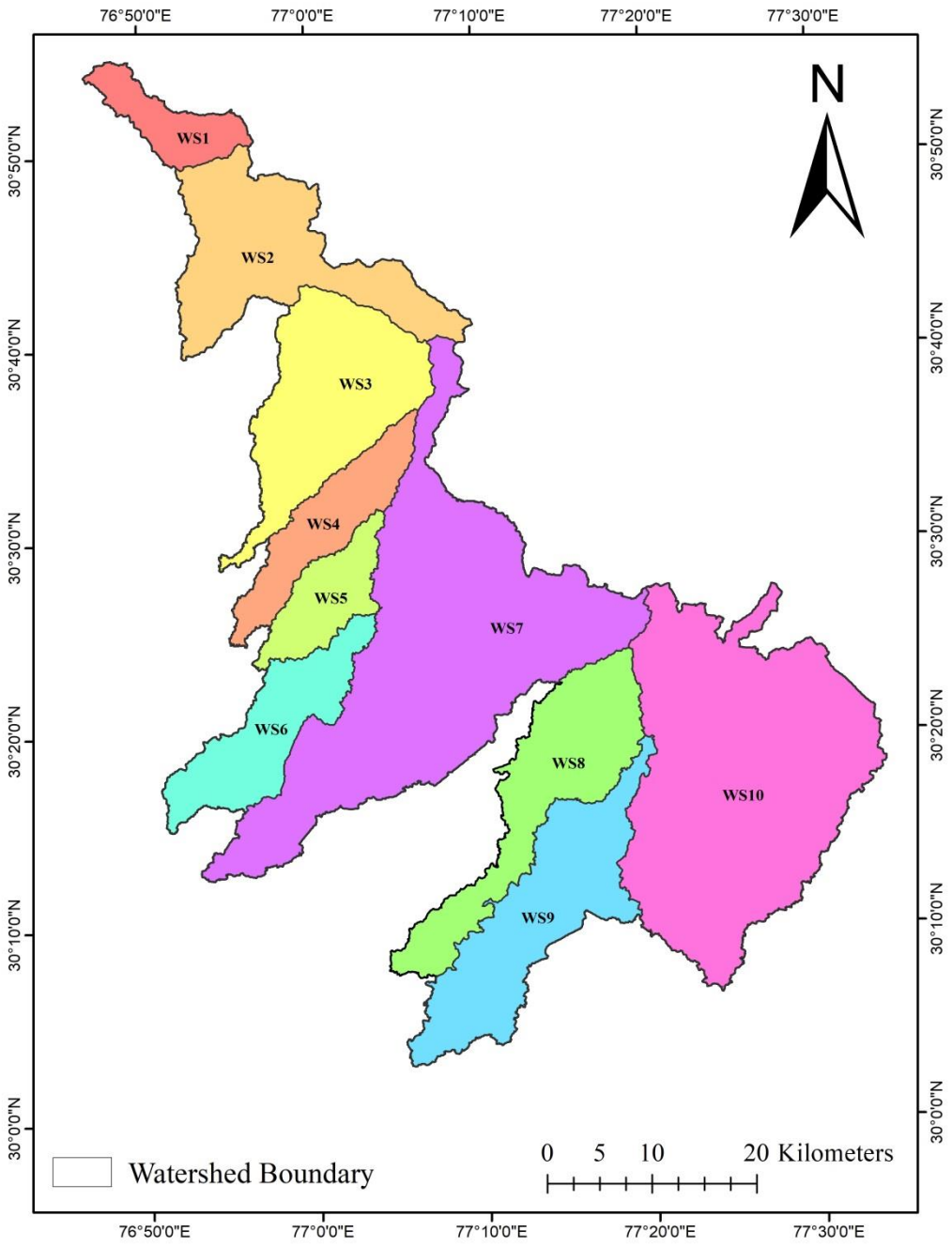

Fig. 4.1: Map of the study area

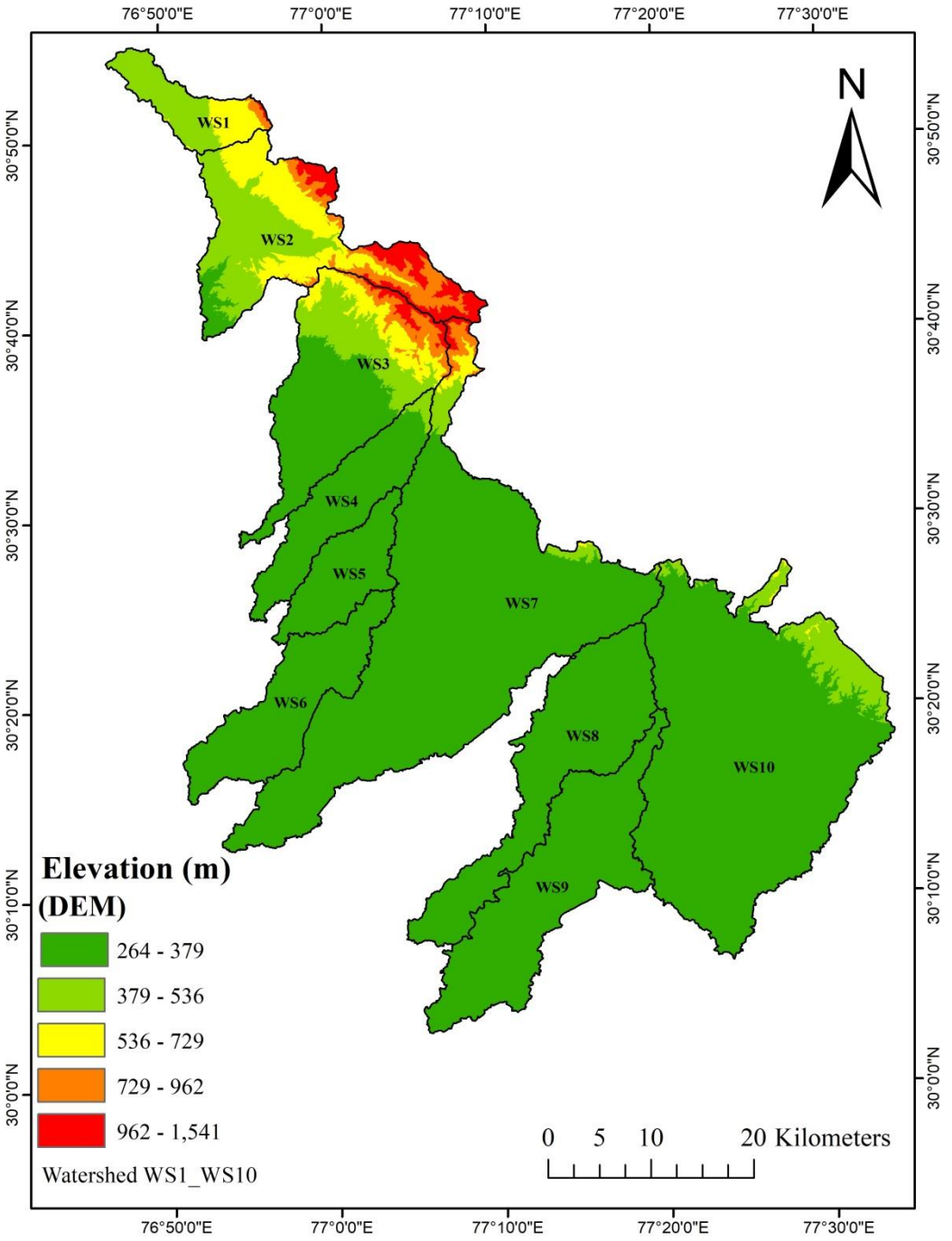

Fig. 4.2: Elevation map of the study area

Table 4.1: Area distribution under selected watersheds in Shivalik foothills

Name of Watershed	Area (km^2)	Area (%)
WS1	65.12	2.57
WS2	236.96	9.34
WS3	241.84	9.53
WS4	111.97	4.41
WS5	80.91	3.19
WS6	142.86	5.63
WS7	616.53	24.29
WS8	210.75	8.30
WS9	233.3	9.19
WS10	597.71	23.55
Total	2537.95	100.00

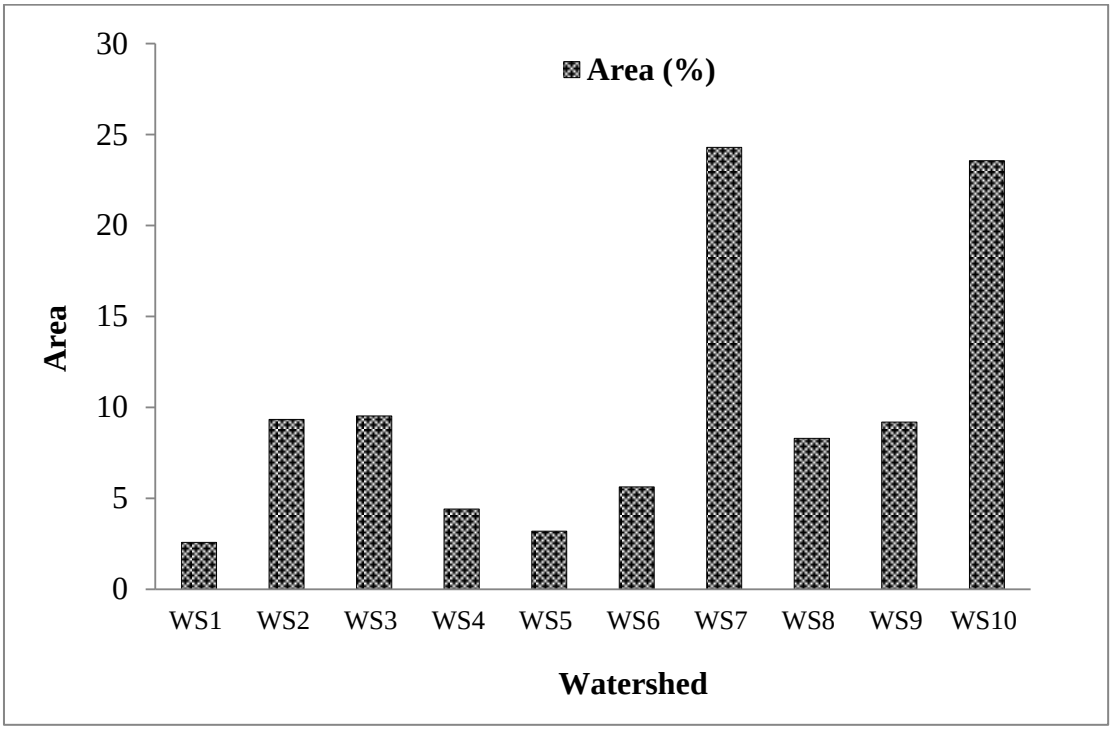

Fig. 4.3: Area (%) under selected watersheds in study area

4.1.2 Land use land cover mapping

The thematic map of LULC of the individual watershed is shown in Fig. 4.4 to Fig 4.13. The LULC map of study area comprises of the selected watersheds is presented in Fig. 4.14. The five major LULC classes were identified in study area i.e. barren land, waterbody, plantation, built up and agriculture. The classification theme used for identification of five major LULC class in the study are presented in Table 3.3. The LULC distribution under barren land, waterbody, plantation, built up class of the whole study area

is given in Table 4.2. The LULC distribution in the study area under barren land, waterbody, plantation, built up and agriculture class was 304.08 km^2, 35.38 km^2, 614.62 km^2, 51.23 km^2 and 1532.64 km^2, respectively, out of total area under each identified class of all the watersheds. The LULC distribution of the study area showed that agriculture was the major class followed by plantation, barran land, built up and waterbody which occupied 60.39%, 24.22%, 11.98%, 2.02% and 1.39% area, respectively, out of total area of all the watersheds.

Table 4.2: Land use land cover distribution of the study area

Class	Land use land cover in 2021	
	Area (km^2)	**Area (%)**
Barren Land	304.08	11.98
Waterbody	35.38	1.39
Plantation	614.62	24.22
Built up	51.23	2.02
Agriculture	1532.64	60.39
Total	2537.95	100.00

The area distribution under LULC classification of watershed WS1, WS2, WS3, WS4, WS5, WS6, WS7, WS8, WS9, and WS10 is given in Table 4.3 to Table 4.12. As per The LULC classification of individual watershed, in WS1 the agriculture class was observed as dominated class followed by plantation while water body has occupied the smallest area as 33.40 km^2, 24.02 km^2 and 0.37 km^2, respectively (Table 4.3). In WS2 the highest area was occupied by plantation class followed by agriculture and lowest area was observed under waterbody as 158.84 km^2, 64.12 km^2 and 1.08 km^2, respectively (Table 4.4). The WS3 has largest area under agriculture class followed by plantation and lowest area was observed under waterbody as 128.90 km^2, 89.45 km^2 and 2.26 km^2, respectively (Table 4.5). In WS4 the largest area was observed under agriculture class followed by plantation and smallest area was under waterbody as 82.77 km^2, 12.94 km^2 and 1.12 km^2, respectively (Table 4.6). The WS5 has the largest area under agriculture as 54.97 km^2 followed by barren land as 13.66 km^2 and smallest area was under waterbody as 0.54 km^2 (Table 4.7). The WS6 has largest area under agriculture followed by barren land and smallest area was noticed under waterbody class as 120.46 km^2, 11.99 km^2 and 2.02 km^2, respectively (Table 4.8). The WS7 has largest area under agriculture class followed by plantation and barren land and smallest area was observed under waterbody as 448.11 km^2, 81.73 km^2, 70.46 km^2 and 5.17 km^2, respectively (Table 4.9). The WS8 has agriculture as dominating class as 145.41 km^2 followed by barren land as 37.58 km^2 and smallest area was found under waterbody as 3.49 km^2 (Table 4.10). The watershed WS9 has largest area under agriculture class followed by barren land and

smallest area was observed under waterbody as 6.06 km^2 (Table 4.11). The agriculture was also dominating land use in WS10 and occupied largest area followed by plantation and smallest area was noticed under waterbody as 281.4 km^2, 194.26 km^2 and 13.27 km^2, respectively (Table 4.12).

The area distribution under identified LULC classes in the all the selected watersheds showed that among all the watersheds, the barren land occupied largest area in watershed WS10 as 95.20 km^2 with 31.31%, and the smallest area was under WS1 as 6.25 km^2 with 2.06% area out of the total area under barren land in all the watersheds. The area under waterbody class was largest in WS10 as 13.27 km^2 with 37.51%, and smallest was observed in WS1 as 0.37 km^2 with 1.05% area out of the total area under waterbody class in all the watersheds. The largest area under plantation was observed in WS10 as 194.26 km^2 with 31.61%, while the smallest area under plantation was in WS6 as 4.56 km^2 with 0.74 % area out of the total area under plantation class of all the watersheds. The largest area under built up class was observed in WS10 as 13.58 km^2 with 26.51%, while the smallest area under built up class was in WS1 as 1.08 km^2 with 2.11% of the total area under built up class of all the watersheds. The largest area under agriculture class was observed in WS7 as 448.11 km^2 with 29.24%, while the smallest area under agriculture class was noticed in WS1 as 33.40 km^2 with 2.18% of the total area under agriculture class of all the watersheds (Table 4.13).

4.1.3 Accuracy assessment

The LULC classification has chances to incur some errors which required accuracy assessment of the developed thematic map through reliable statistical techniques. The precision of LULC classification was defined in terms of the user's exactness and the producer's precision. The LULC categories were checked on the fields with high resolution Google Earth's satellite image. 153 points were drawn at random from classified image, field verifications and Google Earth and verified for accuracy assessment. The user's accuracy is a measure to assess the reliability of the classification to the user and producer's accuracy reflects the accuracy of prediction of the particular class. The kappa coefficient revealed the inter-rate agreement between categorical variables. The user's accuracy ranged from 80% to 100% while producer's accuracy ranged from 75% to 100%. The average user's, producer's, overall accuracies, and kappa coefficient were obtained as 94%, 90.6%, 92%, and 90%, respectively, as shown in Table 4.14. The results obtained in the study are reliable and acceptable for further analysis.

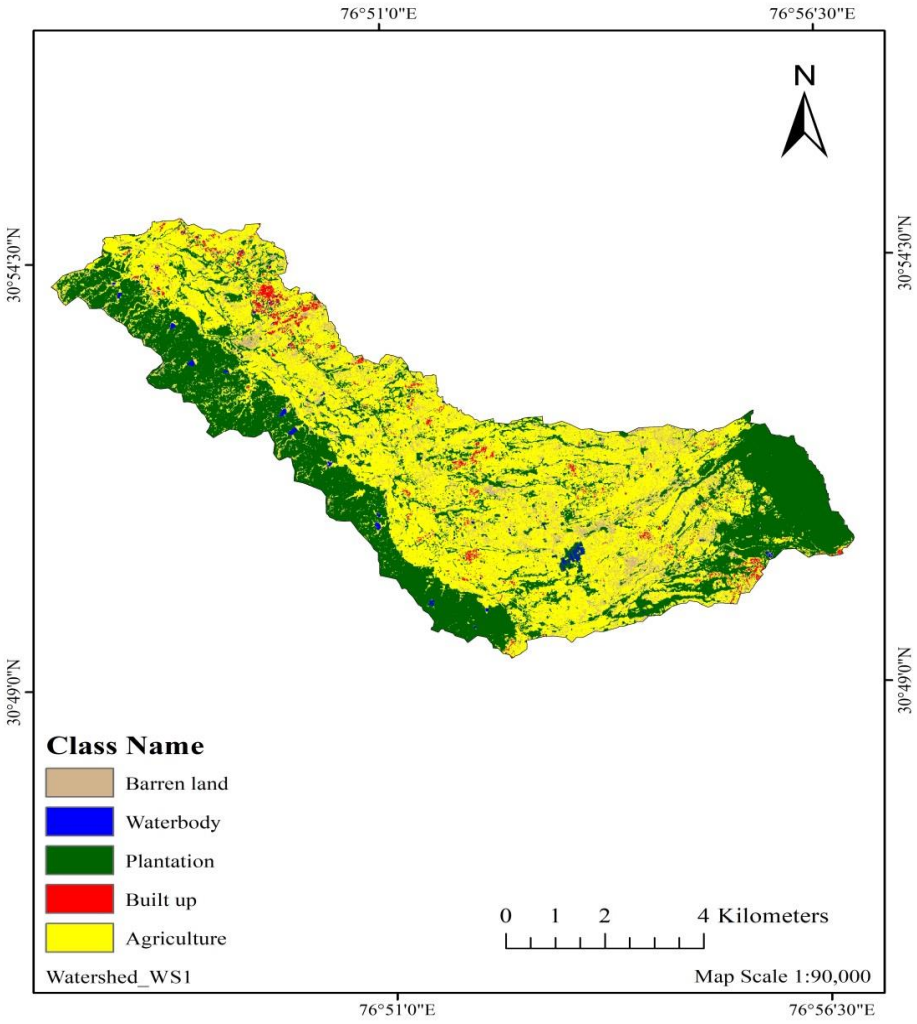

Fig. 4.4: Land use land cover classification map of WS1

Table 4.3: Area distribution under land use land cover classification in WS1

Class	Area (km^2)	Area (%)
Barren land	6.25	9.60
Waterbody	0.37	0.57
Plantation	24.02	36.89
Built up	1.08	1.66
Agriculture	33.40	51.29
Total	65.12	100.00

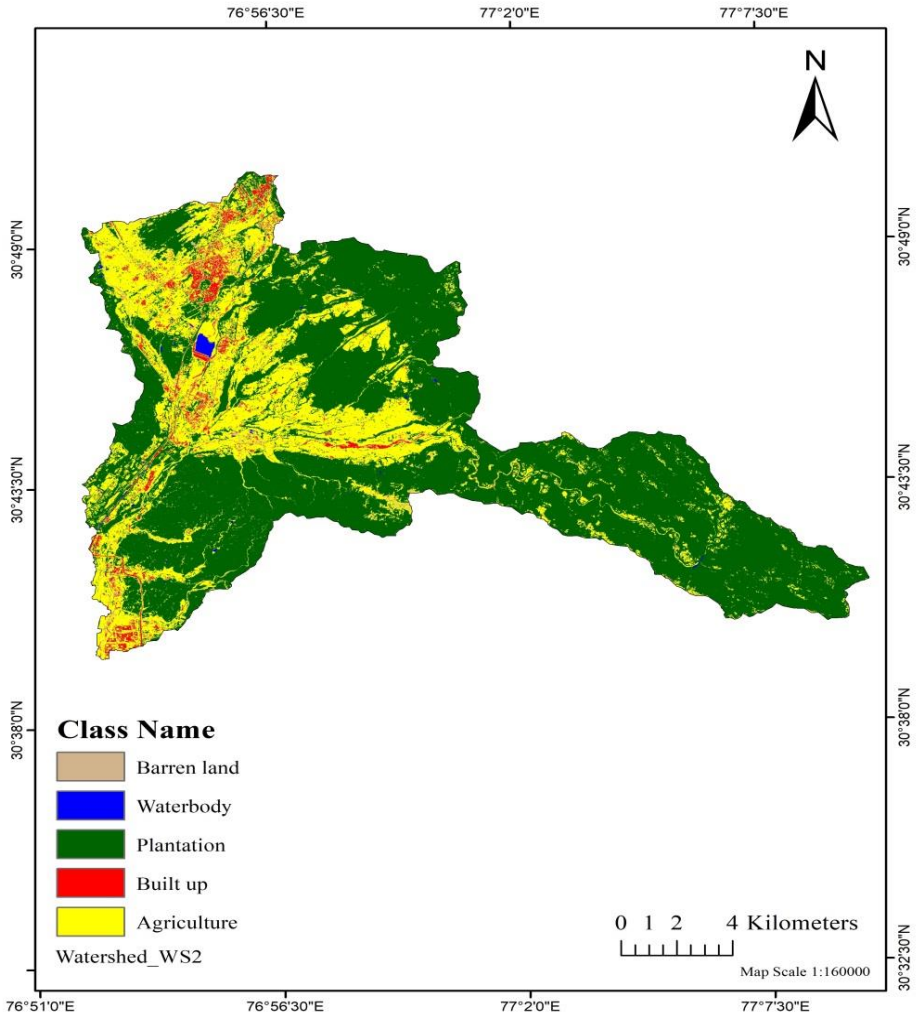

Fig. 4.5: Land use land cover classification map of WS2

Table 4.4: Area distribution under land use land cover classification in WS2

Class	Area (km^2)	Area (%)
Barren land	6.74	2.84
Waterbody	1.08	0.46
Plantation	158.84	67.03
Built up	6.18	2.61
Agriculture	64.12	27.06
Total	236.96	100.00

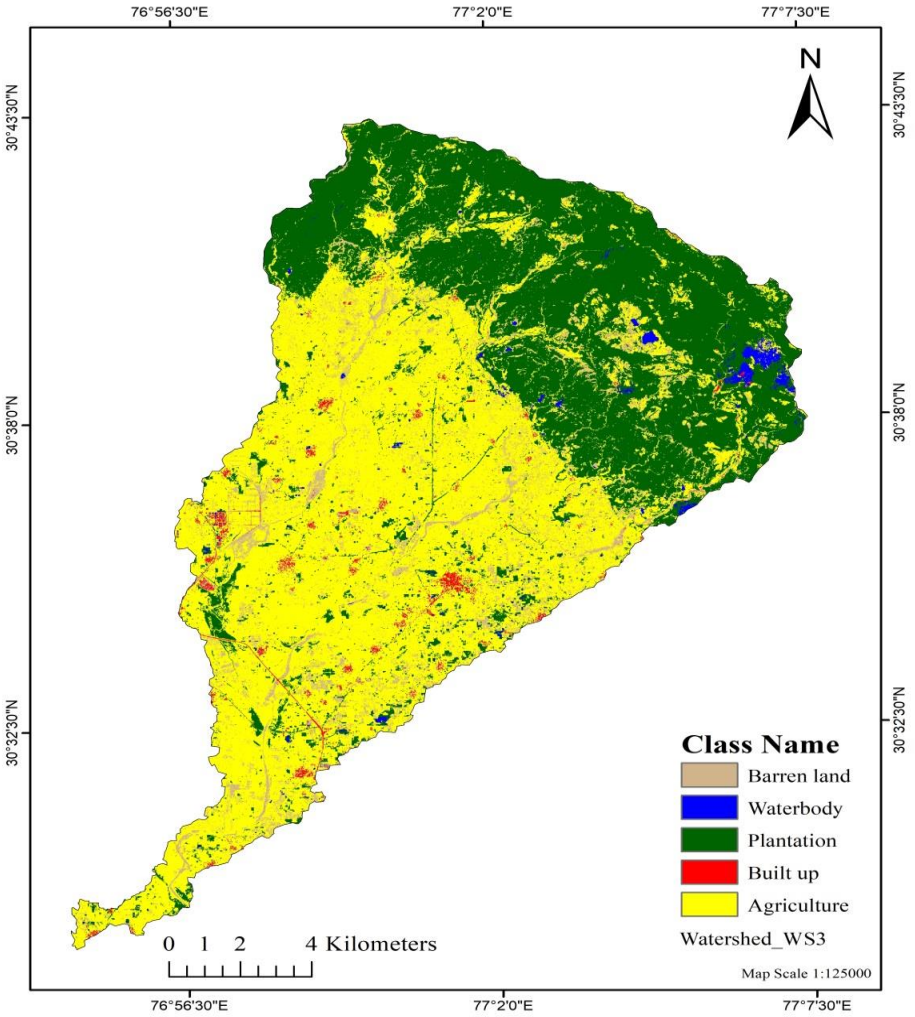

Fig.4.6: Land use land cover classification map of WS3

Table 4.5: Area distribution under land use land cover classification in WS3

Class	Area (km^2)	Area (%)
Barren land	18.88	7.81
Waterbody	2.26	0.93
Plantation	89.45	36.99
Built up	2.35	0.97
Agriculture	128.90	53.30
Total	241.84	100.00

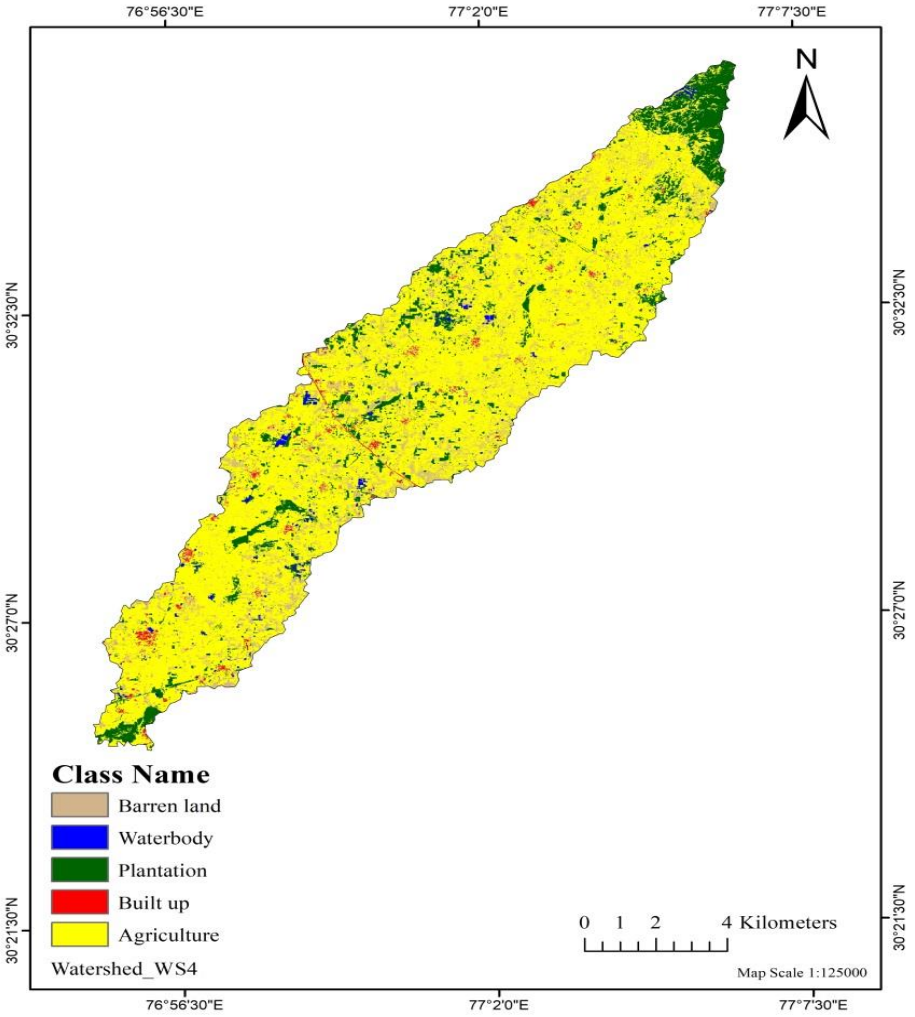

Fig. 4.7: Land use land cover classification map of WS4

Table 4.6: Area distribution under land use land cover classification in WS4

Class	Area (km^2)	Area (%)
Barren land	13.9	12.41
Waterbody	1.12	1.00
Plantation	12.94	11.56
Built up	1.24	1.11
Agriculture	82.77	73.92
Total	111.97	100.00

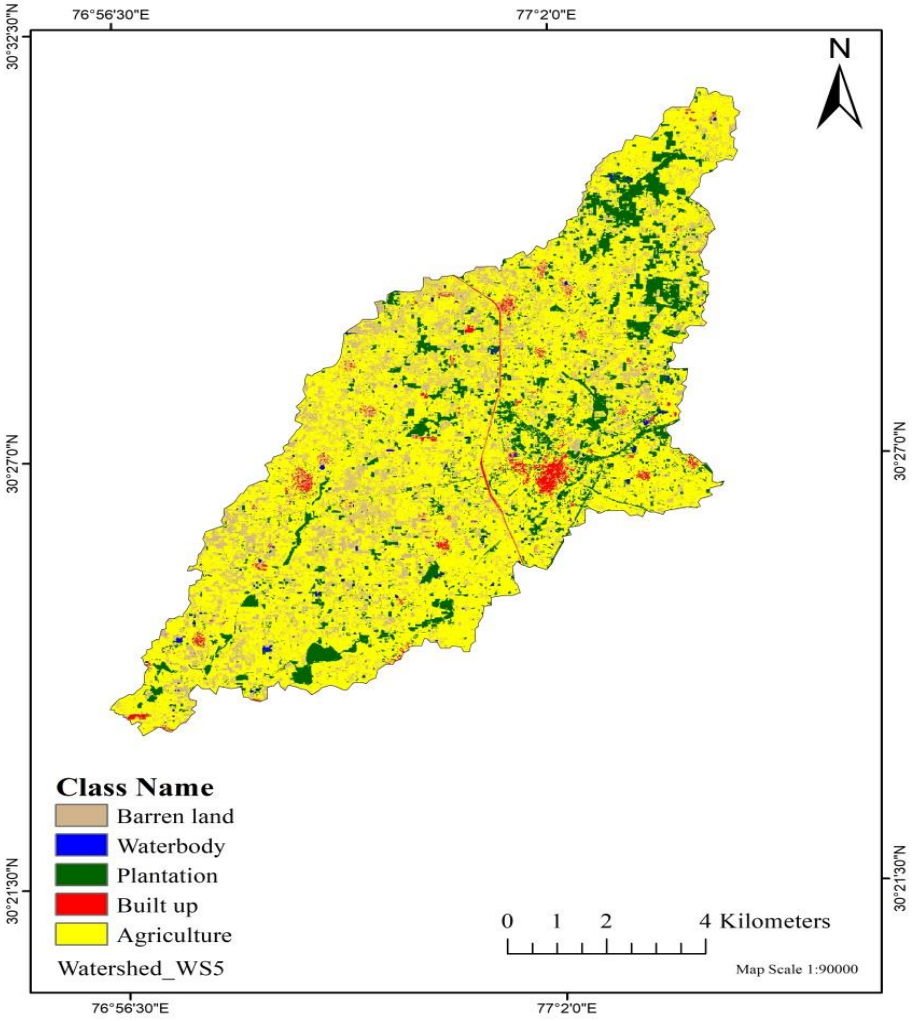

Fig. 4.8: Land use land cover classification map of WS5

Table 4.7: Area distribution under land use land cover classification in WS5

Class	Area (km^2)	Area (%)
Barren land	13.66	16.88
Waterbody	0.54	0.67
Plantation	10.41	12.87
Built up	1.33	1.64
Agriculture	54.97	67.94
Total	80.91	100.00

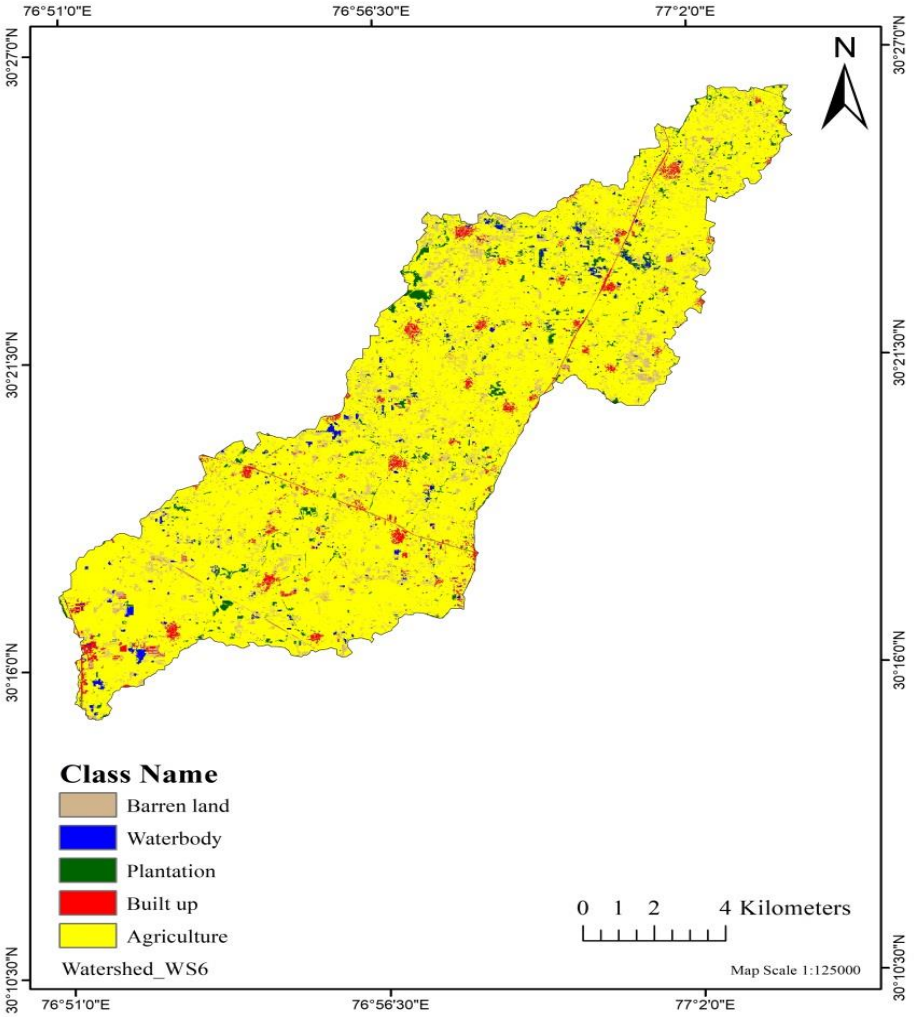

Fig. 4.9: Land use land cover map of WS6

Table 4.8: Area distribution under land use land cover classification in WS6

Class	Area (km^2)	Area (%)
Barren land	11.99	8.39
Waterbody	2.02	1.41
Plantation	4.56	3.19
Built up	3.83	2.68
Agriculture	120.46	84.32
Total	142.86	100.00

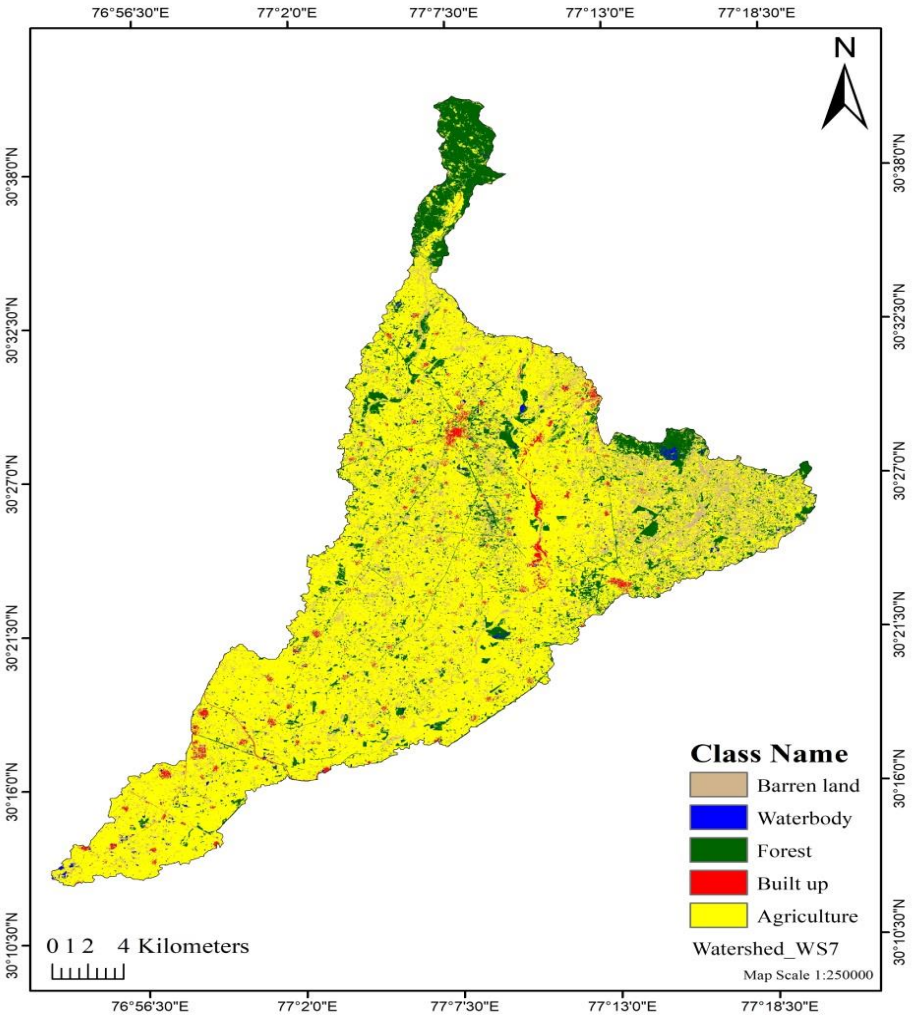

Fig. 4.10: Land use land cover classification map of WS7

Table 4.9: Area distribution under land use land cover classification in WS7

Class	Area (km^2)	Area (%)
Barren land	70.46	11.43
Waterbody	5.17	0.84
Plantation	81.73	13.26
Built up	11.06	1.79
Agriculture	448.11	72.68
Total	616.53	100.00

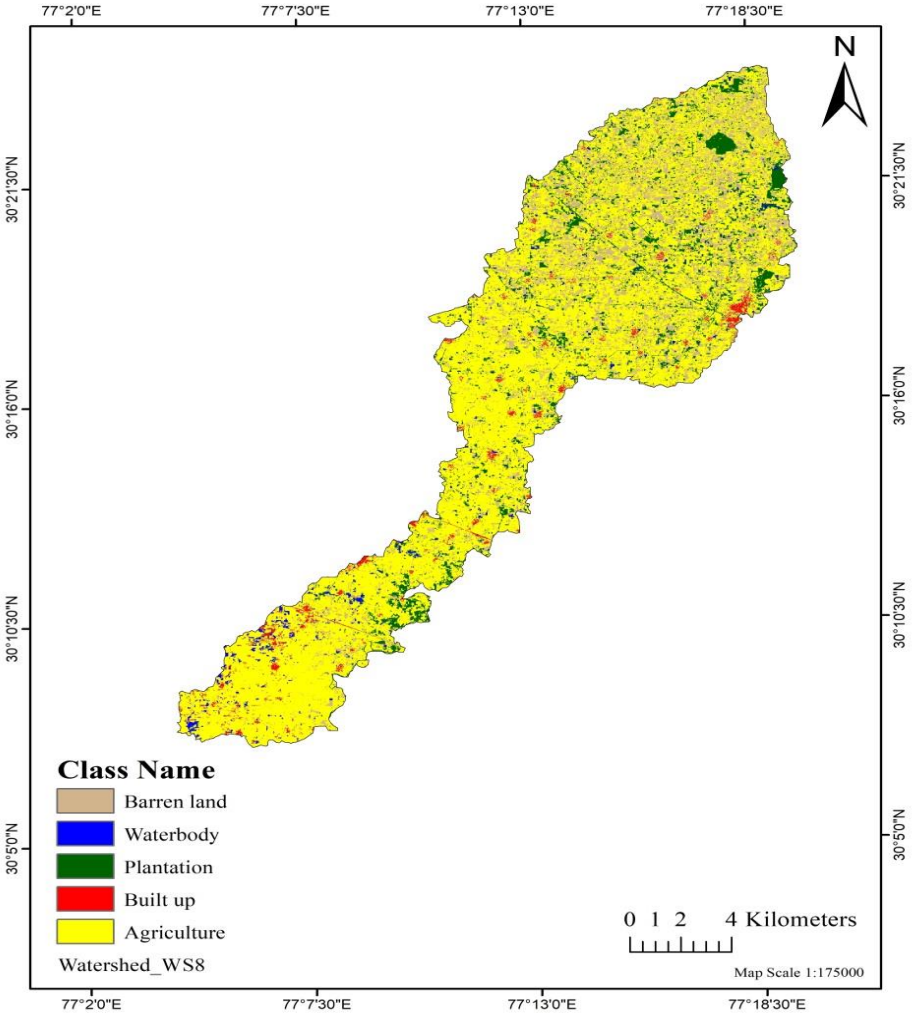

Fig. 4.11: Land use land cover classification map of WS8

Table 4.10: Area distribution under land use land cover classification in WS8

Class	Area (km^2)	Area (%)
Barren land	37.58	17.83
Waterbody	3.49	1.66
Plantation	20.47	9.71
Built up	3.8	1.80
Agriculture	145.41	69.00
Total	210.75	100.00

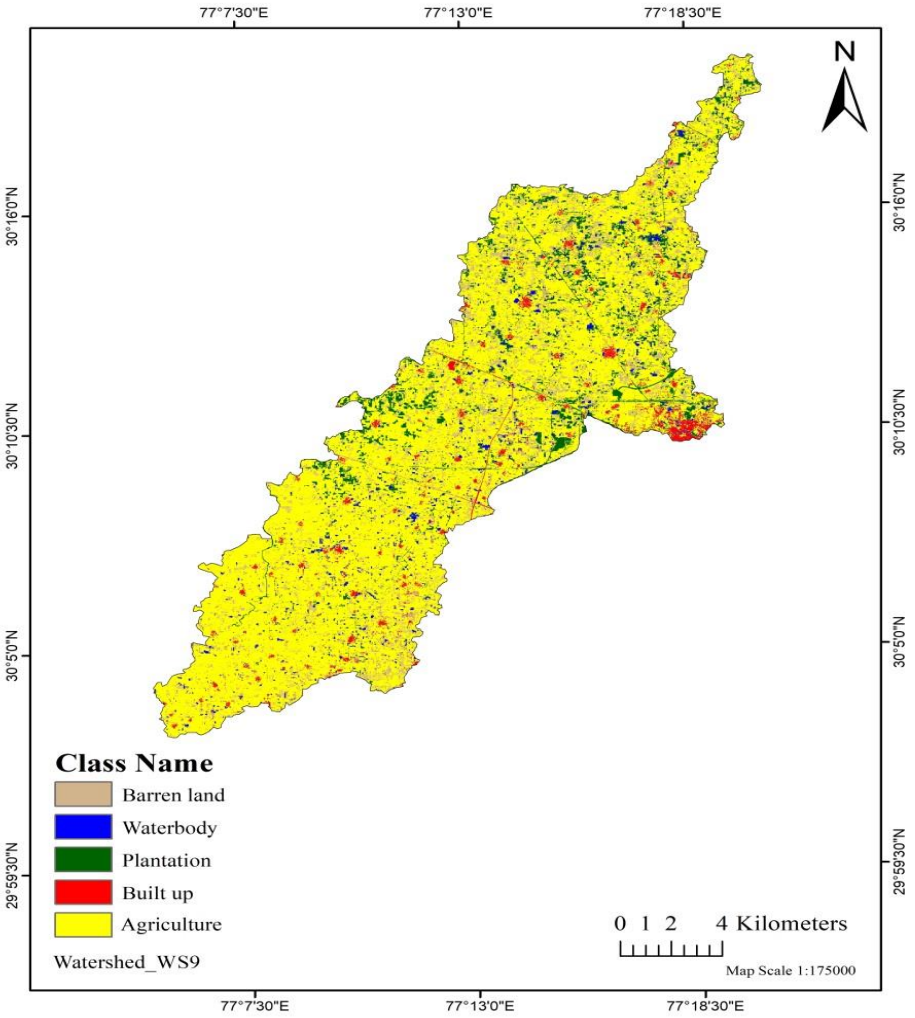

Fig. 4.12: Land use land cover classification map of WS9

Table 4.11: Area distribution under land use land cover classification in WS9

Class	Area (km^2)	Area (%)
Barren land	29.42	12.61
Waterbody	6.06	2.60
Plantation	17.94	7.69
Built up	6.78	2.91
Agriculture	173.1	74.20
Total	233.3	100.00

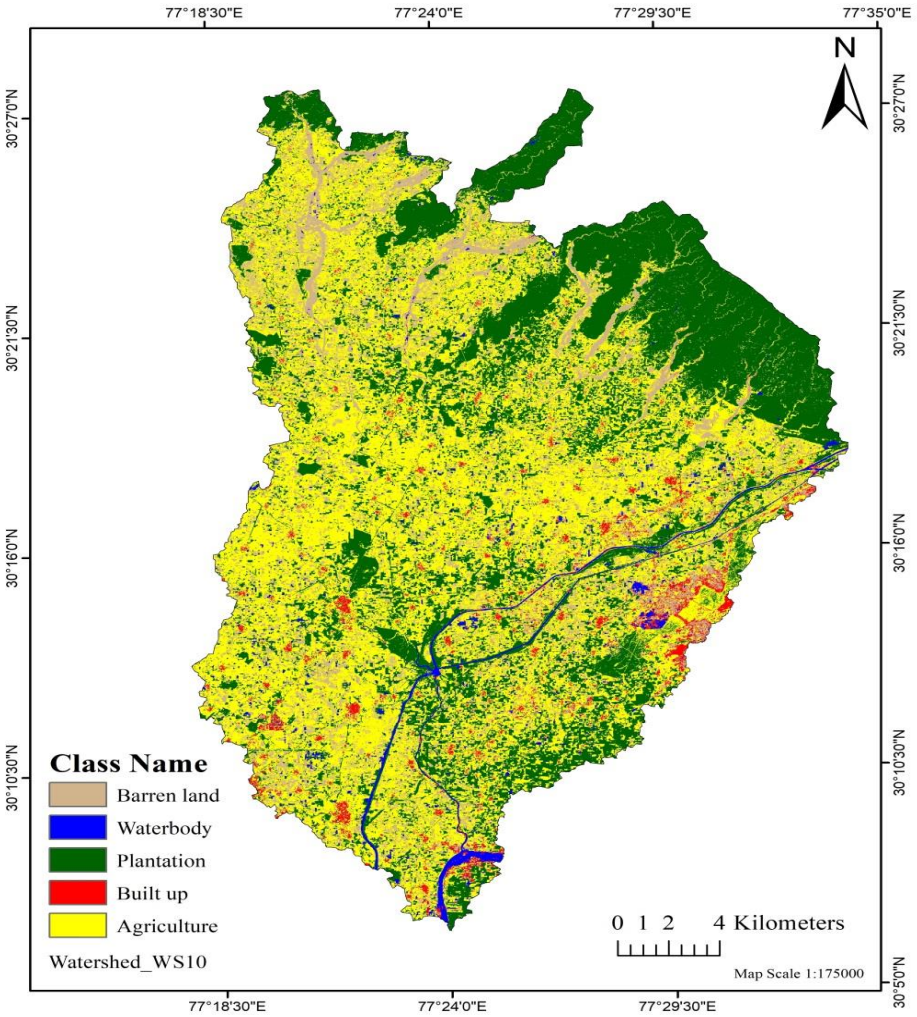

Fig. 4.13: Land use land cover classification map of WS10

Table 4.12: Area distribution under land use land cover classification in WS10

Class	Area (km^2)	Area (%)
Barren land	95.2	15.93
Waterbody	13.27	2.22
Plantation	194.26	32.50
Built up	13.58	2.27
Agriculture	281.4	47.08
Total	597.71	100.00

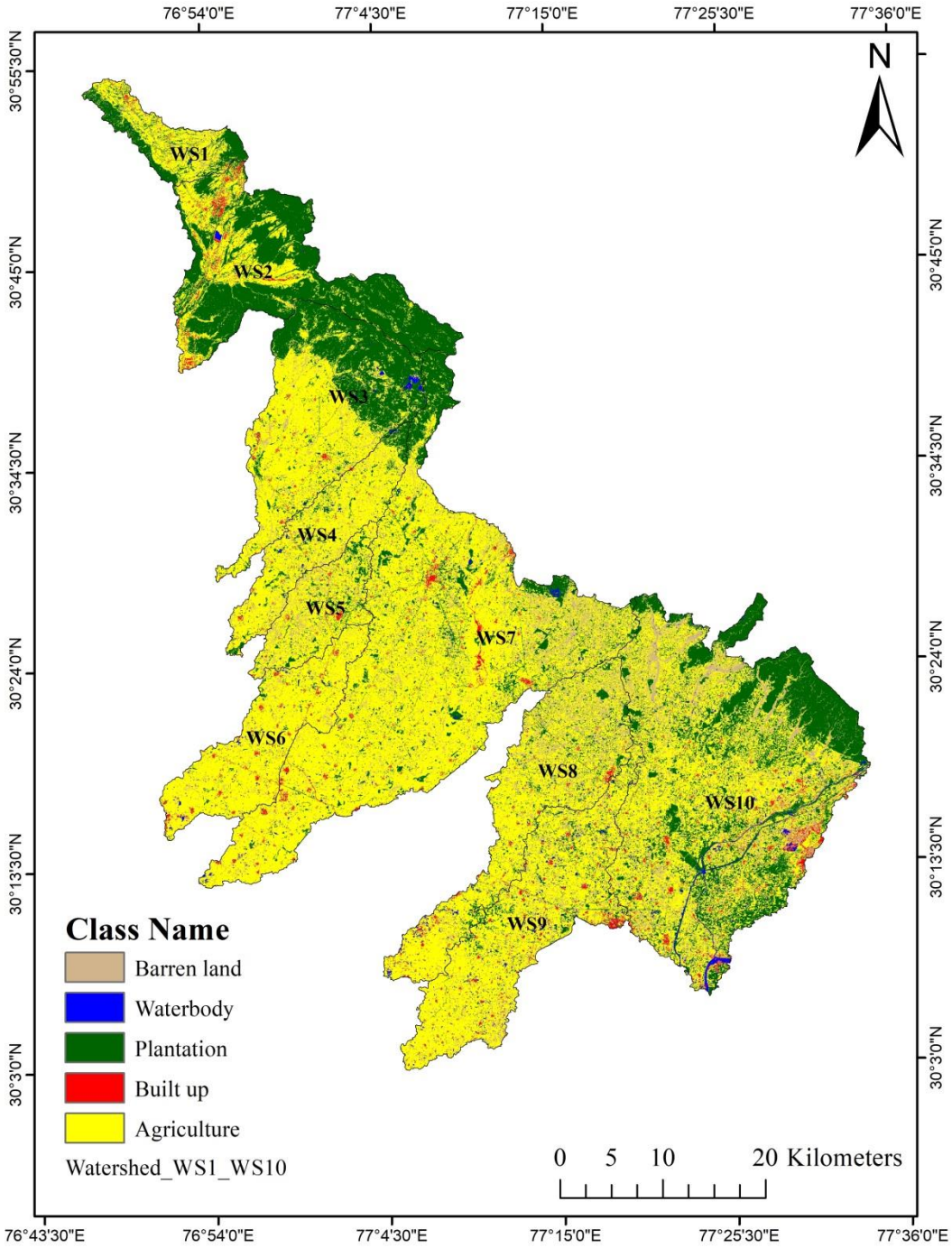

Fig. 4.14: Land use land cover classification map of study area

Table 4.13: Area distribution under land use land cover classification of the selected watersheds in Shivalik foothills

Name of watershed	Class									
	Barren Land		Waterbody		Plantation		Built up		Agriculture	
	Area (km^2)	Area (%)	Area (km^2)	Area (%)	Area (km^2)	Area (%)	Area (km^2)	Area (%)	Area (km^2)	Area (%)
WS1	6.25	2.06	0.37	1.05	24.02	3.91	1.08	2.11	33.40	2.18
WS2	6.74	2.22	1.08	3.05	158.84	25.84	6.18	12.06	64.12	4.18
WS3	18.88	6.21	2.26	6.39	89.45	14.55	2.35	4.59	128.9	8.41
WS4	13.90	4.57	1.12	3.17	12.94	2.11	1.24	2.42	82.77	5.40
WS5	13.66	4.49	0.54	1.53	10.41	1.69	1.33	2.60	54.97	3.59
WS6	11.99	3.94	2.02	5.71	4.56	0.74	3.83	7.48	120.46	7.86
WS7	70.46	23.17	5.17	14.61	81.73	13.30	11.06	21.59	448.11	29.24
WS8	37.58	12.36	3.49	9.86	20.47	3.33	3.80	7.42	145.41	9.49
WS9	29.42	9.68	6.06	17.13	17.94	2.92	6.78	13.23	173.1	11.29
WS10	95.20	31.31	13.27	37.51	194.26	31.61	13.58	26.51	281.40	18.36
Total	304.08	100.00	35.38	100.00	614.62	100.00	51.23	100.00	1532.64	100.00

Table 4.14: Accuracy assessment of land use land cover classification

Class	Plantation	Agriculture	Waterbody	Built up	Barren land	Total	User's Accuracy
Plantation	**30**	0	0	0	0	30	100
Agriculture	0	**30**	0	0	0	30	100
Waterbody	0	3	**27**	0	3	33	90
Built up	0	0	0	**30**	0	30	100
Barren land	0	0	6	0	**24**	30	80
Total	30	33	33	30	27	**153**	94%
Producer Accuracy (%)	100	90	75	100	88		
Overall Accuracy = 92 %							
Kappa Coefficient= 90 %							

4.2 Morphometric analysis of study area

The morphometric analysis of the study area is presented in following sections:

4.2.1 Stream order (μ), stream length (L_μ) and stream number (N_μ)

The study area has been divided into ten watershed namely as WS1 to WS10. The highest order of stream was observed as 6^{th} in the selected watersheds. The basic parameters of the selected watersheds are shown in Table 4.15. It showed that WS7 and WS10 both have highest order of stream as 6^{th} order whereas WS1, WS4 and WS8 have only 4^{th} order streams. The rest of watersheds as shown in the table have 5^{th} order of streams. The maximum number of 1^{st} order streams was observed in WS7 as 813 whereas minimum number of 1^{st} order streams was observed in WS1 as 89. The maximum number of 2^{nd} order streams was observed in as 164 in both WS7 and WS10 whereas minimum number of 2^{nd} order streams was observed in WS1 as 17. The maximum number of 3^{rd} order streams was observed in WS10 as 32 whereas minimum number of 3^{rd} order streams was observed in WS1 as 3. In all the watersheds the stream length (L_μ) is higher for 1^{st} order stream. The maximum number of 4^{th} order streams was observed in WS10 as 8 whereas minimum number of 4^{th} order streams was observed in WS1, WS4 and WS8 as 1 only. The maximum number of 5^{th}order streams was observed in WS7 and WS10 as 2 whereas minimum number of 5^{th} order streams was observed in WS2, WS3, WS5, WS6 and WS9 as 1 only. The two watershed i.e. WS 7 and WS1 have 6^{th} order streams with only one in number.

Table 4.15: Basic parameters of selected watersheds

Watershed		Stream order (μ)					
		I	**II**	**III**	**IV**	**V**	**VI**
WS1	Stream number (N_μ)	89	17	3	1	-	-
	Stream length (L_μ)	70.77	37.12	8.05	9.42	-	-
WS2	Stream number (N_μ)	271	57	13	4	1	-
	Stream length (L_μ)	192.72	109.00	49.37	36.07	14.78	-
WS3	Stream number (N_μ)	298	63	15	2	1	-
	Stream length (L_μ)	193.50	108.13	71.00	33.35	12.31	-
WS4	Stream number (N_μ)	144	30	6	1	-	-
	Stream length (L_μ)	97.37	47.69	20.92	24.37	-	-
WS5	Stream number (N_μ)	104	18	4	2	1	-
	Stream length (L_μ)	63.30	39.08	6.67	17.32	2.12	-
WS6	Stream number (N_μ)	183	36	7	2	1	-
	Stream length (L_μ)	122.77	62.68	44.91	17.76	2.78	-
WS7	Stream number (N_μ)	813	164	30	7	2	1
	Stream length (L_μ)	520.35	260.14	152.74	69.81	31.28	21.54
WS8	Stream number (N_μ)	284	62	12	1	-	-
	Stream length (L_μ)	182.90	80.46	58.63	35.87	-	-
WS9	Stream number (N_μ)	313	72	16	4	1	-
	Stream length (L_μ)	203.90	92.61	60.12	17.40	30.26	-
WS10	Stream number (N_μ)	758	164	32	8	2	1
	Stream length (L_μ)	512.39	282.46	170.770	63.60	38.24	11.73

The stream order maps of the selected watershed have been presented in Fig. 4.15 to 4.24. The different streams on the map were represented by the different colour compositions. The different stream order (μ) in the thematic map is represented by the separate coloured line The thematic maps clearly showed that the streams of different orders in the respective watersheds join the stream of highest order to accomplish the flow.

Table 4.16: Mean stream length (L_{sm}) of selected watersheds based on stream order (μ)

Watershed	Mean stream length (L_{sm})					
	I	II	III	IV	V	VI
WS1	0.80	2.18	2.68	9.42	0	0
WS2	0.71	1.91	3.80	9.02	14.78	0
WS3	0.65	1.72	4.73	16.68	12.31	0
WS4	0.68	1.59	3.49	24.37	0	0
WS5	0.61	2.17	1.67	8.66	2.12	0
WS6	0.67	1.74	6.42	8.88	2.78	0
WS7	0.64	1.64	5.09	9.97	15.64	21.54
WS8	0.64	1.30	4.89	35.87	0	0
WS9	0.65	1.29	3.76	4.35	30.26	0
WS10	0.68	1.72	5.34	7.95	19.12	11.73

Table 4.17: Stream length ratio (R_L) of selected watersheds

Watershed	Stream length ratio (R_L)				
	I-II	II-III	III-IV	IV-V	V-VI
WS1	0.52	0.22	1.17	0.00	0.00
WS2	0.57	0.45	0.73	0.41	0.00
WS3	0.56	0.66	0.47	0.37	0.00
WS4	0.49	0.44	1.16	0.00	0.00
WS5	0.62	0.17	2.60	0.12	0.00
WS6	0.51	0.72	0.40	0.16	0.00
WS7	0.52	0.57	0.46	0.45	0.69
WS8	0.44	0.73	0.00	0.00	0.00
WS9	0.45	0.65	0.29	1.74	0.00
WS10	0.55	0.60	0.37	0.60	0.31

Table 4.18: Bifurcation ratio (R_b) of selected watersheds

Watershed	Bifurcation ratio (R_b)				
	I-II	II-III	III-IV	IV-V	V-VI
WS1	5.24	5.67	3.00	0.00	0
WS2	4.75	4.38	3.25	4.00	0
WS3	4.73	4.20	7.50	2.00	0
WS4	4.80	5.00	6.00	0.00	0
WS5	5.78	4.50	2.00	2.00	0
WS6	5.08	5.14	3.50	2.00	0
WS7	4.96	5.47	4.29	3.50	2
WS8	4.58	5.17	12.00	0.00	0
WS9	4.35	4.50	4.00	4.00	0
WS10	4.62	5.13	4.00	4.00	2

The stream length is a characteristics property related to drainage network component of drainage basin (Strahler, 1964). The mean stream length (L_{sm}) based on stream order (μ) of different watersheds (WS1 to WS10) had the different values and it showed that higher the stream order longer the length of stream (Table 4.16). The L_{sm} value is directly proportional to the size and topography of the basin (Rai *et al*., 2017). In the selected watersheds the WS8 has the highest average L_{sm} as 10.67 km. The average L_{sm} in all the watersheds (WS1 to WS10) ranged from 3.05 to 10.67 km (Table 4.19).

The stream length ratio (R_L) is ratio of the mean stream length (L_{sm}) of the one order to the next lower order of stream segment. The R_L between selected watershed WS1 to WS10 for stream order I-II, II-III, III-IV, IV-V and V-VI was ranged from 0.44 to 0.62, 0.17 to 0.73, 0.29 to 2.60, 0.12 to 1.74 and 0.31 to 0.69 (Table 4.17).

The mean bifurcation ratio (R_{bm}) of the selected watersheds (WS1 to WS10) was ranged from 3.93 to 7.25 for watershed WS1 to WS10 (Table 4.19). Individually on the basis of stream orders, WS5, WS1, WS8 has highest bifurcation ratio (R_b) as 5.78, 5.67 and 12.00 for order I-II, II-III and III-IV respectively (Table 4.18). The watershed WS2, WS9, WS10 has highest and equal R_b as 4.00 for the order IV-V. The WS7 and WS10 have highest R_b as 2.00 for order V-VI.

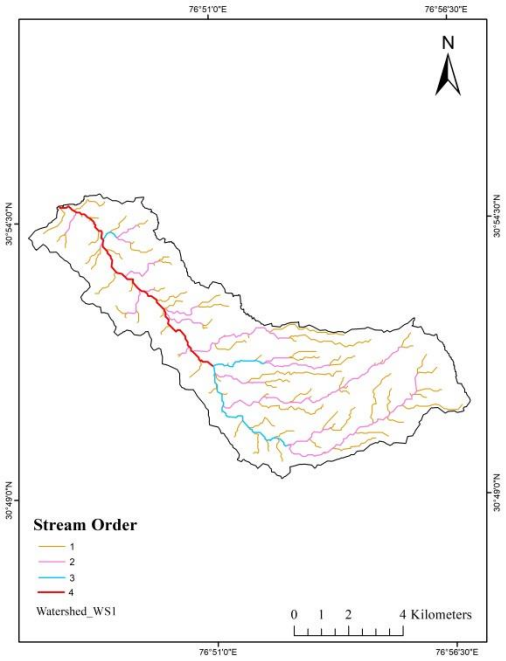

Fig. 4.15: Stream order map of WS1

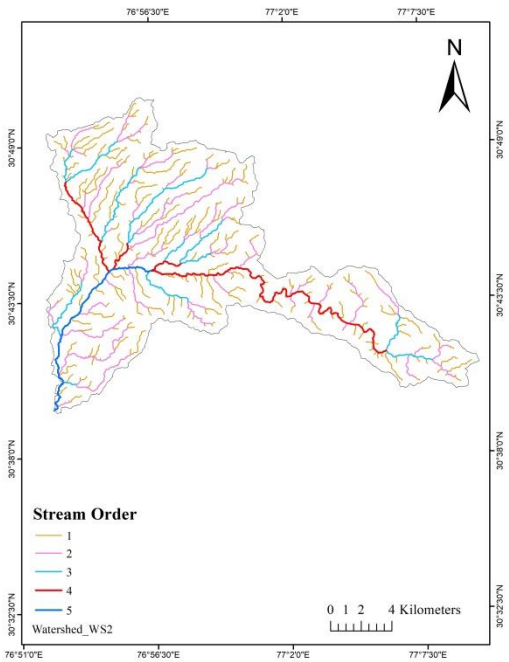

Fig. 4.16: Stream order map of WS2

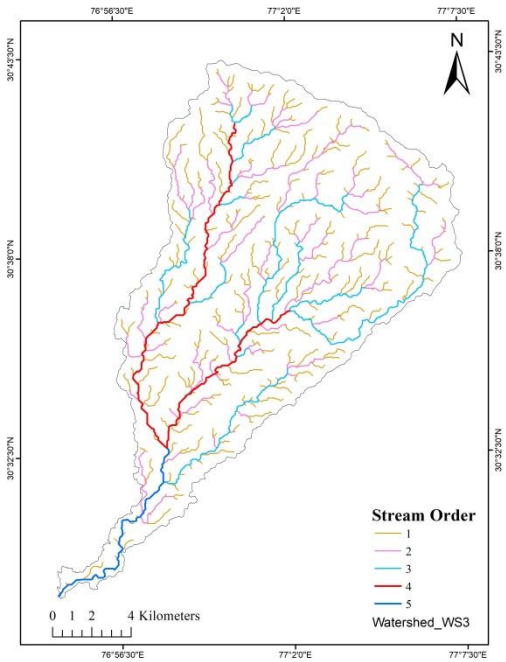

Fig: 4.17: Stream order map of WS3

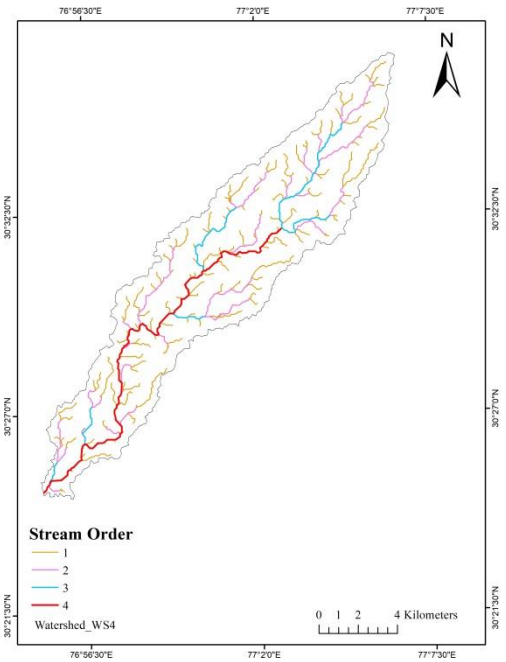

Fig. 4.18: Stream order map of WS4

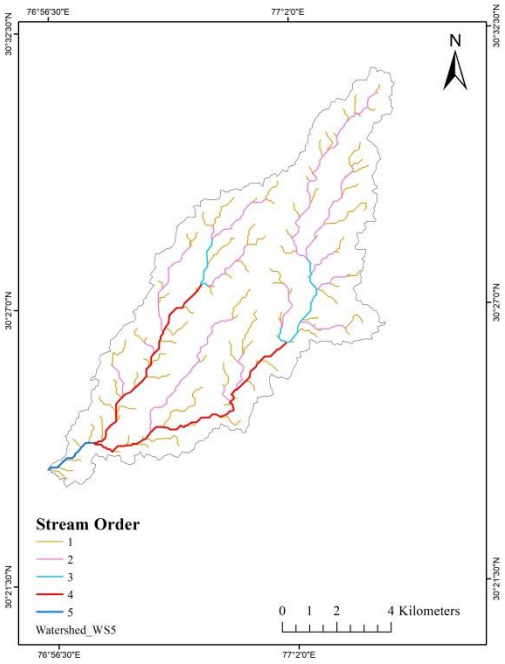

Fig. 4.19: Stream order map of WS5

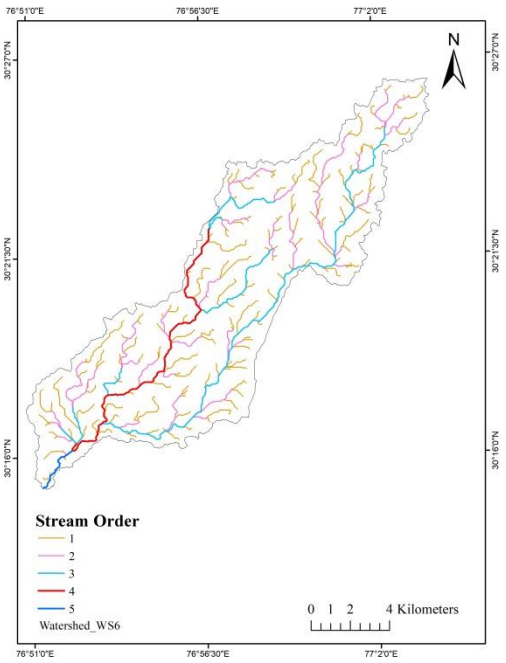

Fig. 4.20: Stream order map of WS6

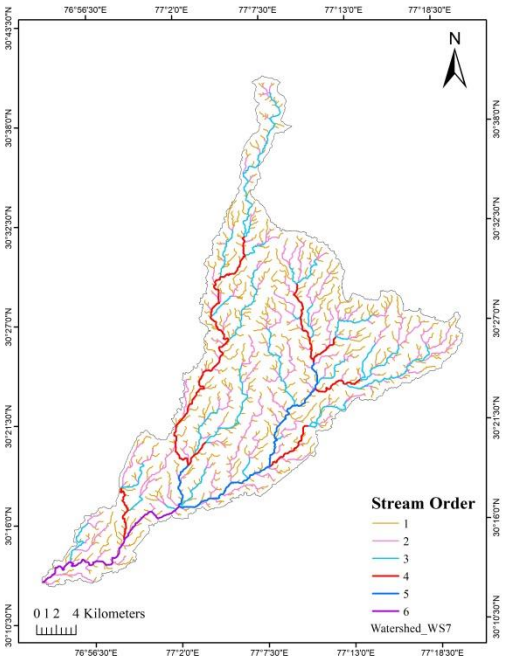

Fig. 4.21: Stream order map of WS7

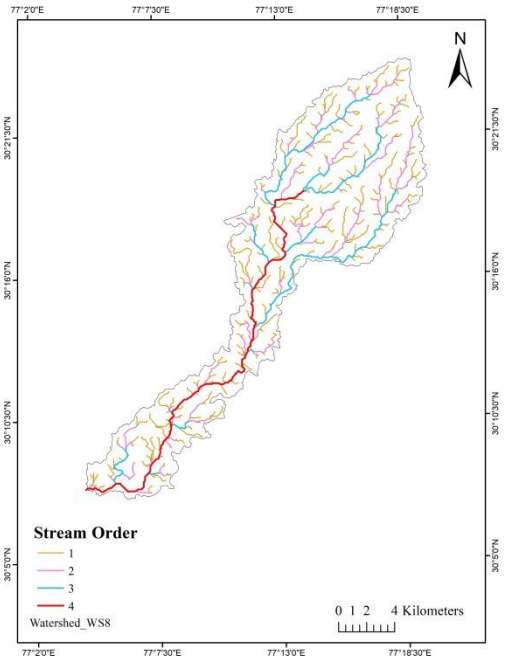

Fig. 4.22: Stream order map of WS8

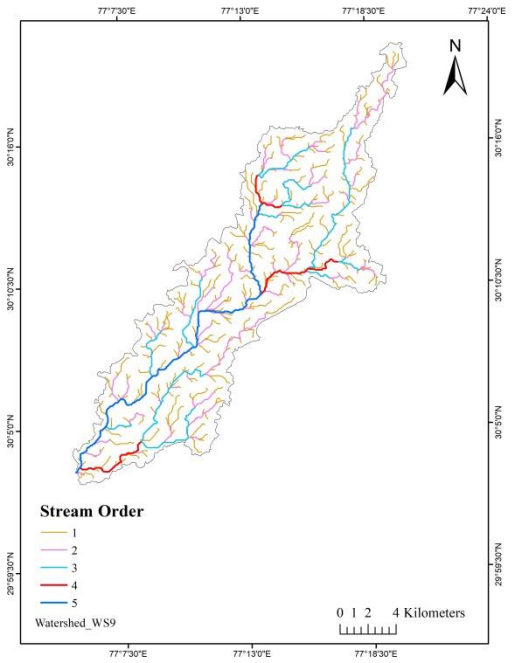

Fig. 4.23: Stream order map of WS9

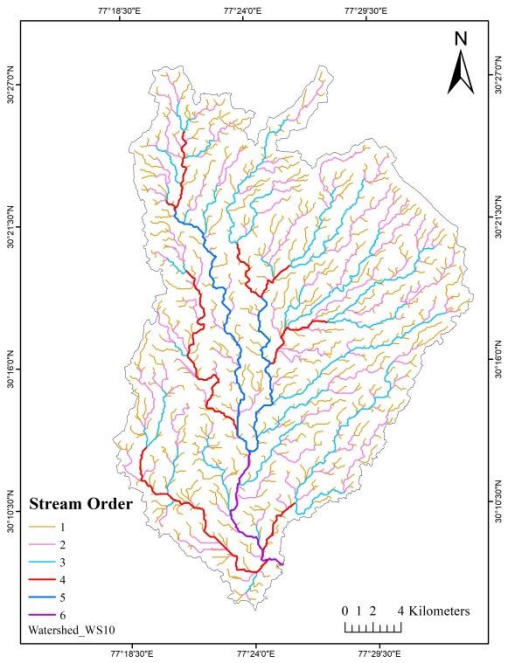

Fig. 4.24: Stream order map of WS10

The stream order map of the Shivalik region, comprising the selected watersheds of study area, has been shown in Fig. 4.25 which clearly showed that study area has 6th order as highest order of stream. Fig. 4.26 showed the drainage density (D_d) map of selected watersheds in the Shivalik foothills region. The D_d indicated the length of the stream per unit area in the selected watershed, and it ranged from 0.29 km/km^2 to 6.03 km/km^2.

4.2.2 Drainage network

The drainage network of the selected watershed is shown in Table 4.19. The table showed watershed wise values of total no. of streams (N_μ), total stream length (L_u), mean stream length (L_{sm}), stream length ratio (R_L), and mean bifurcation ratio (R_{bm}). The WS 7 has the maximum total N_μ, i.e. 1017, and WS 10 has the maximum total L_μ, i.e. 1079.19 km, whereas WS1 has the minimum total N_μ, as well as minimum total L_μ, i.e., 110 and 125.36 km, respectively. The total L_{sm} of the respective watersheds as depicted in the Table 4.19 showed that WS8 has a maximum value of 10.67 whereas WS5 has a minimum value (3.05). The WS6 has a minimum value of average R_L of 0.44, whereas the WS5 has the highest average R_L of 0.88. According to the tabulated values, WS5 has the lowest R_{bm} as 3.57, while WS8 has the highest R_{bm} 7.25.

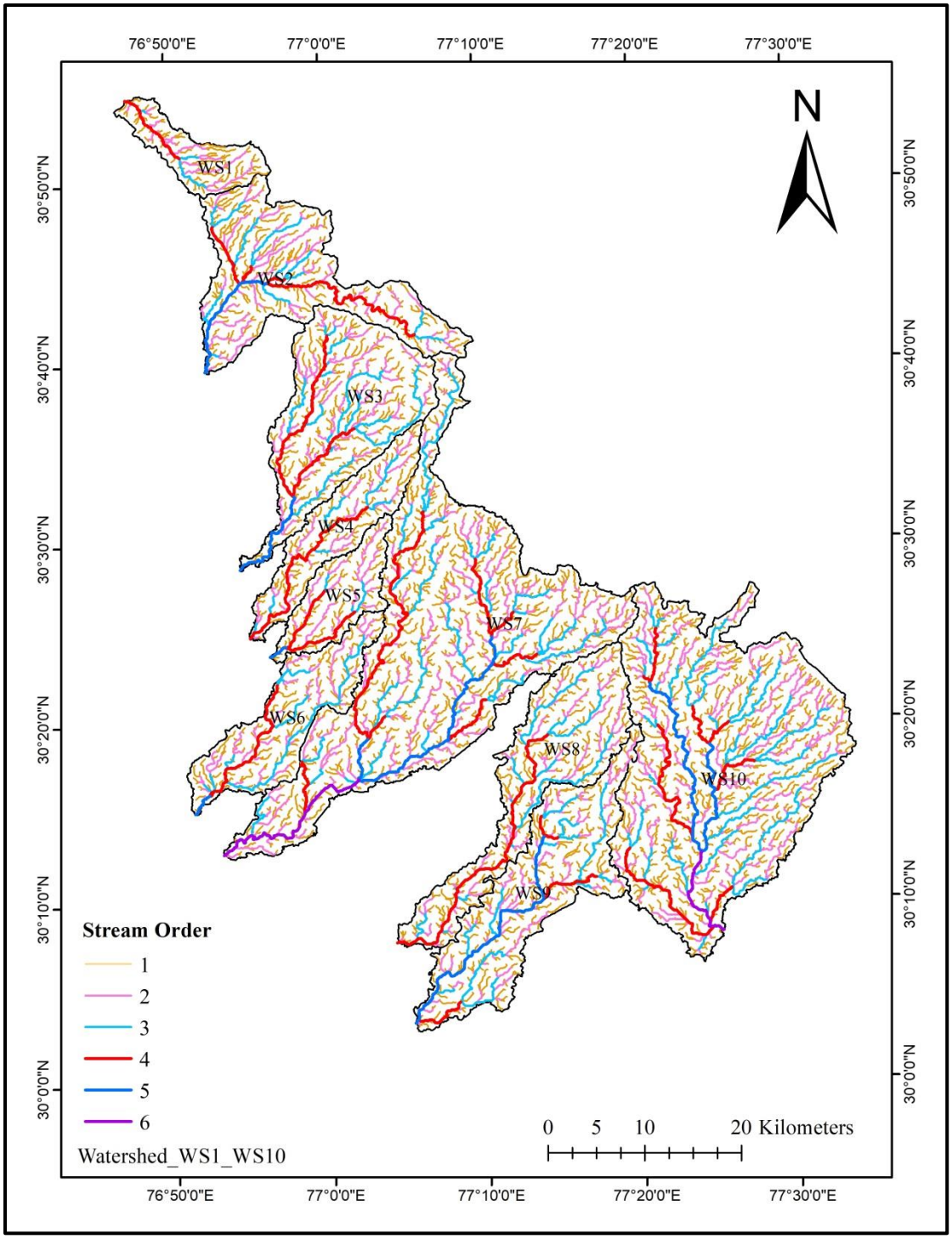

Fig. 4.25: Stream order map of selected watersheds of Shivalik region

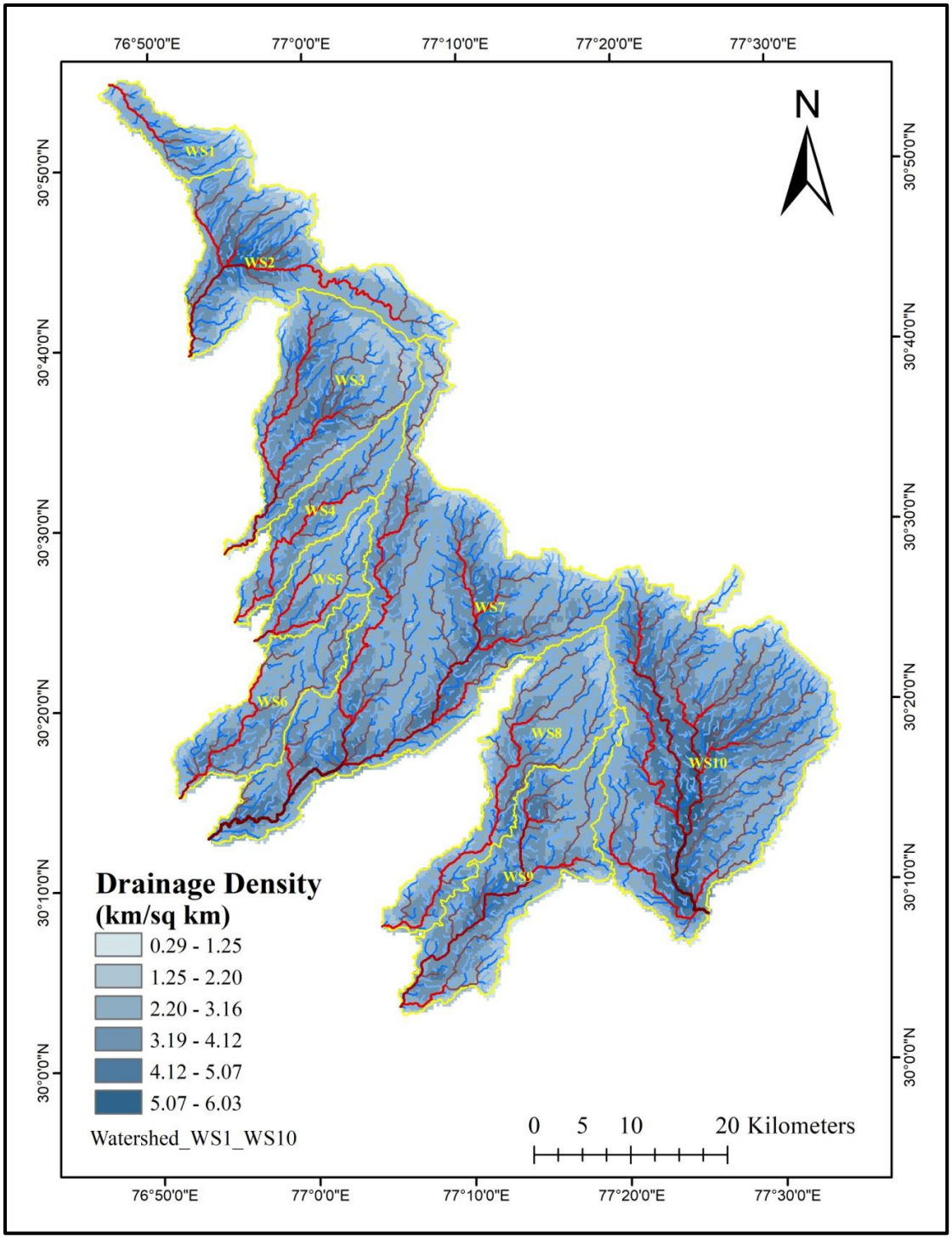

Fig. 4.26: Drainage density map of selected watersheds of Shivalik Region

Table 4.19: Drainage network

Watershed	Total no. of streams (N_μ)	Total stream length (L_μ)	Mean stream length (L_{sm})	Stream length ratio (R_L)	Mean bifurcation ratio (R_{bm})
WS1	110	125.36	3.77	0.64	4.63
WS2	346	401.94	6.04	0.54	4.10
WS3	379	418.29	7.22	0.51	4.61
WS4	181	190.35	7.53	0.70	5.27
WS5	129	128.49	3.05	0.88	3.57
WS6	229	250.90	4.10	0.44	3.93
WS7	1017	1064.86	9.09	0.54	4.04
WS8	359	357.86	10.67	0.58	7.25
WS9	406	404.29	10.08	0.78	4.21
WS10	965	1079.19	7.76	0.49	3.95

4.2.3 Drainage geometry

The drainage geometry parameters are shown in Table 4.20. The table showed watershed wise values of basin area (km^2), perimeter (km), circulatory ratio (R_c), elongation ratio (R_e), compactness constant (C_c), form factor (F_f), and basin length (km). The results showed that WS7 has a maximum basin area and perimeter of 616.53 km^2 and 207.46 km,

Table 4.20: Drainage geometry

Watershed	Basin area (km^2)	Perimeter (km)	Circulatory ratio (R_c)	Elongation ratio (R_e)	Compactness constant (C_c)	Form factor (F_f)	Basin length (L)
WS1	65.12	51.02	0.31	0.406	1.78	0.13	22.43
WS2	236.96	113.73	0.23	0.387	2.08	0.12	44.81
WS3	241.84	93.73	0.35	0.468	1.70	0.17	37.50
WS4	111.97	76.68	0.24	0.328	2.04	0.08	36.36
WS5	80.91	59.01	0.29	0.418	1.85	0.14	24.29
WS6	142.86	86.34	0.24	0.364	2.04	0.10	37.00
WS7	616.53	207.46	0.18	0.340	2.36	0.09	82.29
WS8	210.75	125.89	0.17	0.326	2.45	0.08	50.18
WS9	233.30	133.07	0.17	0.333	2.46	0.09	51.74
WS10	597.71	163.97	0.28	0.587	1.89	0.27	47.01

whereas WS1 has a minimum basin area and perimeter of 65.12 km^2 and 51.02 km. The WS8 and WS9 have a minimum R_c of 0.17, whereas WS3 has the highest R_c of 0.35. The table showed that WS10 has the maximum R_e as 0.587 and WS8 has the minimum R_e value as 0.326. The WS3 has minimum value C_c as 1.70, whereas WS9 has the maximum value C_c as 2.46. The WS4 and WS8 have a minimum value of F_f as 0.08 and the WS10 has the maximum value of F_f as 0.27. The basin length (L) of the WS7 was observed as maximum i.e., 82.29 km, and WS1 has found as minimum basin length (L) of 22.43 km.

4.2.4 Drainage texture

The watershed wise drainage texture analysis is shown in Table 4.21. The drainage texture analysis involved the values of drainage density (D_d), stream frequency (F), constant of channel maintenance (C), shape factor (B_s), drainage texture (T_s), and length of overland flow (L_o). The tabulated results showed that in the selected watersheds in the study area, WS1 has a maximum value of D_d as 1.93 whereas WS5 has a minimum value of D_d as 1.59. The observed results for F showed that WS2 has a maximum value of F as 74 whereas WS2 has a minimum value of F as 1.46. The tabulated results for C showed that WS5 has a maximum value of C as 0.63 whereas WS1 has a minimum value of C as 0.52. The results showed that WS8 has a maximum value of B_s as 11.95, whereas WS10 has a minimum value of B_s as 3.70. The WS2 has a minimum value of T_s as 2.48 whereas WS1 has a maximum value of T_s as 3.25. In the tabulated results, the maximum value for the length of overland flow was observed as 0.260 of WS1 and the minimum value was 0.315 of WS5.

Table 4.21: Drainage texture

Watershed	Drainage density (D_d)	Stream frequency (F_s)	Constant of channel Maintenance (C)	Shape factor (B_s)	Drainage texture (T_s)	Length of overland flow (L_o)
WS1	1.93	1.69	0.52	7.73	3.25	0.260
WS2	1.70	1.46	0.59	8.47	2.48	0.295
WS3	1.73	1.57	0.58	5.81	2.71	0.289
WS4	1.70	1.62	0.59	11.81	2.75	0.294
WS5	1.59	1.59	0.63	7.29	2.53	0.315
WS6	1.76	1.60	0.57	9.58	2.82	0.285
WS7	1.73	1.65	0.58	10.98	2.85	0.289
WS8	1.70	1.70	0.59	11.95	2.89	0.294
WS9	1.73	1.74	0.58	11.47	3.02	0.289
WS10	1.81	1.61	0.55	3.70	2.92	0.277

4.2.5 Relief characteristics

The relief characteristics of the selected watersheds (WS1 to WS10) were analysed during the study. The analysed results of the relative relief (R_r), relief ratio (R_h) and ruggedness number (R_n) are presented in the Table 4.22. The result showed that value of R_r ranged from 48 to 1233 in WS1 to WS10. The WS2 has highest value of R_r as 1233 whereas WS6 has lowest value of R_r 48. The R_h ranged in the selected watersheds from 0.001 to 0.03. The results for R_h showed that WS1 has maximum value as 0.033 whereas WS6, WS8, WS9 has minimum value as 0.001. The R_n ranged in the selected watersheds (WS1 to WS10) from 0.10 to 2.09. The observed results for R_n showed that WS2 has maximum value as 2.09 whereas WS6 has minimum value as 0.08.

Table 4.22: Relief characteristics

Watershed	Relative relief (R_r)	Relief ratio (R_h)	Ruggedness no. (R_n)
WS1	734	0.033	1.41
WS2	1233	0.028	2.09
WS3	907	0.024	1.57
WS4	269	0.007	0.46
WS5	62	0.003	0.10
WS6	48	0.001	0.08
WS7	1025	0.012	1.77
WS8	70	0.001	0.12
WS9	55	0.001	0.10
WS10	385	0.008	0.70

4.3 Soil loss estimation using RUSLE on watershed basis

The estimation of soil loss using RUSLE with integration of RS and GIS was carried out in selected watersheds in Shivalik foothills. The key factors which are required to derive RUSLE equation for soil estimation are discussed below.

4.3.1 Rainfall-runoff erosivity factor (R)

The average annual rainfall erosivity factor (R) value varied from 174 to 616 MJ mm ha^{-1} h^{-1} yr^{-1}over the entire study area as shown in Fig. 4.27.

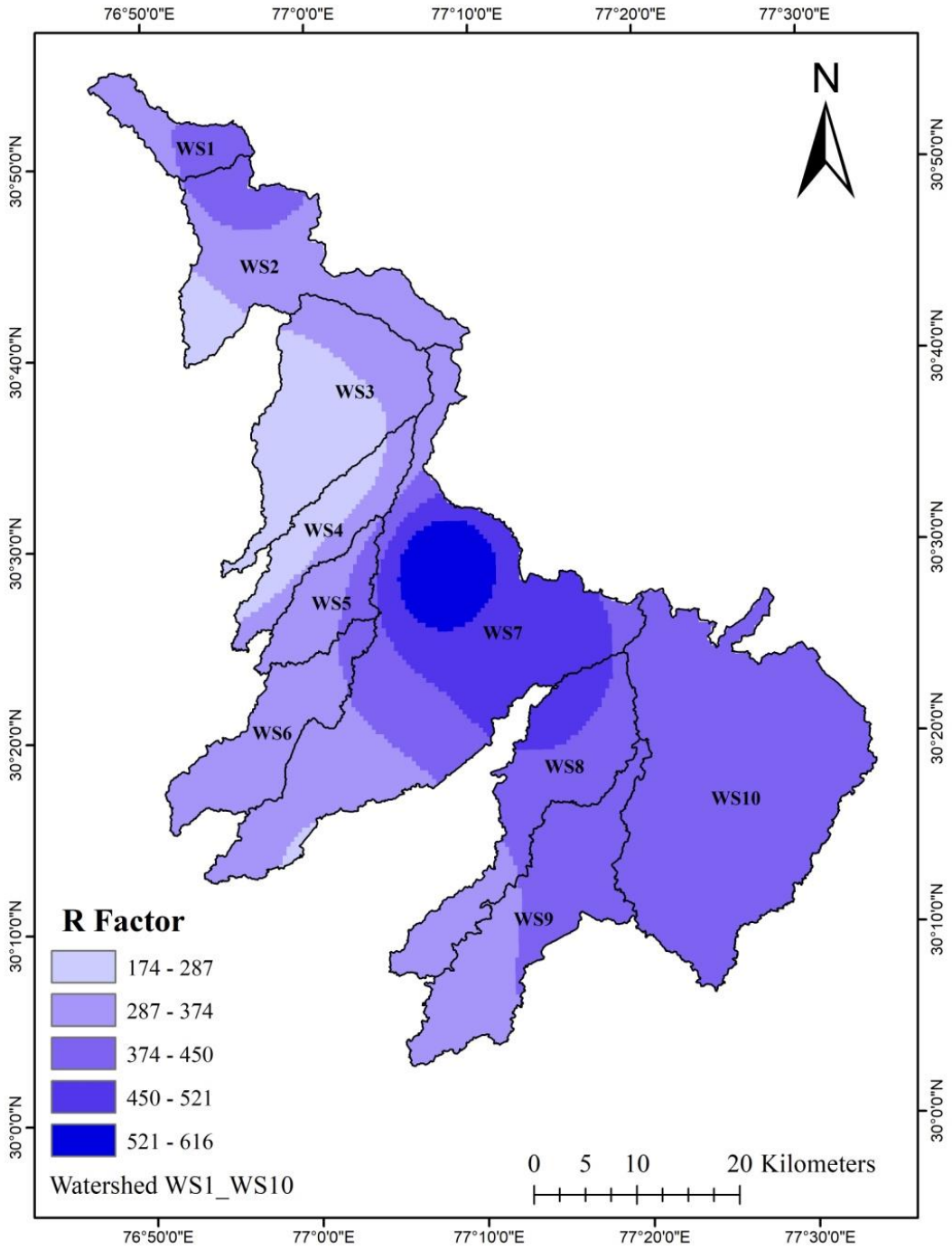

Fig. 4.27: Rainfall erosivity map of the study area

4.3.2 Soil erodibility factor (K)

4.3.2.1 Soil properties

The FAO digital soil map of the world (DSMW) was used for information about the soil physical properties of the study area. The shapefile of the study area was masked and extracted from the global data set and the attributes of the raster image were analysed and the percentage of sand, silt, clay and organic matter (OM) of the top (0-15 cm) soil layer of the

study area were obtained as shown in Fig. 4.28, 4.29, 4.30 and 4.31, respectively. The soil physical properties, soil permeability class and structure code of the study area are shown in Table 4.23 and Table 4.24, respectively. The percentages of sand, silt, clay, and organic matter in loam soil ranged from 36.40% to 48.70%, 29.90% to 37.20%, 21.60% to 26.40% and 0.64% to 1.07%, respectively. In sandy loam textural class, the percentages of sand, silt, clay, and organic matter varied from 68.30% to 76.00%, 9.90% to 15.10%, 14.10% to 16.60%, and 0.41% to 0.50%, respectively (Table 4.23).

Table 4.23: Soil physical properties of the study area

Soil unit symbol	Soil texture Class	sand (%) topsoil	%silt topsoil	clay (%) topsoil	OM (%) topsoil
BE	Loam Soil	36.40	37.20	26.40	1.07
JC	Loam Soil	39.60	39.90	20.60	0.65
XK	Loam Soil	48.70	29.90	21.60	0.64
LO	Sandy Loam	76.00	9.90	14.10	0.41
RE	Sandy Loam	68.30	15.10	16.60	0.50

The textural class of loam soil has permeability code of 3, permeability class as moderate and soil structure code of 2. In case of sandy loam, the table depicts permeability code of 2, permeability class as moderate fast and soil structure code of 2 (Table 4.24). Table 4.25 depicts the area under different soil types in study area. As per the obtained data, the loam soil covered 70.75% area whereas sandy loam covered 29.25% area.

Table 4.24: Soil permeability class and structure code of the study area

FAO Soil unit symbol	Soil texture Class	Permeability Code	Permeability Class	Soil Structure Code
BE	Loam Soil	3	Moderate	2
JC	Loam Soil	3	Moderate	2
XK	Loam Soil	3	Moderate	2
LO	Sandy Loam	2	Moderate Fast	2
RE	Sandy Loam	2	Moderate Fast	2

Table 4.25: Area under different soil types in study area

Soil texture Class	Area (km^2)	Area (%)
Loam Soil	1795.59	70.75
Sandy Loam	742.36	29.25

4.3.2.2 Soil textural class

The soil structure codes have been obtained from the soil databank of FAO. The thematic maps of soil textural information have been prepared and related information has displayed through legends in maps. The soil texture triangle was used to derive soil texture classes, followed by designating permeability codes, permeability classes, and soil structure codes.

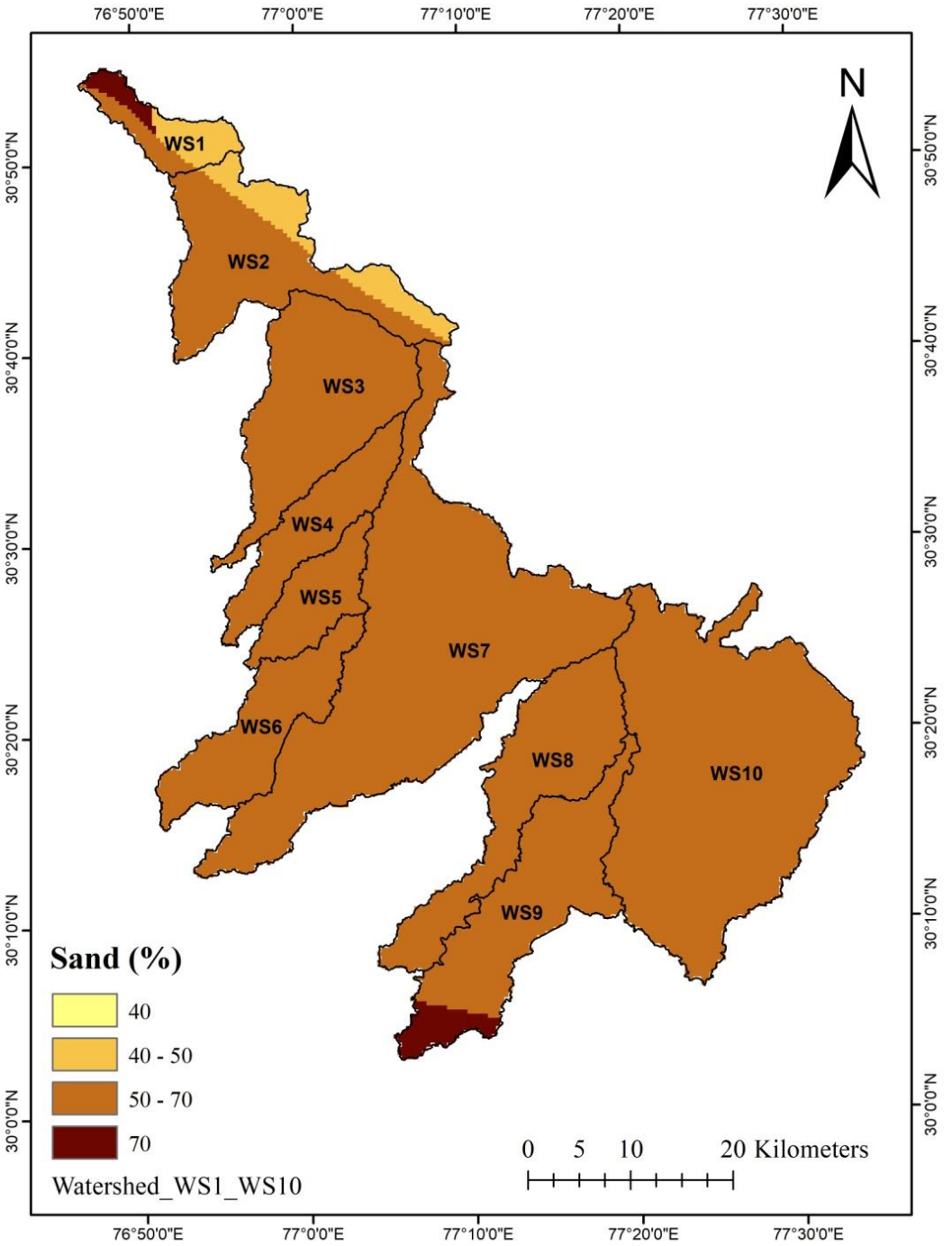

Fig. 4.28: Sand percent in the study area

The K factor quantitatively describes the erodibility of a particular soil type. It represents the susceptibility of soil particles to detachment and transport by rainfall and runoff. It gets influenced by soil texture, soil structure, organic matter and permeability of particular soil. The K factor in the study area ranged from 0.095 to 0.134 t ha h $ha^{-1}MJ^{-1}$ mm^{-1}. The K factor thematic map has shown in Fig. 4.32.

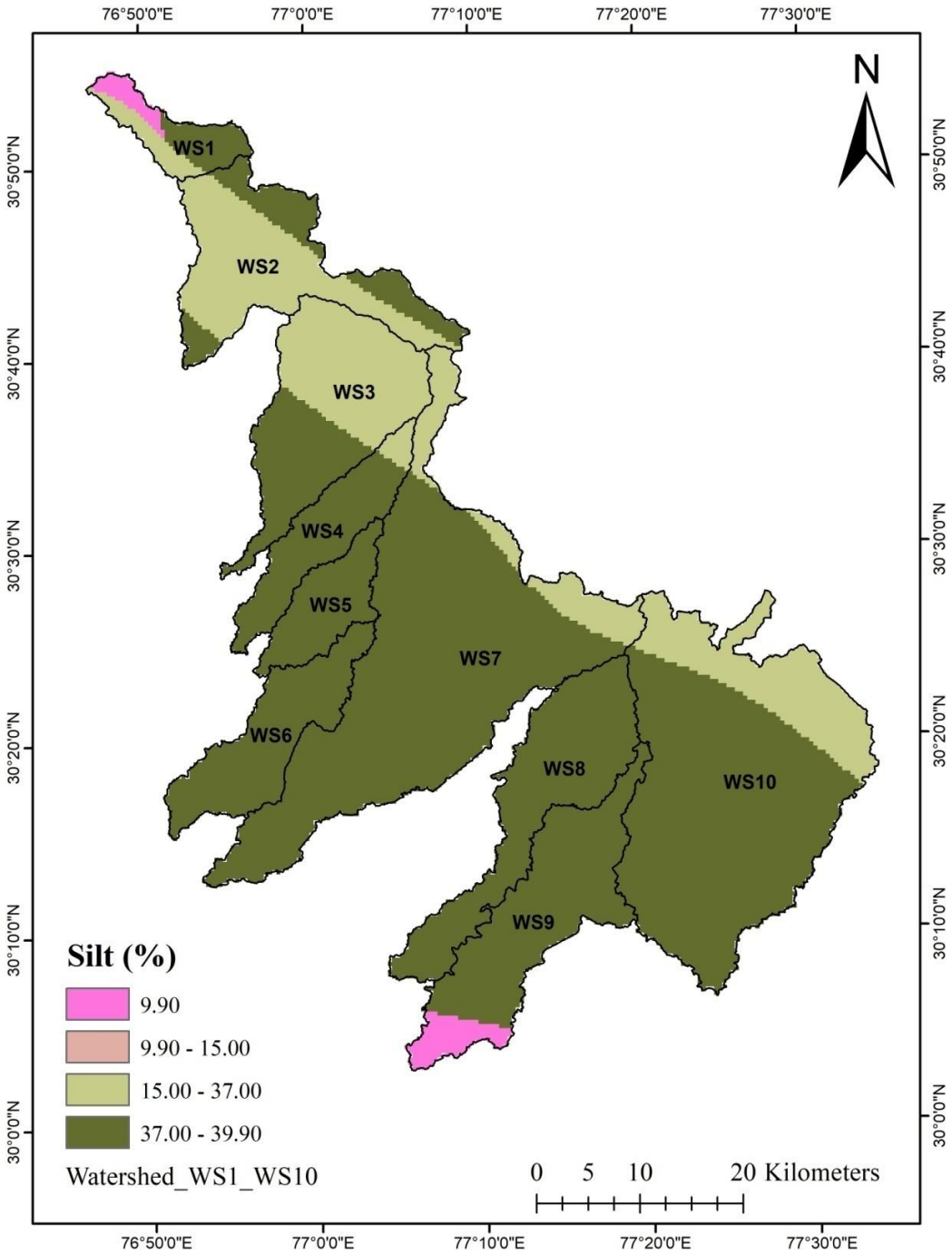

Fig. 4.29: Silt percent in the study area

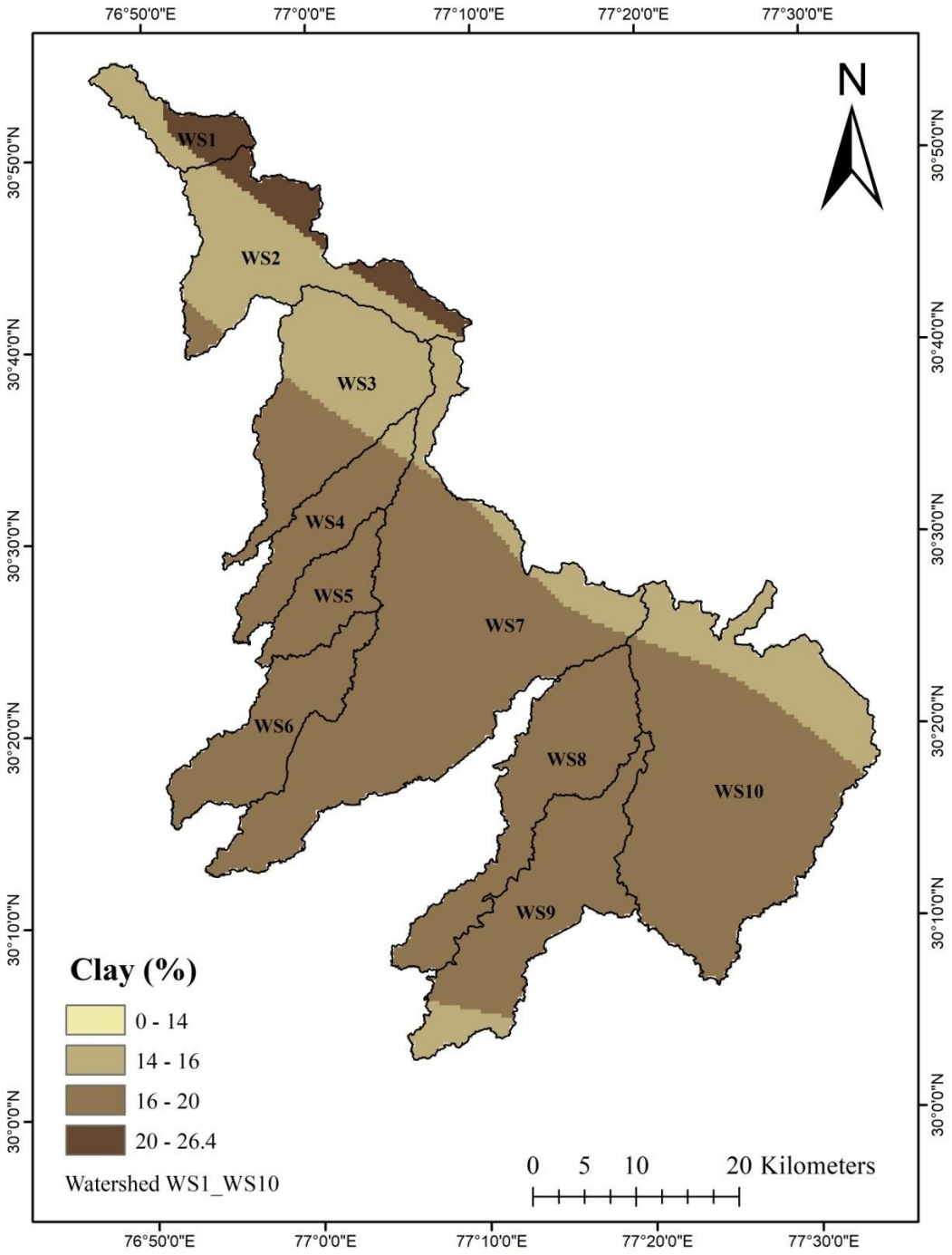

Fig. 4.30: Clay percent in the study area

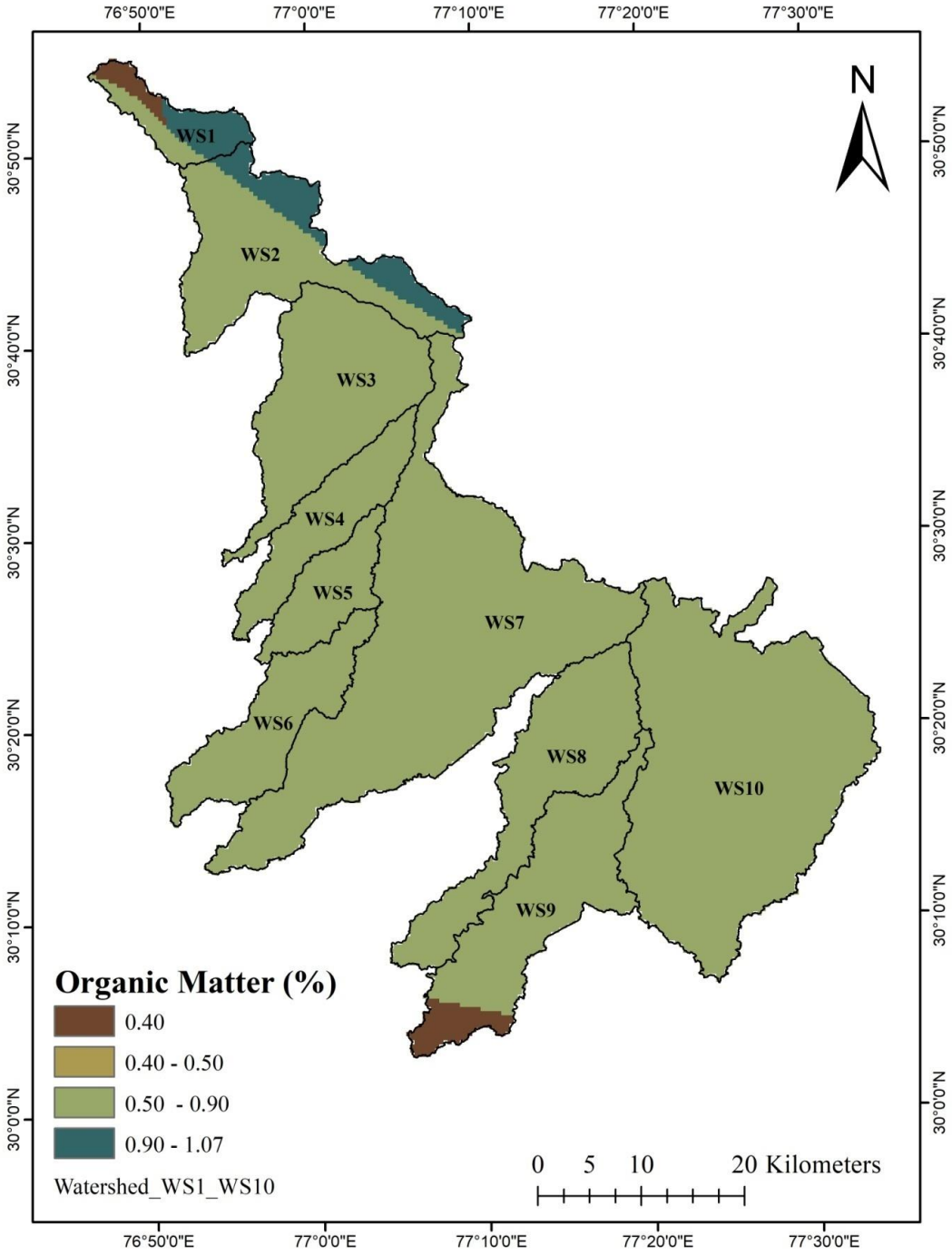

Fig. 4.31: Organic matter percent in the study area

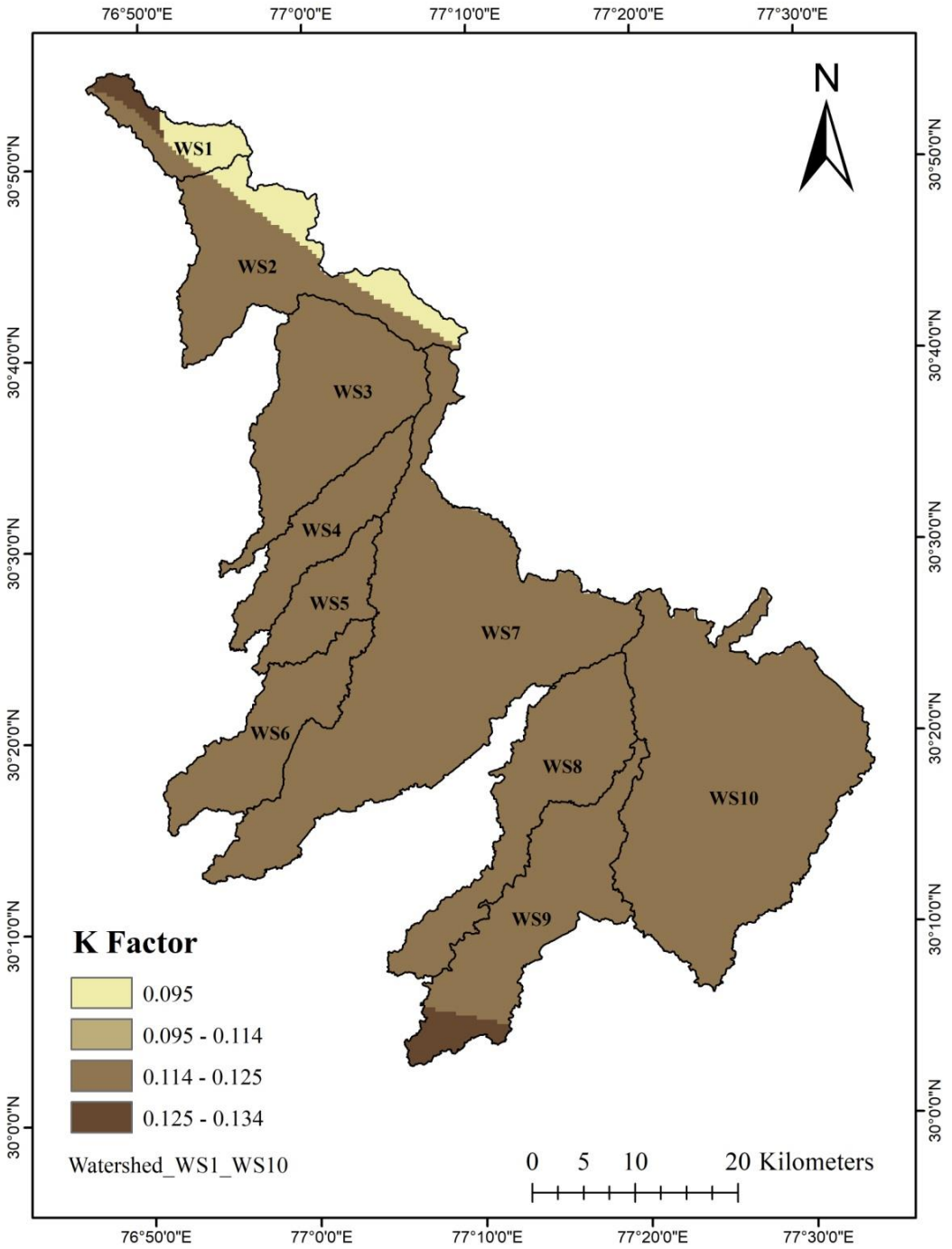

Fig. 4.32: K factor map of study area

4.3.3 Slope length steepness factor (LS)

4.3.3.1 Flow accumulation

The natural flow of water, received through precipitation, flows from areas of higher elevation to lower elevation in a steady way, due to which adjacent regions also gets accumulated. The flow accumulation over the study area in the Shivalik foothills region is shown in Fig. 4.33.

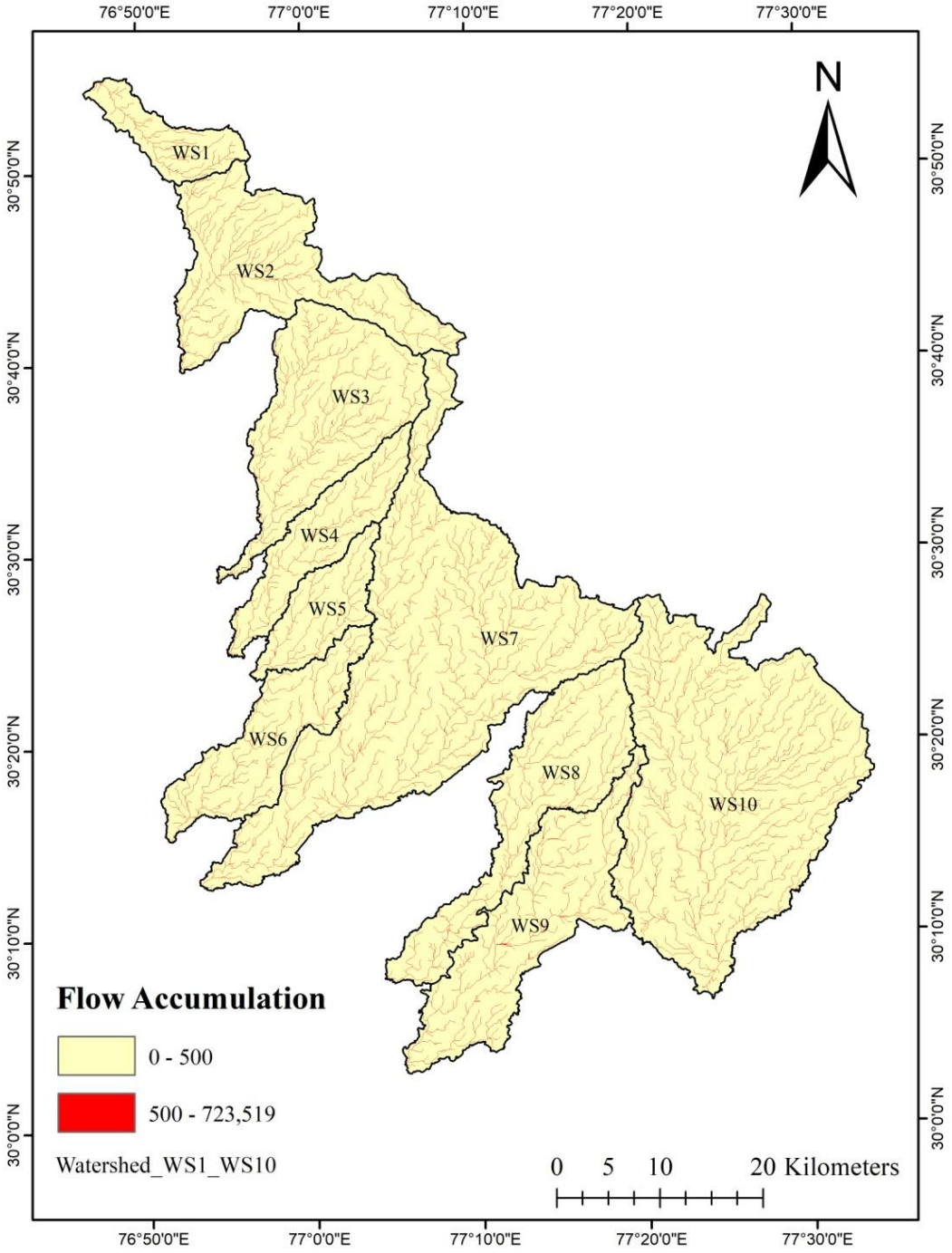

Fig. 4.33: Flow accumulation map of study area

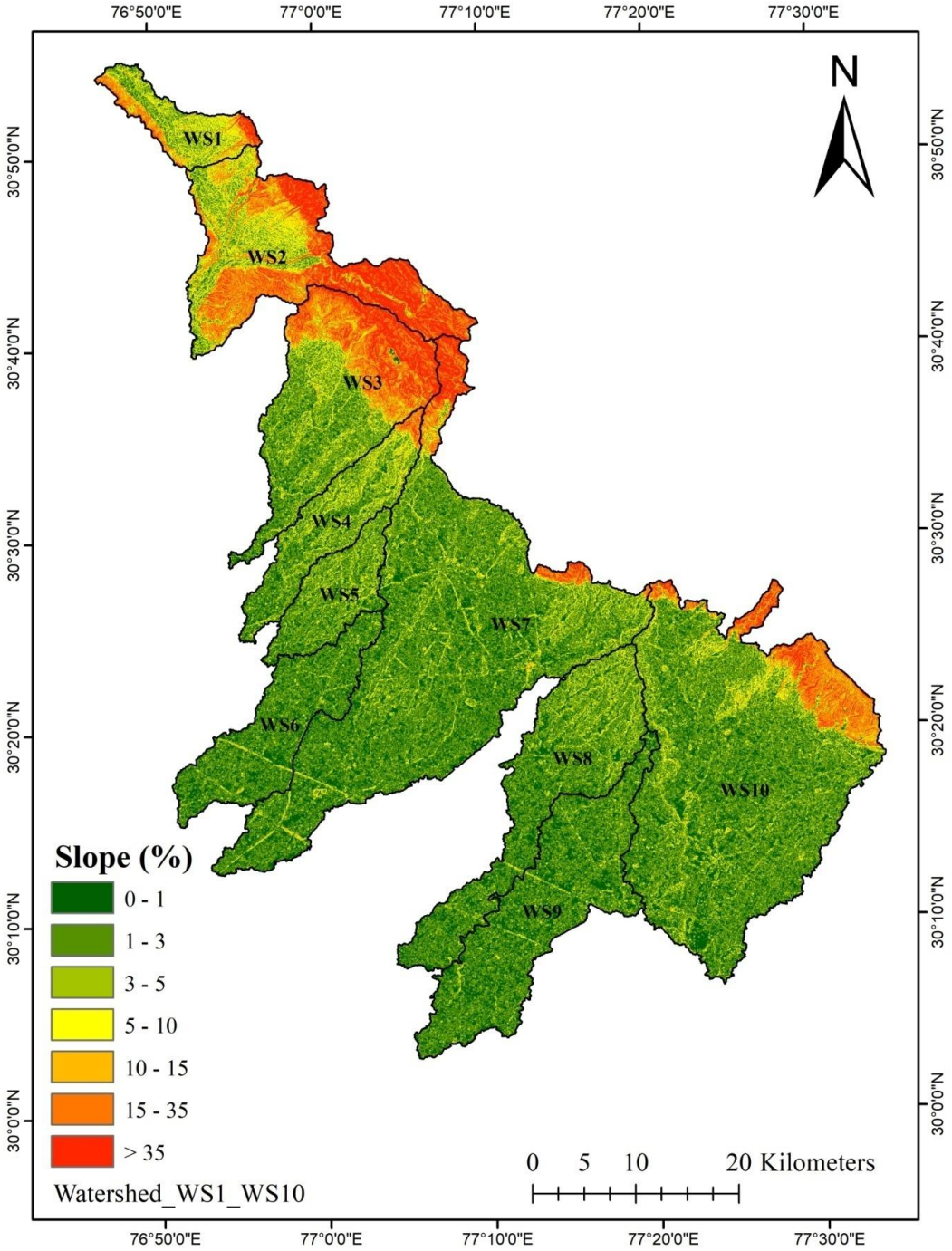

Fig. 4.34: Slope percent map of study area

4.3.3.2 Land slope

The soil losses are prominently affected by the slope of the land. Therefore, DEM data is used to generate the slope layer of the watersheds in the study area. The hydrological module of ArcGIS was used to derive slope from the digital elevation map (DEM) of the region. The slope (%) of the Shivalik region is shown in Fig. 4.34. The slope (%) was reclassified into seven category intervals, i.e., 0-1, 1-3, 3-5, 5-10, 10-15, 15-35, and more than 35. The slope classification in the selected watershed is presented in Table 4.27.

Table 4.26: Slope classification of study area

Watershed	Slope % category	Class	Area (km^2)	Area (%)
WS1	0-1	Nearly level	3.05	4.68
	1-3	Very gentle	10.64	16.34
	3-5	Gentle	15.27	23.45
	5-10	Moderate	18.23	27.99
	10-15	Strong	5.74	8.81
	15-35	Moderately steep	8.87	13.62
	>35	Very steep	3.32	5.10
WS2	0-1	Nearly level	5.56	2.35
	1-3	Very gentle	18.31	7.73
	3-5	Gentle	28.77	12.14
	5-10	Moderate	42.5	17.94
	10-15	Strong	20.95	8.84
	15-35	Moderately steep	62.46	26.36
	>35	Very steep	58.41	24.65
WS3	0-1	Nearly level	26.14	10.81
	1-3	Very gentle	53.84	22.26
	3-5	Gentle	43.75	18.09
	5-10	Moderate	27.43	11.34
	10-15	Strong	12.2	5.04
	15-35	Moderately steep	45.24	18.71
	>35	Very steep	33.24	13.74
WS4	0-1	Nearly level	19.97	17.84
	1-3	Very gentle	38.68	34.54
	3-5	Gentle	31.47	28.11
	5-10	Moderate	16.1	14.38
	10-15	Strong	1.87	1.67
	15-35	Moderately steep	3.02	2.70
	>35	Very steep	0.86	0.77
WS5	0-1	Nearly level	18.1	22.37
	1-3	Very gentle	33.57	41.49
	3-5	Gentle	22.19	27.43
	5-10	Moderate	6.81	8.42
	10-15	Strong	0.22	0.27
	15-35	Moderately steep	0.02	0.02
	>35	Very steep	-	-
WS6	0-1	Nearly level	52.15	36.50
	1-3	Very gentle	63.68	44.58
	3-5	Gentle	22.92	16.04
	5-10	Moderate	3.74	2.62
	10-15	Strong	0.32	0.22
	15-35	Moderately steep	0.05	0.03

	>35	Very steep	-	-
WS7	0-1	Nearly level	173.42	28.13
	1-3	Very gentle	251.03	40.72
	3-5	Gentle	124.03	20.12
	5-10	Moderate	35.3	5.73
	10-15	Strong	5.02	0.81
	15-35	Moderately steep	14.02	2.27
	>35	Very steep	13.71	2.22
WS8	0-1	Nearly level	62.33	29.58
	1-3	Very gentle	89.21	42.33
	3-5	Gentle	46.51	22.07
	5-10	Moderate	12.27	5.82
	10-15	Strong	0.42	0.20
	15-35	Moderately steep	0.01	0.00
	>35	Very steep	-	-
WS9	0-1	Nearly level	90.19	38.66
	1-3	Very gentle	100.67	43.15
	3-5	Gentle	36.97	15.85
	5-10	Moderate	5.32	2.28
	10-15	Strong	0.14	0.06
	15-35	Moderately steep	0.01	0.00
	>35	Very steep	-	-
WS10	0-1	Nearly level	145.84	24.40
	1-3	Very gentle	219.13	36.66
	3-5	Gentle	126.13	21.10
	5-10	Moderate	43.51	7.28
	10-15	Strong	12.48	2.09
	15-35	Moderately steep	36.45	6.10
	>35	Very steep	14.17	2.37

The results showed that in WS1, approximately 27.99% of its total area falls under the 5-10% slope category with a moderate slope class, 23.45% area falls under the 3-5% slope category with a gentle slope class, the 16.34% area was under the 1-3% slope category with a very gentle slope class. Apart from that, 5.10% of its area was under the very steep class, having a slope of more than 35%, the 13.62% area was under moderately steep class with 15-35% slope and 8.81% area was under strong slope class with 10-15% slope category. Only 4.68% area of WS1 was noticed under nearly levelled slope class with 0-1% slope category.

In WS2, about 26.36% of its area was found under the 15-35% slope category with a moderate steep slope class, followed by 24.65% of its area under more than 35% slope category with a very steep slope class. The 17.94% area was under the 5-10% slope category with a moderate slope class. Aside from that, 12.14% of the area is classified as gentle, with a slope of 3-5%, the remaining 7.73% and 2.35% of area were observed as very gentle with 1-3% slope category and nearly levelled with 0-1% slope category, respectively.

Approximately 22.36% area of WS3 falls under the 1-3% slope category with a gentle slope class, while 18.71% falls under the 15-35% slope category with a moderate steep slope class, 18.09% area falls under 3-5% slope category with gentle slope class. Apart from that, 13.74% of its area is under the very steep class, having a slope of more than 35%. The remaining 10.81% area was nearly levelled under 0-1% slope category while 5.04% area was found under 10-15% slope category with strong slope class.

In WS4 the 34.54% of its area was found under the 1-3% slope category with a very gentle slope class, 28.11% area falls under the 3-5% slope category with a gentle slope class, 17.84% area was under 0-1% slope category with nearly level classes, about 14.38% of its geographical area was found under the 5-10% slope category with a moderate slope class, 2.70% area was classified under very moderate steep with 15-35% slope category, 1.67% area was noticed under strong slope class with 10-15% slope category. Only 0.77% area was noticed under very steep slope class with a slope of more than 35%, respectively.

In WS5, 41.49% of its area was found under the 1-3% slope category with a very gentle slope class, 27.43% area was under the 3-5% slope category with a gentle slope class, 22.37% area was under 0-1% slope category with nearly levelled slope, 8.42% of area was found under the 5-10% slope category with a moderate slope, 0.27% area was under 10-15% slope category with strong slope, apart from that, very less area under moderately steep class with 15-35% slope category and no area under very steep slope with more than 35% slope category was noticed, respectively.

In WS6, about 44.58% of its area was found under the 1-3% slope category with a very gentle slope class, 36.50% area was under 0-1% slope category with nearly levelled slope, 16.04% area falls under the 3-5% slope category with a gentle slope, 2.62% area falls under the 5-10% slope category with a moderate slope, 0.22% area was noticed under 10-15% slope category with strong slope, apart from that only 0.03% area was found under 15-35% slope category with moderate steep slope while no area was noticed under very steep slope class having more than 35% slope, respectively.

In WS7 about 40.72% of its area was observed under 1-3% slope category having very gentle slope class, 28.13% area was under 0-1% slope category having nearly levelled slope, 20.12% area was under 3-5% slope category with gentle slope class, 5.73% area was under 5-10% slope category with a moderate slope class, 2.27% of the area was classified under 15-35% slope category with moderate steep slope while 2.22% area was found under more than 35% slope category with very steep slope and only 0.81% was noticed under 10-15% slope category with strong slope, respectively.

In WS8 about 42.33% of its area was under the 1-3% slope category with very gentle slope, 29.58% area was under 0-1% slope category with nearly levelled slope, 22.07% area was under 3-5% slope category with gentle slope, 5.82% area was noticed under 5-10% slope category under moderate slope. Only 0.20% area was under 10-15% slope category with strong slope while almost nil area was noticed under 10-35% and more than 35% slope category with moderate and very steep slope class, respectively.

In WS9 about 43.15% of its area was under the 1-3% slope category with a very gentle slope class, 38.66% area was under 0-1% slope category with nearly levelled slope, 15.85% area was found under 3-5% slope category with gentle slope, 2.28% area was observed under 5-10% slope category with moderate slope, 0.6% area was noticed under 10-15% slope category with strong slope class. Almost nil area was noticed under 15-35% and more than 35% slope category with moderately steep and very steep slope class, respectively.

In WS10, about 36.66% of its area was under the 1-3% slope category with a very gentle slope class, 24.40% area was under 0-1% slope category with nearly levelled slope, 21.10% area was observed under 3-5% slope category with gentle slope, 7.28% area was observed under 5-10% slope category with moderate slope, 6.10% area was noticed under 15-35% slope category with moderate steep slope, 2.37% area was noticed under more than 35% slope category with very steep slope, about 2.09% was found under 10-15% slope category with strong slope class, respectively.

The thematic map of LS factor was prepared using slope map of the study area and Eq. 8, in ArcGIS environment. Flow accumulation was derived from DEM using the spatial analyst tool in ArcGIS. At first, the DEM has to be filled and then flow direction has to be performed. Using flow direction as an input, flow accumulation was derived in ArcGIS. The slope angle for each was found by using the Spatial Analyst tool in ArcGIS. Finally, the LS factor map shown above was prepared for the study area.

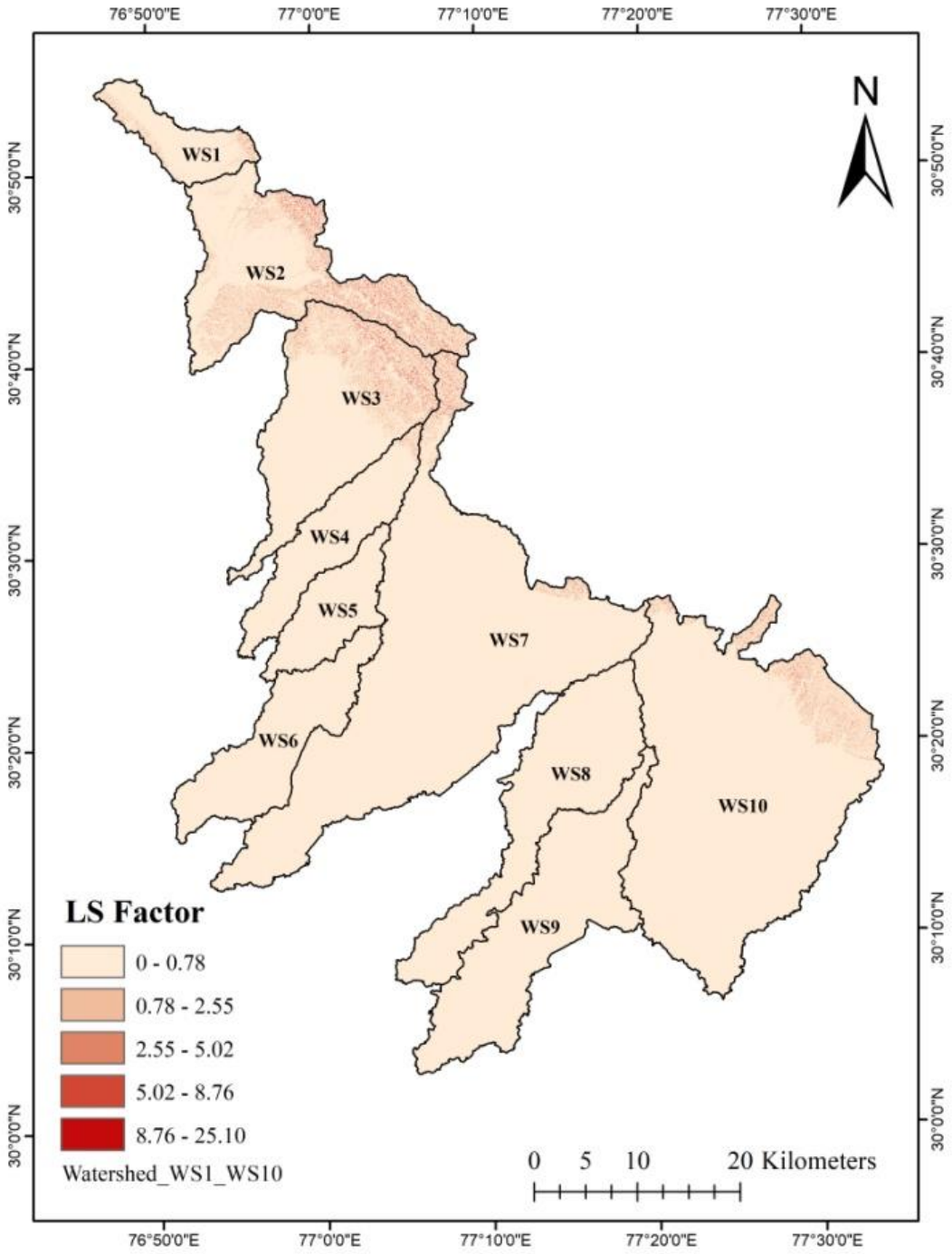

Fig. 4.35: Length of slope and steepness (LS) factor map

4.3.4 Crop management factor (C)

The C factor is considered according to the land use type. This factor C factor signifies the effects of plants, soil biomass and soil distressing actions on erosion. The information related to the land use helps in understanding of the land utilization characteristics. RS and GIS technique are capable to produce a thematic layer of LULC of a study area. The C factor map for study area is shown in Fig. 4.36. The value of C factor in study area (WS1 to WS10) was ranged from 0 to 0.63.

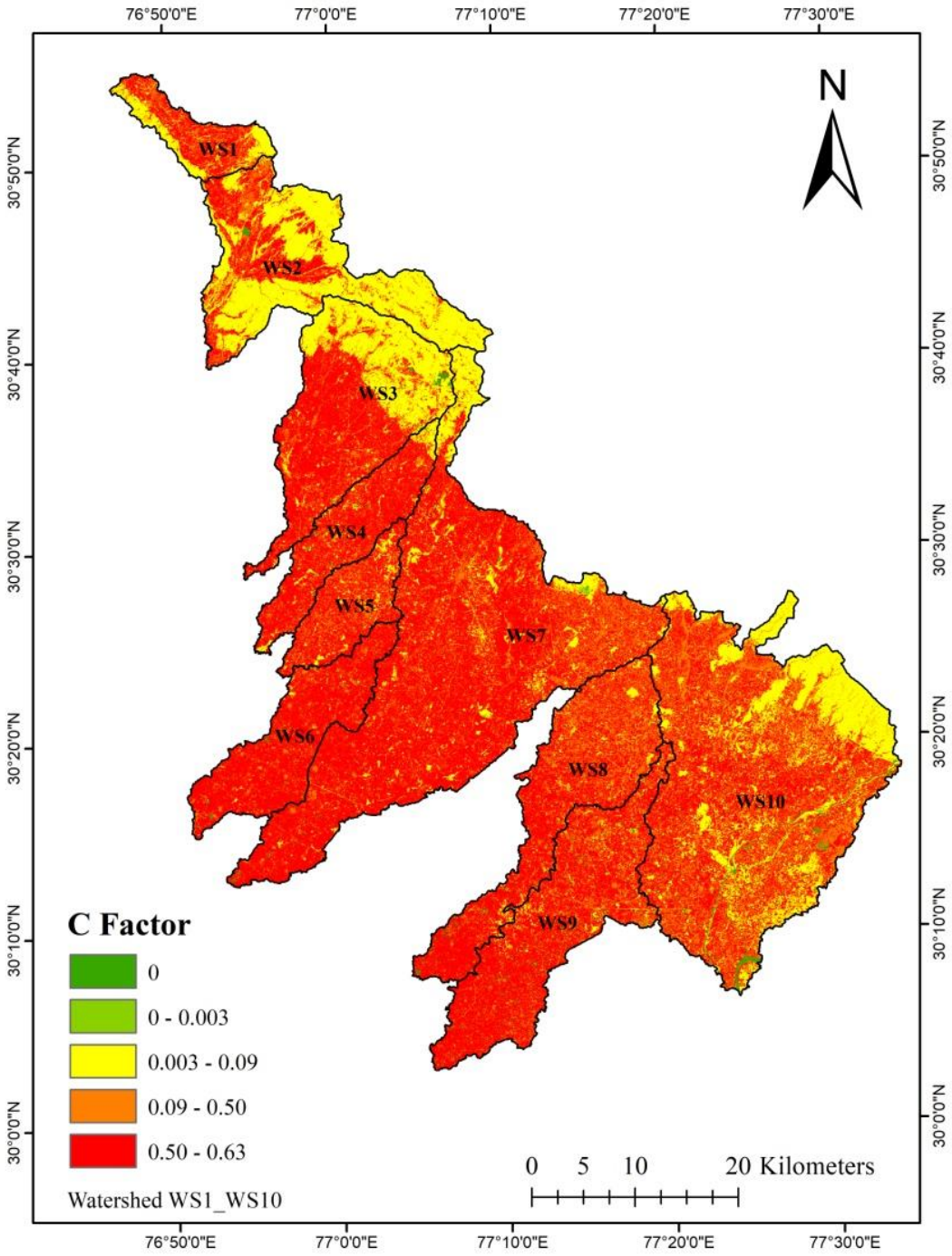

Fig. 4.36: Crop management factor (C) map

4.3.5 Erosion control practices factor (P)

The P factor values on different slope gradients was calculated and described in Chapter 3. The P-factor reflects the impact of support practices on the soil erosion rate. The P factor of the study area is shown in the Fig. 4.37. The value of P factor in the study area (WS1-WS10) was ranged from 0.5 to 1.

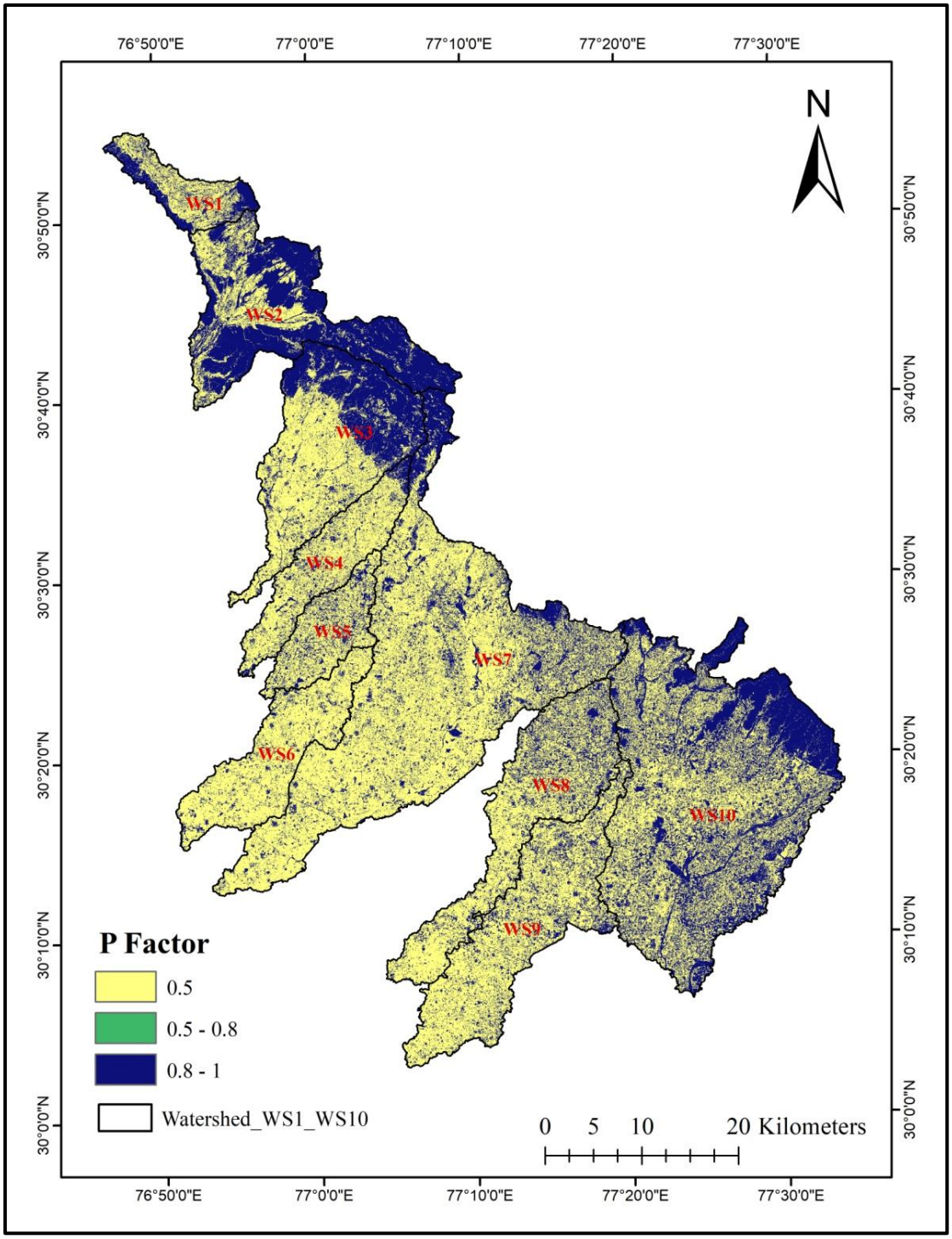

Fig. 4.37: Erosion control practices factor (P) map

4.3.6 Soil loss (A)

The RUSLE parameters i.e. R, K, LS, C and P factors were used to obtain annual soil loss in the selected watersheds of the study area. These factors were generated through integration of RS, ArcGIS and RUSLE factors. The generated RUSLE parameters i.e. raster images of R,K,LS, C & P were overlapped to attain the value which provides annual soil erosion map of the study area. The soil erosion class was assigned on the basis of Indian condition. Table 4.28 shows that 98.07 % of the total area lies under erosion rate of 0-5 t ha^{-1}

yr^{-1} followed by 1.45% under 5-10 t ha^{-1} yr^{-1}, 0.26% under 10-20 t ha^{-1} yr^{-1}, 0.13% under 20-40 t ha^{-1} yr^{-1} and 0.08% area under greater than 40 t ha^{-1} yr^{-1} (Table 4.27).

Table 4.27: Area and erosion rate distribution in the study area

Erosion Rate (t ha^{-1} yr^{-1})	Area (km^2)	% Area
0-5	2489.05	98.07
5-10	36.83	1.45
10-20	6.71	0.26
20-40	3.28	0.13
>40	2.08	0.08

4.4 Priority areas assessment for efficient implementation of soil erosion control program

The priority area was determined based on the estimated erosion rate and was classified as slight, moderate, high, very high and severe. The highest priority (1) was given to the area that has experienced an erosion rate of more than 40 t ha^{-1} yr^{-1}. Table 4.28 showed the conservation priority given to the designated classes. The maximum area was found under the slight erosion class and has been given the least priority for soil conservation measure (Table 4.27 & 4.28).

Table 4.28: Soil erosion class by severity and conservation priority

Erosion Rate (t ha^{-1} yr^{-1})	Class	Conservation Priority
0-5	Slight	5
5-10	Moderate	4
10-20	High	3
20-40	Very High	2
>40	Severe	1

Table 4.29: Erosion rate based watershed wise priority

Soil Loss (t ha^{-1} yr^{-1})	Area (km^2)										
	WS1	WS2	WS3	WS4	WS5	WS6	WS7	WS8	WS9	WS10	Class
0-5	62.09	228.88	235.95	110.67	80.14	142.13	603.30	206.71	232.15	587.03	Slight
5-10	2.34	4.87	2.40	0.98	0.71	0.48	11.10	3.86	1.12	8.97	Moderate
10-20	0.49	1.90	1.52	0.15	0.05	0.25	1.21	0.17	0.03	0.94	High
20-40	0.15	0.89	1.18	0.11	0.01	-	0.48	0.01	-	0.45	Very High
>40	0.05	0.42	0.79	0.06	-	-	0.44	-	-	0.32	Severe
Total	65.12	236.96	241.84	111.97	80.91	142.86	616.53	210.75	233.3	597.71	2537.95

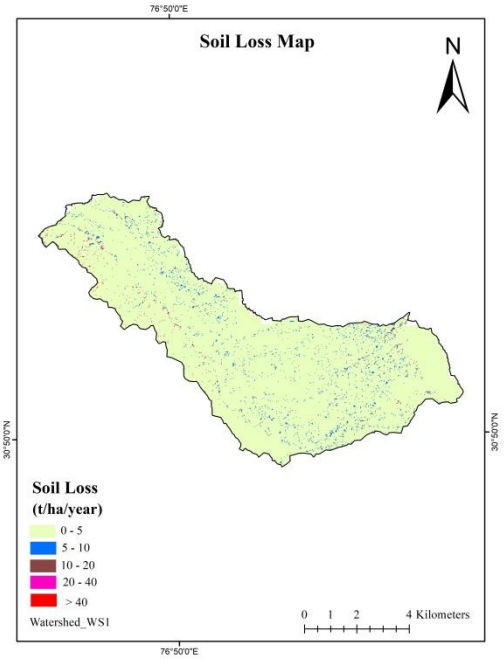

Fig. 4.38: Soil loss map of WS1

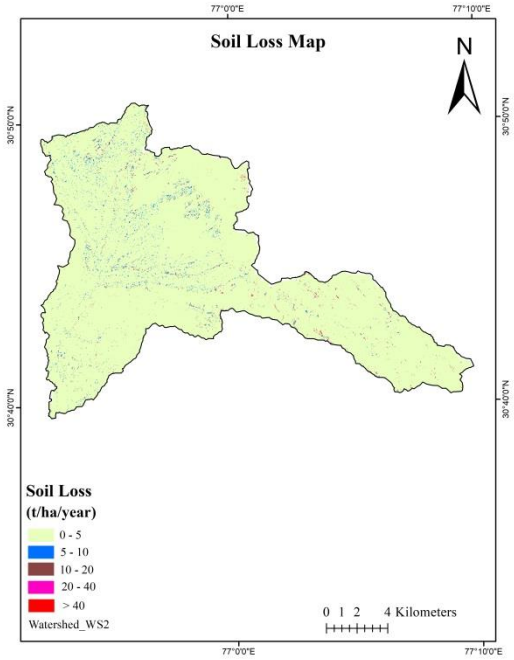

Fig. 4.39: Soil loss map of WS2

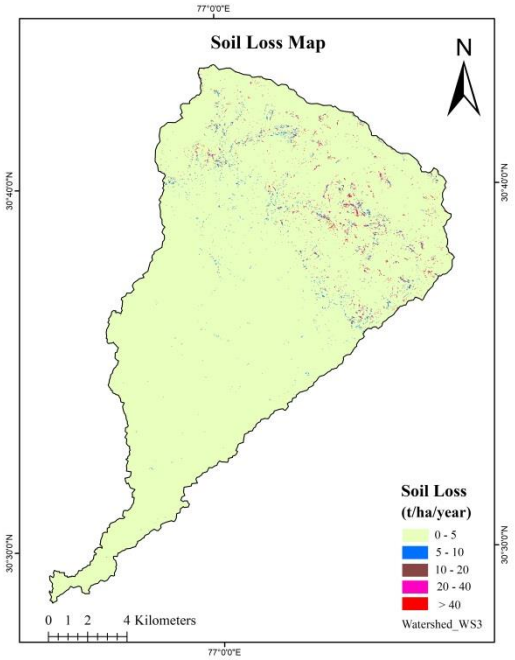

Fig. 4.40: Soil loss map of WS3

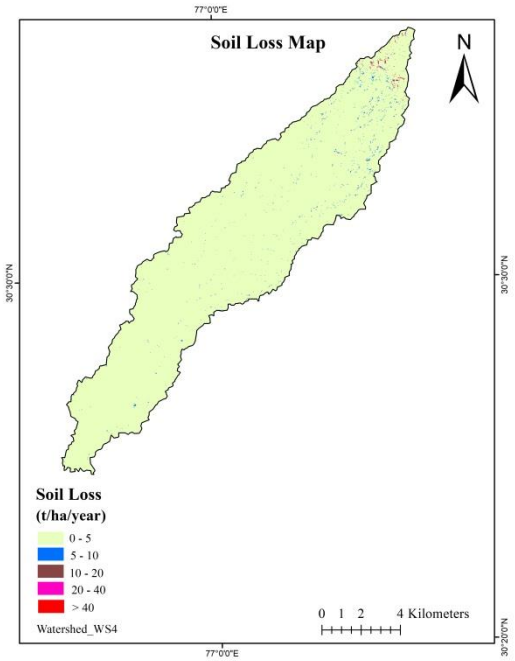

Fig. 4.41: Soil loss map of WS4

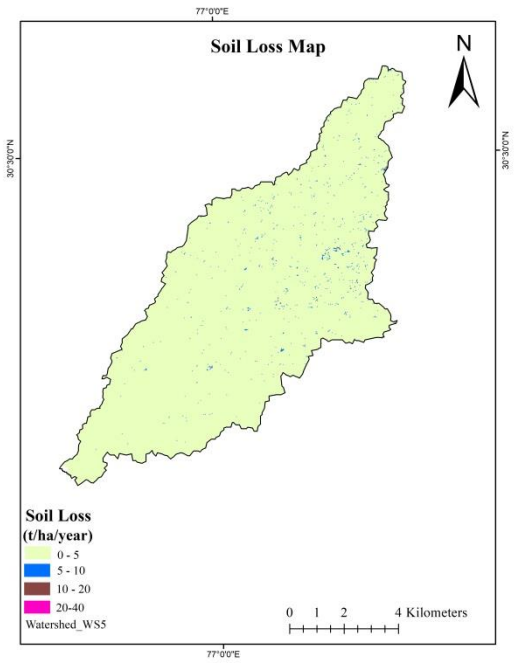

Fig. 4.42: Soil loss map of WS5

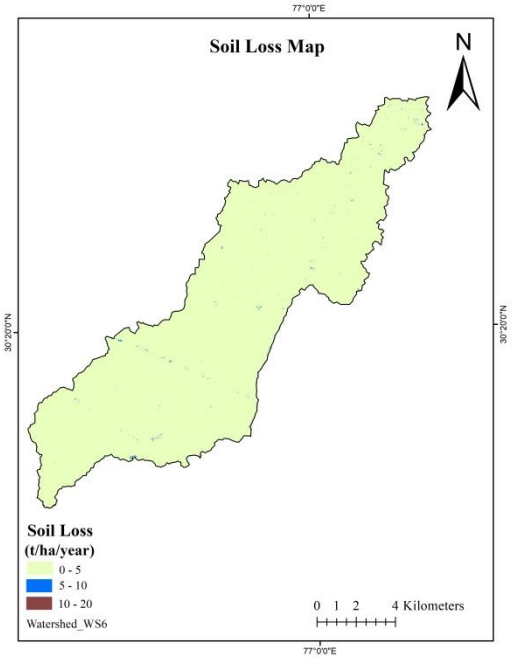

Fig. 4.43: Soil loss map of WS6

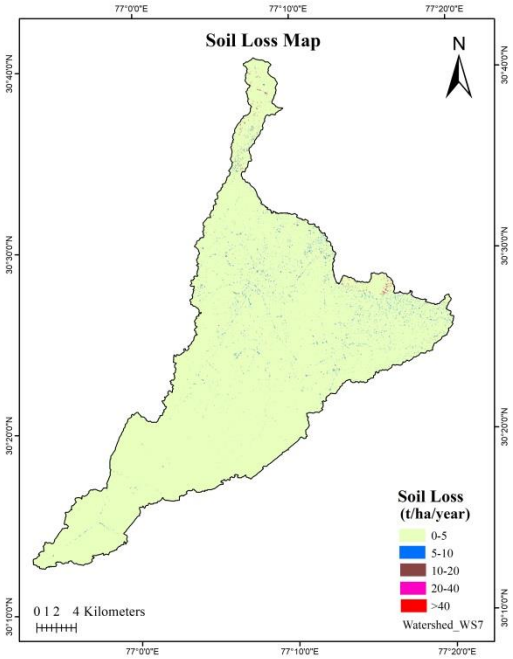

Fig. 4.44: Soil loss map of WS7

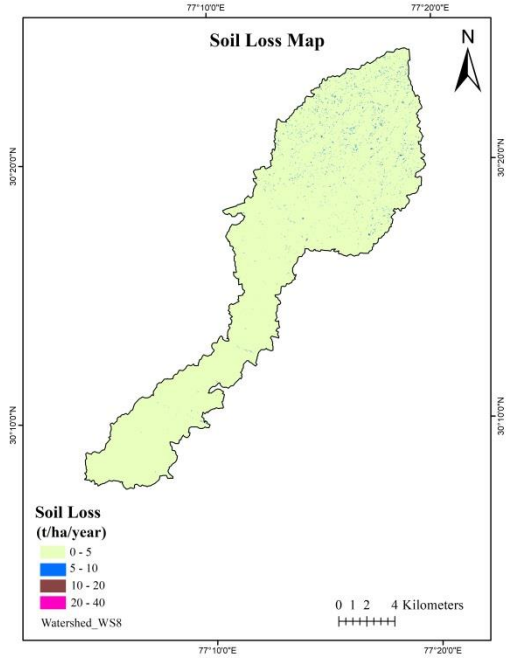

Fig. 4.45: Soil loss map of WS8

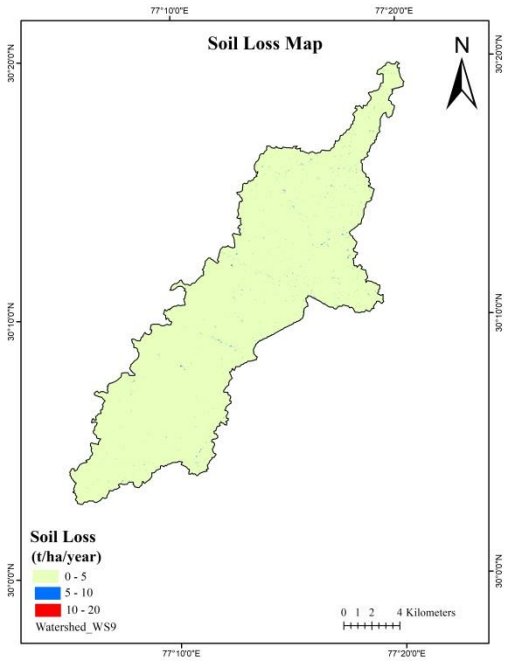

Fig. 4.46: Soil loss map of WS9

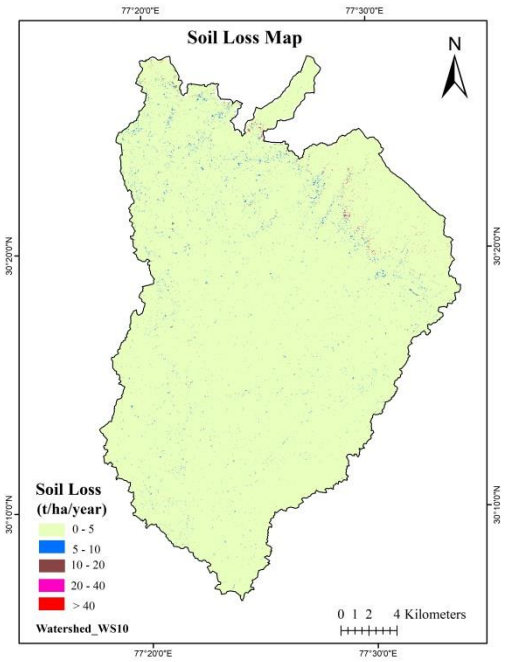

Fig. 4.47: Soil loss map of WS10

4.4.1 Watershed level soil loss

The various ranges of erosion mapped in selected watersheds are shown by thematic erosion maps. Subsequently, the nature of watersheds can be obtained by accessing harshness of soil erosion in individual watersheds. The average soil loss from individual watershed was computed by overlaying the watershed boundaries on raster-based soil loss thematic map. The soil loss for the watersheds in the study area has been depicted in Fig. 4.38 to Fig. 4.47.The soil loss for the entire study area is shown in Fig. 4.48 ranged between 0-5, 5-10, 10-20, 20-40 and more than 40. The watershed priority on the basis of erosion rate is shown in table 4.29. It showed that all selected watershed has maximum area under slight erosion class. WS1, WS2, WS3, WS4, WS7 and WS10 have area under severe erosion class (>40 t ha^{-1} yr^{-1}), hence given to 1st conservation priority. The WS5, WS6, WS8 and WS9 have no area under severe erosion class.

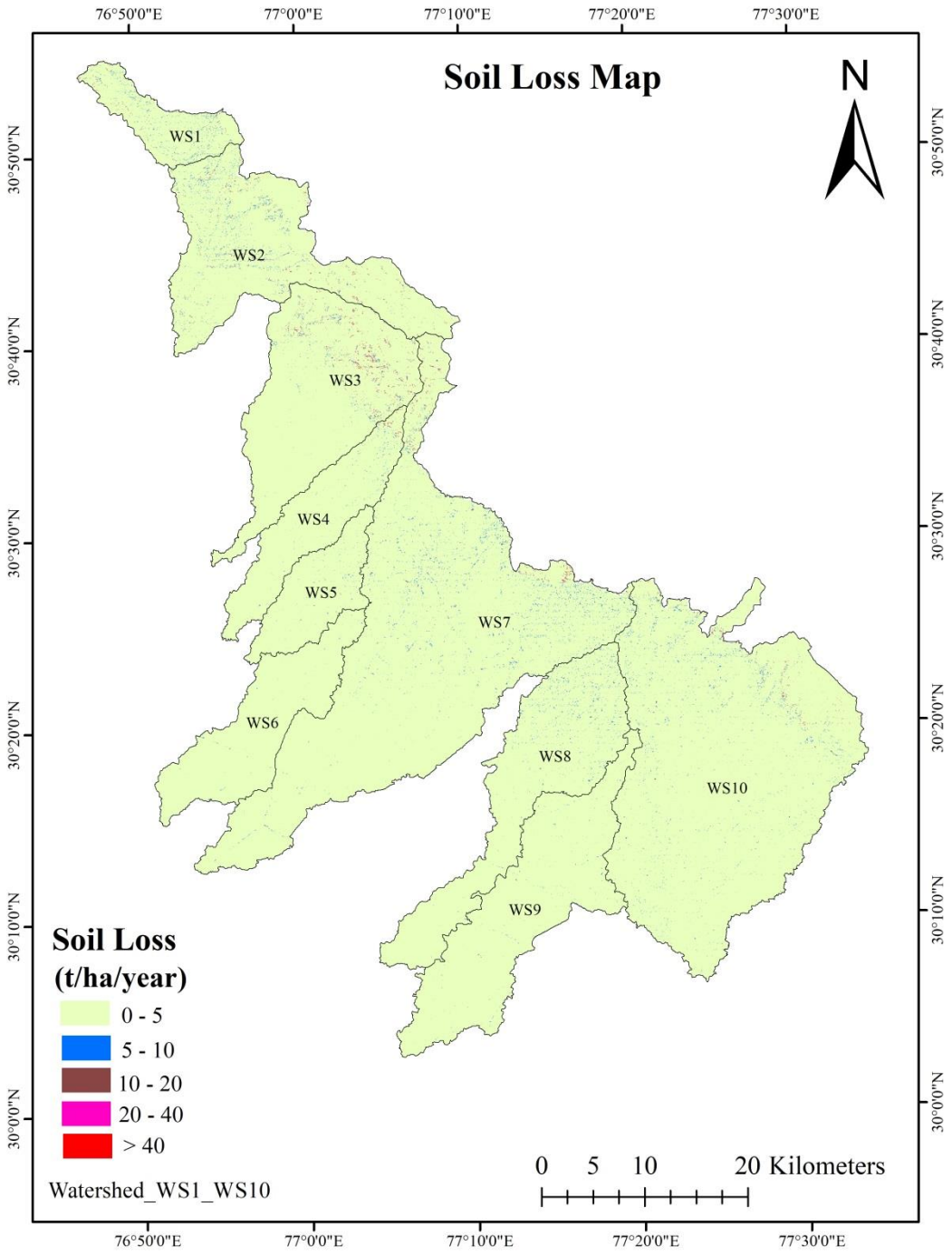

Fig. 4.48: Soil loss map of study area

CHAPTER–V

DISCUSSION

This chapter discussed the results presented in the previous chapter. Analysis of LULC has been carried out and different thematic maps have been prepared so as to analyse the status of LULC under different land use classes, to analyse the morphometric behaviour and to estimate the potential soil losses in the selected watersheds of the study area.

5.1 Thematic mapping related to land use and land cover classification of the study area

Geospatial technologies are widely used for thematic mapping of the earth's surface to have information about the status of LULC through considering an appropriate LULC classification scheme. Land use refers to how the land is being used, what activities are being carried out on the land surface. While land cover describes the surface cover on the ground, whether it is urban infrastructure, natural vegetation, plantation, water, barren land etc., the thematic map indicates the link between a single component and multiple other factors, as well as the range of different features. Depending on the situation, the theme map could be qualitative or quantitative. Quantitative thematic maps represent numerical data connected to dimensions, while qualitative thematic maps primarily display spatial coordinates and the distribution of particular features. Land use, land cover, height, slope, morphometric parameters, soil characteristics, and so on are examples of variables that could be mapped together under thematic mapping.

The study area has been delineated and 10 watersheds in the Shivalik foothills were selected. The result showed that among all the watersheds, WS7 was found as the largest watershed and occupied (24.29%) the maximum area, while WS1 was the smallest one and had the minimum area (2.57%) of the cumulative area of the selected watersheds. The area under different LULC classes in different watersheds varied from each other. As per the cumulative area of all the watersheds, the area under barren land was observed to be the highest (31.31%) in WS10 out of the cumulative area of all the watersheds. The WS10 adjoins the Yamuna river and is the 2nd largest watershed according to size among all the watersheds. The minimum area under barren land (2.06%) was observed under the smallest watershed (WS1). The highest area under waterbody (37.51%) was also noticed in WS10 and the lowest area under waterbody (1.05%) was observed in the smallest watershed (WS1) of the cumulative area of all watersheds. The WS10 had the highest plantation land (31.61%), while the WS6 had the lowest plantation area (0.74%) of the total area of all watersheds. The second largest WS10 has the most area under built up (26.51%), while the smallest watershed has the least (2.11%) area out of the total area of all the watersheds. The largest watershed,

WS7, was dominated by agriculture LULC with highest area (29.24%), while the smallest watershed, WS1, has the lowest area under agriculture LULC (2.18%) of the total area of all watersheds. The land use under agriculture class (60.39%) was observed as dominated class out of the cumulative area of distinct watersheds, followed by the area under plantation class (24.22%). The land use under plantation was observed as the other major LULC class in the study area. While the area covered under other LULC classes such as barren land, built up and waterbody was 11.98%, 2.20% and 1.39%, respectively out of the cumulative area of all watersheds (Table 4.2).

The result obtained after analysing the area under different LULC classes in individual watersheds showed that the WS1 has agriculture as the dominated LULC (51.29%), followed by plantation LULC (36.89%) of its total area. The WS2's dominant LULC class is plantation (67.03%), followed by agriculture LULC (27.06%). The WS3 is also dominated by agricultural LULC (53.30%) and followed by plantation LULC (36.99%) of its total area. Similarly, the WS4 also has agriculture as its dominated LULC (73.92%) followed by an area under barren LULC class (12.41%). Similarly, agriculture (67.94%) LULC dominated in WS5, followed by barren LULC class (16.88%). The agricultural land use dominated in the WS6 (84.32%), followed by land use under barren land (8.39%). The WS7 was also dominated with agriculture land use (72.68%), with plantation land use as second (13.26%). The agriculture LULC class dominated in the WS8 (69.00%), followed by the barren LULC (17.83%).The watershed WS9 has the highest area under agriculture LULC (74.20%) followed by the area under barren land use (12.61%). The WS10 has agriculture as its dominant LULC (47.08%), followed by plantation LULC (32.50%). The LULC in this region was also analysed by Kumar *et al*. (2021b) and they identified the waste land in Shivalik (Haryana) and obtained the possibility and potential sites for sericulture practises in suitable seasons in this region. Priyanka (2017) also analysed the LULC of Ambala district in the Shivalik region and noticed the drastic changes in LULC since 2001, particularly in barren land and water bodies.

The classified image was verified for accuracy assessment using Google Earth, field visits, and 153 random points. The average user's, producer's, overall accuracies, and Kappa coefficient were obtained as 94%, 90.6%, 92%, and 90%, respectively.

5.2 Morphometric analysis of study area

In the study area, the highest order of stream was observed to be the 6^{th} and the lowest order of stream was the 4^{th}. The WS7 and WS10 have the highest order of stream at 6^{th} order, whereas WS1, WS4 and WS8 have only 4^{th} order streams. The rest of the watersheds, as shown in the Table 4.15, have 5^{th} order of stream. The maximum number of 1^{st} order streams (813) was observed in WS7, whereas the minimum number of 1^{st} order streams (89) was observed in WS1. The maximum number of 2nd order streams (164) was observed in WS7

and WS10, whereas the minimum number of 2nd order streams (17) was observed in WS1. The maximum number of 3rd order streams (32) was observed in WS10, whereas the minimum number of 3rd order streams (3) was observed in WS1. The maximum number of 4th order streams (8) was observed in WS10, whereas the minimum number of 4th order streams (1) was observed in WS1, WS4, and WS8. The maximum number of 5th order streams (2) was observed in WS7 and WS10, whereas the minimum number of 5th order streams (1) was observed in WS2, WS3, WS5, WS6, and WS9. Only two watersheds, i.e., WS7 and WS1, have 6th order streams (1).

As per Horton's law, the number of streams and the number of stream segments decreases with increasing order. Generally, the lowest stream order (μ) had the maximum number of streams, and the higher stream order (μ) had a lower number of streams, whereas the highest stream order (μ) had only one stream. Similar results were obtained in this study and are presented in Table 4.15. The largest watershed, WS7, has the highest total number of streams (1017), while the smallest watershed, WS1, has the lowest total number of streams (110), indicating that the watershed having the highest total number of streams is large in size. The results showed that in all watersheds, the first order stream had the longest length and decreased as the stream order number increased, indicating that first order streams occupied the longest length (Ghosh and Gope, 2021).The stream length (Lμ) and stream order (μ) were further analysed and the bifurcation ratio, drainage texture, and stream frequency were obtained in this study.

The mean stream length is a property of the drainage network and its components (Strahler, 1964). Any stream order's mean stream length value is larger than that of the lower order but less than that of the next higher order in the basin. The mean stream length value of different watersheds, WS1 to WS10, has different values. The mean stream length value is directly proportional to the size and topography of the basin (Rai *et al*. 2017). In the study area, the Mean stream length (Lsm) in WS1 with 1st order ranged from 3.05 to 10.67 km, as presented in Table 4.16. The stream length ratio is the ratio of the mean stream length of one order to the next lower order of stream segment. In the study area, the stream length ratio (R_L) between the streams of different orders showed a change in each watershed.

The bifurcation ratio of the stream segment of the given order to the number of segments of the higher order is a dimensionless property and shows the degree of integration. It provides information regarding relief and categorization. The lower bifurcation value of watersheds indicates that these watersheds were less disturbed. Also, there was no distortion in the drainage pattern and vice versa (Balasubramani *et al*. 2019). The mean bifurcation ratio (R_{bm}) for WS8 was observed as 7.25, which means there is the potential for flash floods during the strong events with early hydrograph peaks.

The circularity ratio is related to the length and frequency of the stream, geological structure, land use, land cover, climate, relief, and slope of the basin, which indicates the dendritic stage of the watershed. In the selected watersheds, the circularity ratio (R_c) ranged from 0 to 1, in which 1 means a perfectly round shape, and the lower the value, the higher the irregularity. The obtained values which lies between 0.17 and 0.35, showed less circularity in basins. The elongation ratio (R_e) of selected watersheds except WS10 has a value of less than 0.5, which means these watersheds are more elongated. Due to a value higher than 0.5, WS10 was found to be in the category of elongated watershed. The lower value of the compactness constant showed less vulnerability to risk factors, whereas the higher value has the opposite tendency (Ahirwar *et al*. 2019). The form factor (F_f) of the watersheds was observed to be a maximum of 0.27, which means all the selected watersheds are in the category of elongated watersheds.

The range of the drainage density (D_d) of the selected watersheds lies between 1.59 and 1.93, which indicated the moderate permeability of the soil and better vegetation cover. The range of the stream frequency (F_s) of the selected watersheds lies from 1.46 to 1.74. The higher value of stream frequency (F_s) in the WS9 indicated the high degree of surface runoff. The observed values of constant channel maintenance (R) showed moderate to high permeability, moderate slope, and moderate surface runoff. The drainage texture (T_s) of the watersheds was less than 4, which means the watersheds lie in the category of coarse (Choudhari *et al*. 2018). The length of overland flow (L_o) describes the length of time water flows over the ground. The value of the length of overland (L_o) ranged from 0.260 to 0.315, which indicates the potential to cause quicker runoff.

The relative relief (R_f) of the selected watersheds is in the range of 48 to 1233, which indicates that the WS5, WS6, WS8 and WS9 have basin slopes nearly level to gentle due to low relative relief (R_f) values. It means the areas within these watersheds can be used for agricultural activities due to their being flat in nature. The lower value of the relief ratio (R_b) of WS6, WS8, and WS9 indicated the low degree of slope. The ruggedness number (R_n) is relatively low for all the selected watersheds except WS1, WS2, WS3 and WS7, which indicates that these watersheds are prone to erosion.

5.3 Soil loss estimation using RUSLE on watershed basis

Rainfall erosivity (R), soil erodibility (K), length of slope and steepness (LS), crop management (C), and conservation practise (P) are the six primary elements utilised in the RUSLE equation to calculate soil loss. The soil loss in the study area was calculated by independent investigation of these variables.

The mean annual rainfall data of 14 raingauge stations located within and outside the selected watersheds was analysed in a GIS environment and interpolated using the IDW method. The highest rainfall was recorded at Sadhaura block, located in WS7, whereas the

lowest rainfall was recorded at Barwala block, located at the boundary of WS3. Soil erosion is caused by a quantity called R, which is a quantitative expression of the rainfall-runoff connection. The amount of runoff that occurs after a rainstorm and how long it lasts both has significant effects on it (Kumar *et al*., 2021a). Both the total intensity of precipitation and the typical rainfall duration are considered into to the R value. A thematic map of the R factor was created and its value ranged from 174 to 616 MJ mm ha^{-1} h^{-1} yr^{-1}.

Texture, structure, organic matter content, and permeability are all important factors in determining the soil erodibility. The study area falls under the loam and sandy loam soil textural classes as per information extracted from the digital soil map of the world (DSMW) for the study area. The loam soil has a moderate permeability class, whereas sandy loam soil has a moderately fast permeability class. The area under loam soil was found to be 70.75% and sandy loam covers 29.25% of the study area. Erosion in soil is controlled by a wide variety of physical and chemical characteristics, and its value is often assessed by experimentation (Shinde *et al*. 2010). Using DSMW soil map and textural table, values of the K factor analysed and were used to create a GIS based K factor map. The K factor for the study area was found to have a range of 0.095 - 0.0134.

The slope length calculated from a DEM is predicated on the assumption that each slope plane has a uniform slope and vegetation cover, which may not be the case in practice. GIS approaches tend to forecast excessively long slope lengths on flat to very gentle slopes when calculating topographic parameters, which can lead to overestimation of soil loss (Kumar *et al*., 2021a). As a result, despite its usefulness as a measure of the sediment transport capacity of runoff from the landscape, the LS factor fails to adequately account for the hydrological processes that drive runoff and erosion. The slope map in percent and degree was created using an SRTM DEM. ArcGIS was used to create an LS factor map using the slope map and equations. The LS factor value for the study area was ranged from 0 to 25.10.

Land use data allows for a better understanding of the land use features of agriculture, barren land, plantations, built up and waterbodies etc. which is essential for development planning and erosion studies. Thematic layers of LULC can be generated for an area using remote sensing and GIS techniques. The research area has been divided into five LULC classifications. Different land use patterns were allocated to a crop management component. The C factor map was created in ArcGIS using the LULC map and C factor values was determined and ranged in 0 to 0.63 in the study area. The P factor ranged from 0.5 to 1. Agriculture and vegetation were dominated LULC in the study area, therefore the maximum area was in the range of 0.5 to 0.8.

For selected watersheds (WS1 to WS10), annual soil loss was computed using the annual average R, K, LS, C, and P components. All of the layers, R, K, LS, C, and P, were created in GIS and overlaid to produce a result that provides annual soil erosion map for the

study region. The total soil loss in a selected watershed was used to calculate the soil erosion rate (t ha^{-1} yr^{-1}). The risk of soil erosion has been used to priorities selected watersheds. The watershed erosion maps displayed the ranges of erosion in various watersheds, revealing the nature of watersheds based on the severity of soil erosion in them. Soil loss was classified as 0-5, 5-10, 10-20, 20-40, and more than 40 t $ha^{-1}yr^{-1}$ with erosion grades of slight, moderate, high, very high and severe. The area under soil loss of 0-5 t $ha^{-1}yr^{-1}$ was found to be 98.07% of the entire area, followed by 5-10 t $ha^{-1}yr^{-1}$ as 1.45%. The remaining categories, 10-20, 20-40, and more than 40 t $ha^{-1}yr^{-1}$, cover 0.26%, 0.13%, and 0.08% of the land, respectively.

5.4 Priority areas assessment for efficient implementation of soil erosion control program

The prioritization of watershed was assigned on the basis of soil erosion rate and erosion class. The conservation priority was given according to the soil erosion class i.e. severe, very high, high, moderate and slight as 1,2,3,4, and 5 respectively. The watershed having soil erosion more than 40 t $ha^{-1}yr^{-1}$ was given first priority. Similarly, the priority was given to rest of the classes on decreasing soil loss. The WS1, WS2, WS3, WS4, WS7, and WS10 are classified as having severe soil erosion and hence received top priority for soil conservation measures. WS7 is larger in size; however the erosion is worse in WS3. The slopes of the ground and soil organic matter have a substantial influence on soil erosion. The region of moderate to very steep soil erosion has a high amount of erosion. A very steep slope not only creates a lot of runoff, but it also provides lot of momentum to the runoff, which erodes the soil round the year.

CHAPTER–VI

SUMMARY AND CONCLUSION

Soil erosion is most serious environmental threats as it removes fertile soil and transports it to the water bodies which ultimately increase the sedimentation into water bodies. The eroded soil psget deposited into water bodies and ultimately reduced the carrying and storage capacity canal, river and reservoirs and the soil erosion results in damaging the cultivable lands increase the probability of floods. So it is necessary to identify region prone to erosion so that it may get prioritised and necessary erosion control measure may be adopted well in time. Assessment and identification of soil erosion prone areas through traditional techniques particularly in hilly tract is tedious and expensive. The integration soil erosion model (RUSLE) with RS and GIS found suitable for assessment and prioritization erosion prone areas in quick manner.

The study entitled **"Priority areas assessment for soil erosion control in a watershed using geospatial technology in the Shivalik foothills (Haryana)"** was undertaken to with the following objectives:

- Thematic mapping related to land use and land cover classification of the study area
- Soil loss estimation using RUSLE on watershed basis
- Priority areas assessment for efficient implementation of soil erosion control programmes

The Shivalik foothills are spread in the Panchkula, Ambala, and Yamunanagar districts of the Haryana state. In these districts, the watersheds were delineated using satellite imaginary and ArcGIS 10.7.1 software, and ten watersheds were identified and designated as WS1, WS2, WS3, WS4, WS5, WS6, WS7, WS8, WS9, and WS10 and further analysed for LULC attributes using Sentinel-2A satellite imaginary and image processing software, Erdas Imagine. The morphometric parameters, i.e., basic parameters of watersheds, drainage network, drainage geometry, and drainage textural analysis of all selected watersheds were carried out. The integration of RUSLE with geospatial technology was used to estimate soil loss in different watersheds, and all six RUSLE parameters were calculated in ArcGIS 10.7.1 software. The estimated soil loss was reclassified in the GIS environment in the range of 0-5, 5-10, 10-20, 20-40, and >40 t $ha^{-1}yr^{-1}$ and assigned the severity class and priority class as slight, moderate, high, very high, and severe and 5,4,3,2,1 respectively to the selected watershed.

The major observation and results obtained from the above study are summarised as follow:

- The WS1 was observed as the smallest watershed and WS7 as the largest watershed, with an area of 65.12 km^2 and 616.53 km^2 and occupied 2.57% and 24.29% area of the selected watersheds, respectively.
- The area covered by barren LULC was highest in WS10 and lowest in WS1, with 95.20 km^2 and 6.25 km^2 occupying 31.31% and 2.06% area of selected watersheds, respectively.
- The area under waterbody LULC was also found maximum under WS10 and minimum under WS1 as 13.27 km^2 and 0.37 km^2 which occupied 37.51% and 1.05% area of the selected watersheds, respectively.
- The area under plantation LULC was also observed maximum under WS10 while minimum was under WS6 as 194.26 km^2 and 4.56 km^2 and occupied 31.61% and 0.74% area of the selected watersheds, respectively.
- The area under built up LULC was also observed maximum under WS10 and minimum was under WS1 as 13.58 km^2 and 1.08 km^2 and occupied 26.51% and 2.11% area of all the selected watersheds, respectively.
- The area under agriculture LULC was also found maximum under WS7 and minimum under WS1 as 448.11 km^2 and 33.40 km^2 and occupied 29.24% and 2.18% of all the selected watersheds, respectively.
- In the study area, the highest stream order (μ) was observed as 6^{th} order, and the lowest stream order (μ) was the observed as 4^{th} order. The WS7 and WS10 have the highest stream order (μ), whereas WS1, WS4 and WS8 have only 4^{th} order stream. The rest of the watersheds have 5^{th} stream order (μ).
- The mean stream length (L_{sm}) value of different watersheds (WS1 to WS10) has different values. In the study area, the mean stream length (L_{sm}) in WS1 to WS10 ranged from 3.05 to 10.67 km. The stream length ratio (R_L) between the streams of different orders showed a change in each watershed.
- In the selected watersheds WS1 to WS10, the circularity ratio (R_c) ranged from 0.17 to 0.35, showing less circularity nature of the basins. The elongation ratio (R_e) of selected watersheds except WS10 has a value of less than 0.5, which means these watersheds are more elongated. Due to a value higher than 0.5, WS10 was found to be in the category of elongated watershed.
- The form factor (F_f) of the selected watersheds was observed to be a maximum of 0.27, which means the selected watersheds are in the category of elongated watersheds.

- The drainage density (D_d) of the selected watersheds ranged from 1.59 to 1.93, which indicated the moderate permeability of the soil and better vegetation cover.
- The stream frequency (F_s) of the selected watersheds ranged from 1.46 to 1.74. The higher value of stream frequency (F_s) in the WS9 indicated the high degree of surface runoff.
- The observed values of constant channel maintenance (R) showed moderate to high permeability, moderate slope, and moderate surface runoff. The drainage texture (T_s) of the watersheds was less than 4, indicated that a watershed lies in the category of coarse.
- The length of overland flow (L_o) describes the length of water flows over the ground. The value of length of overland ranged from 0.260 to 0.315 which indicated the potential to cause quicker runoff.
- The relative relief (R_f) of the selected watersheds is in the range of 48 to 1233, which indicated that the WS5, WS6, WS8 and WS9 have basin slopes nearly level to gentle. It means the areas within these watersheds can be used for agricultural activities due to their being flat in nature. The lower value of the relief ratio (R_h) of WS6, WS8, and WS9 indicated the low degree of slope.
- The R factor value incorporates total precipitation intensity and the duration pattern of rainfall. The value of the R factor for the study area varied from 174 to 616 MJ mm ha^{-1} h^{-1} yr^{-1} and the thematic map of the R factor was prepared.
- The thematic map of K factor map was prepared in ArcGIS and K factor values were calculated. The value of K factor ranged from 0.095 to 0.0134 for the study area.
- The thematic map of the LS factor map was prepared. The value of the LS factor for the study area ranged from 0 to 25.10 for the study area.
- The study area has been classified into five LULC classes. The crop management factor was assigned to different land use patterns. Using LULC map and C factor values, a C factor map was prepared in ArcGIS and the C factor was ranged from 0 to 0.63 in the study area.
- The value of the P factor ranged from 0.5 to 1 in the study area. The maximum area lies in the range of 0.5-0.8 as agriculture and vegetation dominated LULC class in the study area.
- The annual soil loss for selected watersheds was calculated by using the RUSLE and its parameters R, K, LS, C, and P factors. All the layers, viz., R, K, LS, C, and P, were generated in GIS and overlaid to obtain the product, which gives an annual soil erosion map for the study area. The area under soil loss of 0-5 t $ha^{-1}yr^{-1}$ was found to be 98.07%, followed by 5-10 t $ha^{-1}yr^{-1}$ as 1.45% of the total area. The rest of the categories, i.e., 10-

20, 20-40, and more than 40 t $ha^{-1}yr^{-1}$, cover 0.26%, 0.13%, and 0.08% of the area, respectively.

- The WS1, WS2, WS3, WS4, WS7, and WS10 was observed under the severe soil erosion class with more than 40 t $ha^{-1}yr^{-1}$ and thus assigned first priority for soil conservation measures. However, WS7 is the largest in size, even though the higher rate soil erosion was observed in WS3.
- Soil erosion is strongly influenced by the slope of land and soil organic matter. A high amount of soil erosion is found in the region of moderate to very steep soil erosion class.

Based on the result obtained from the study, following conclusion may be drawn:

- The WS1 was found as the smallest watershed (2.57%) and WS7 was the largest watershed (24.29%) among the selected watersheds in the study area.
- The agriculture (60.39%) was dominated LULC class in the study area.
- Highest and lowest order of stream was observed as 6^{th} order, and 4^{th} order in the study area.
- The elongation ratio (R_e) of selected watersheds indicated that watersheds are more elongated.
- The value of length of overland flow (L_o) ranged from 0.260 to 0.315 which indicated that selected watersheds have potential to cause quicker runoff.
- The relative relief (R_f) indicated that the WS5, WS6, WS8 and WS9 have basin slopes nearly level to gentle. It means the areas within these watersheds can be used for agricultural activities due to their being flat in nature.
- About 98.07%, area of the selected watersheds was found under the slight erosion class with soil erosion rate of 0-5 t $ha^{-1}yr^{-1}$.
- Some of watersheds i.e. WS1, WS2, WS3, WS4, WS7 and WS10 falls under the severe soil erosion class category with soil loss more than 40 t ha^{-1} yr^{-1} thus assigned with first priority for soil conservation measures.

Policy recommendation

It was observed during the study that WS3, WS7, WS2, WS10 are affected with severe erosion with erosion rate more than 40 t $ha^{-1}yr^{-1}$. So these watersheds need to be taken care on priority in suggested order while planning for soil and water conservation measures in Shivalik region (Haryana). such kind of prioritization may also be undertaken in different watersheds proposed to be treated under IWMP for optimum resource allocation.

REFERENCES

Ahirwar, R., Malik, M.S., & Shukla, J.P. (2019). Prioritization of sub-watersheds for soil and water conservation in parts of Narmada River through morphometric analysis using remote sensing and GIS. *Journal Geological Society of India, 94,* 515-524.

Alaguraja, P., Durairaju, S., Yuvaraj, D., Sekar, M., Muthuveerran, P., Manivel, M., & Thirunavukkarasu, A. (2010). Land use and land cover mapping–Madurai District, Tamilnadu, India using remote sensing and GIS techniques. *International Journal of Civil and Structural Engineering, 1(1),* 91-100.

Ashiagbor, G., Forkuo, E.K., Laari, P., & Aabeyir, R. (2013). Modelling soil erosion using RUSLE and GIS tools. *International Journal of Remote Sensing & Geoscience, 2(4),* 7-17.

Balasubramani, K., Gomathi, M., Bhaskaran, G., & Kumaraswamy, K. (2019). GIS-based spatial multi-criteria approach for characterization and prioritization of micro-watersheds: A case study of semi-arid watershed, South India. *Applied Geomatics, 11,* 289-307.

Benavidez, R., Jackson, B., Maxwell, D., & Norton, K. (2018). A review of the (Revised) Universal Soil Loss Equation ((R)USLE): with a view to increasing its global applicability and improving soil loss estimates. *Hydrology and Earth System Sciences, 22,* 6059-6086.

Beniwal, A., Kumar, V., & Arya, V.S. (2014). Application of Geo-informatics for cadastral level land use/land cover mapping in Adalpur micro watershed of Mahendergarh District for sustainable agriculture management. *Journal of Remote Sensing & GIS, 5(3),* 1-6.

Bera, A. (2017). Estimation of soil loss by USLE model using GIS and remote sensing techniques: A case study of Muhuri River basin, Tripura, India. *Eurasian Journal of Soil Science,6(3),* 206-215.

Bouhadeb, C.E., Menani, M.R., Bouguerra, H., & Derdous, O. (2018). Assessing soil loss using GIS based RUSLE methodology. Case of the BouNamoussa watershed, North-East of Algeria. *Journal of Water and Land Development, 36(1),* 27-35.

Choudhari, P.P., Nigam, G.K., Singh, S.K., & Thakur, S. (2018). Morphometric based prioritization of watershed for groundwater potential of Mula River basin, Maharashtra, India. *Geology, Ecology and Landscapes, 2(4),* 256-267.

Choudhury, D., Das, K., & Das, A. (2019). Assessment of land use land cover changes and its impact on variations of land surface temperature in Asansol-Durgapur development region. *The Egyptian Journal of Remote Sensing and Space Sciences,22(2),* 203-218.

Choudhury, M., Hasan, M.E., & Abdullah-Al-Mamun, M.M. (2020). Land use/land cover change assessment of Halda watershed using remote sensing and GIS. *The Egyptian Journal of Remote Sensing and Space Sciences, 23(1),* 63-75.

Dabral, P.P., Baithuri, N., & Pandey, A. (2008). Soil erosion assessment in a hilly catchment of North Eastern India using USLE, GIS and RS. *Water Resources Management, 22,* 1783-1798.

Fayas, C.M., Abeysingha, N.S., Nirmanee, K.G.S., Samaratunga, D., & Mallawatantri, A. (2019). Soil loss estimation using RUSLE model to prioritize erosion control in KELANI river basin in Sri Lanka *International Soil and Water Conservation Research, 7,* 130-137.

Fistikoglu, O., & Harmancioglu, N.B. (2002). Integration of GIS with USLE in assessment of soil erosion. *Water Resources Management*, *16*, 447-467.

Foster, G.R., Mc Cool, D.K., Renard, K.G., & Moldenhauer, W.C. (1991). Conversion of the universal soil loss equation to SI metric units. *Journal of soil and water conservation*, *36*, 356-359.

Foster, G.R., Toy, T. E., & Renard, K.G. (2003). Comparison of the USLE, RUSLE1.06c and RUSLE2 for application to highly disturbed lands. *Proceeding of the 1st Interagency Conference on Research on Watersheds*, 154-160.

Gajbhiye, S., Sharma, S.K., & Meshram C.S. (2014). Prioritization of watershed through sediment yield index using RS and GIS approach. *International Journal of u- and e- Service, Science and Technology*, *7(6)*, 47-60.

Ganasri, B.P., & Ramesh, H. (2016). Assessment of soil erosion by RUSLE model using remote sensing and GIS-A case study of Nethravathi basin. *Geoscience Frontiers*, *7*, 953-961.

Gaubi, C.A. Mammou, A.B., & Hamza, M.H. (2017). A GIS-based soil erosion prediction using the Revised Universal Soil Loss Equation (RUSLE) (Lebna watershed, Cap Bon, Tunisia). *Natural Hazards*, *86*, 219-239. https://doi.org/10.1007/s11069-016-2684-3

Ghosh, K., De, S.K., Bandyopadhyay, S., & Saha, S. (2013). Assessment of soil loss of the Dhalai River basin, Tripura, India Using USLE. *International Journal of Geosciences*, *4*, 11-23.

Ghosh, M., & Gope, D. (2021). Hydro-morphometric characterization and prioritization of sub-watersheds for land and water resource management using fuzzy analytical hierarchical process (FAHP): a case study of upper Rihand watershed of Chhattisgarh State, India. *Applied Water Science*, *11*, 17.

Grewal, S.S., Samra, J.S., Mittal, S.P., & Agnihotri, Y. (1995). Sukhomajri concept of integrated watershed management. Tech. Bull. No T-26/C-5, Central Soil and Water Conservation Research and Training Institute, Research Centre, Chandigarh, 157.

Guler, M., Yomralıoglu, T., & Reis, S. (2007). Using Landsat data to determine land use/land cover changes in Samsun, Turkey. *Environmental Monitoring and Assessment*, *127(1-3)*, 155-167.

Hadley, R., & Schumm, S. (1961). Sediment sources and drainage basin characteristics in upper Cheyenne river basin. US Geological Survey Water-supply Paper, 1531-B, 137-146.

Helmer, E.H., Brown, S., & Cohen, W.B. (2000). Mapping montane tropical forest successional stage and land use with multi-date Landsat imagery mapping. *International Journal of Remote Sensing*, *21(11)*, 2163-2183.

Horton, R.E. (1932). Drainage basin characteristics. *Transactions American Geophysical Union*, *13*, 350–361.

Horton, R.E. (1945). Erosional development of streams and their drainage basins: Hydrophysical approach to quantitative morphology. *Bulletin of the Geological Society of America*, *56*, 275–370.

Jain, S.K., Kumar, S., & Varghese, J. (2001). Estimation of soil erosion for a Himalayan watershed using GIS technique. *Water Resource Management,15(1)*, 41-54.

Jazouli, A.E., Barakat, A., Ghafiri, A., Moutaki, S.E., Ettaqy, A., & RidaKhellouk, R. (2017). Soil erosion modeled with USLE, GIS, and remote sensing: A case study of Ikkour watershed in Middle Atlas (Morocco). *Geoscience Letter*, *4*, 25.

Jothimani, M., Gunalan, J., Duraisamy, R., & Abebe A. (2021). Study the relationship between LULC, LST, NDVI, NDWI and NDBI in Greater Arba Minch area, Rift Valley, Ethopia. *Proceedings*

of the 3rd International Conference on Integrated Intelligent Computing Communication & Security (ICIIC), 183-193.

Kamaludin, H., Lihan, T., Rahman, Z., Mustapha, M.A., Idris, W.M.R., & Rahim, S.A. (2013). Integration of remote sensing, RUSLE and GIS to model potential soil loss and sediment yield (SY*). Hydrology and Earth System Science Discussion, 10*, 4567-4596.

Khan, M.A., Gupta, V.P., & Moharana, P.C. (2001). Watershed prioritization using remote sensing and geographical information system: A case study from Guhiya, India. *Journal of Arid Environments*, *49*, 465-475.

Khassaf, S.I., & Rammahi, A.A. (2018). Estimation of soil erosion risk of the Euphrates River watershed using RUSLE model, remote sensing and GIS techniques. *Hydrology Days*, Colorado State University, USA, 13-32.

Koirala, P., Thakuri, S., Joshi, S., & Chauhan, R. (2019). Estimation of soil erosion in Nepal using a RUSLE modeling and geospatial tool. *Geosciences*, *9(4)*, 147.

Kothyari, U.C. (1996). Erosion and sedimentation problems in India. Erosion and sediment yield: Global and regional perspectives (*Proceedings of the Exeter Symposium, July 1996*). IAHS Publ. No. 236, 531-540.

Kothyari, U.C., & Jain, S.K. (1997). Sediment yield estimation using GIS. *Hydrological Sciences Journal*,*42*, 833-843.

Kukal, S.S., Sur, H., & Gill, S. (1991). Factors responsible for soil erosion hazards in submontane Punjab, India. *Soil Use and Management*, *7(1)*, 38-44.

Kumar, A., & Dhiman, R. (2014) Manual and automated delineation of watershed boundaries-A case study from Kangra region of Western Himalaya, India. *International Journal of Environmental Sciences*, *5(1)*, 16.

Kumar, D., Dhaloiya, A., Nain, A. S., Sharma, M.P. & Singh, A. (2021a). Prioritization of Watershed Using Remote Sensing and Geographic Information System. *Sustainability*, 13*(16)*, 9456.

Kumar, R., Chauhan, N., Handique, B.K., &, Arya, V.S. (2021b). Site-suitability analysis for sericulture development in Sub-Himalayan region of Haryana, India. *South Asian Research Journal of Engineering and Technology*, *3(4)*, 135-145.

Kushwaha, N.L., Bhardwaj, A., & Verma, V.K. (2016). Hydrologic response of Takarla-Ballowal watershed in Shivalik foot-hills based on morphometric analysis using remote sensing and GIS. *Journal of Indian Water Resource Society*, *36(1)*, 17-25.

Mahala, A. (2018). Soil erosion estimation using RUSLE and GIS techniques - A study of a Plateau Fringe region of tropical environment. *Arabian Journal of Geosciences*, *11*, 335.

Mallupattu, P.K., & Reddy, J.R.S. (2013). Analysis of land use/land cover changes using remote sensing data and GIS at an Urban area, Tirupati, India. *The Scientific World Journal*, 1-6. http:// dx.doi.org/ 10.1155/2013/ 268623

Meshram, S.G., & Sharma, S.K. (2017). Prioritization of watershed through morphometric parameters: A PCA-based approach. *Applied Water Science*, *7*, 1505-1519. https://doi.org/10.1007/s13201-015-0332-9

Miller, V.C. (1953). A quantitative geomorphic study of drainage basin characteristics in the Clinch mountain area Virginia and Tennessee. Department of Geology, Columbia University, New York, 389-402.

Mishra, P.K. Rai, A., & Rai, S.C. (2020). Land use and land cover change detection using geospatial techniques in the Sikkim Himalaya, India. *The Egyptian Journal of Remote Sensing and Space Sciences, 23*, 133-143.

Naqvi, H.R., Mallick, J., Devi, L.M., & Siddiqui, M.A. (2013). Multi-temporal annual soil loss risk mapping employing revised universal soil loss equation (RUSLE) model in Nun Nadi watershed, Uttrakhand (India). *Arabian Journal of Geosciences, 6*, 4045- 4056.

Narayan, V.V.D., & Babu, R. (1983). Estimation of soil erosion in India. *Journal of Irrigation and Drainage Engineering, 109(4)*, 419-434.

Panagos, P., Ballabio, C., Borrelli, P., & Meusburger, K. (2016). Spatio-temporal analysis of rainfall erosivity and erosivity density in Greece. *Catena, 137*, 161-172.

Panaskar, S., Narwade, R., & Nagarajan, K. (2019). Analysis of changes in LULC of Western Ghat by Comparing NDVI and NDWI. *Journal of Remote Sensing & GIS, 8(4)*, 1-7.

Pandey, A., Behra, S., Pandey, R.P., & Singh, R.P. (2011). Application of GIS for watershed prioritization and management: A case study. *International Journal of Environmental Science Development & Monitoring, 2(1)*, 25-42.

Pandey, A., Chowdary, V.M., & Mal, B.C. (2007). Identification of critical erosion prone areas in the small agricultural watershed using USLE, GIS and remote sensing. *Water Resources Management, 21*, 729-746.

Pham, T.G., Degener, J., & Kappas, M. (2018). Integrated universal soil loss equation (USLE) and geographical information system (GIS) for soil erosion estimation in a Sap basin: Central Vietnam. *International Soil and Water Conservation Research, 6*, 99-110.

Pongsai, S., Vogt, D.S., Shrestha, R.P., Clemente, R.S., & Eiumnoh, A. (2010). Calibration and validation of the modified universal soil loss equation (MUSLE) for estimating sediment yield on sloping plots: A case study in Khun Satan catchment of Northern Thailand. *Canadian Journal of Soil Science, 90*, 585-596.

Prasannakumar, V., Shiny, R., Geetha, N., & Vijith, H. (2011). Spatial prediction of soil erosion risk by remote sensing, GIS and RUSLE approach: A case study of Siruvani River watershed in Attapady valley, Kerala, India. *Environmental Earth Science, 64*, 965-972.

Prasannakumar, V., Vijith, H., Abinod, S., & Geetha, N. (2012). Estimation of soil erosion risk within a small mountainous sub-watershed in Kerala, India using Revised Universal Soil Loss Equation (RUSLE) and geo-information technology. *Geoscience Frontiers, 3(2)*,209-215.

Priyanka (2017). Land use/land cover mapping through remote sensing and GIS techniques. *International Journal of Research in Geography, 3(2)*, 22-25.

Puno, G.R., & Puno, R.C.C. (2019). Watershed conservation prioritization using eomorphometric and land use-land cover parameters. *Global Journal of Environmental Science and Management, 5(3)*, 279-294.

Rai, P.K., Mohan, K., Mishra, S., Ahmad, A., & Mishra, V.N. (2017). A GIS-based approach in drainage morphometric analysis of Kanhar River Basin, India.*Applied Water Science, 4(4)*. https://doi.org/10.1007/s13201-014-0238-y

Renard, K.G., & Foster, G.R. (1985). Managing rangeland Soil Resources: The Universal Soil Loss Equation. *Rangelands, 7(3)*, 118-122.

Renard, K.G., Foster, G.R., Weesies, G. A., McCool, D.K., & Yoder, D.C. (1997). Predicting soil erosion by water: A guide to conservation planning with the revised universal soil loss equation (RUSLE). United States Department of Agriculture, Washington, DC.

Renard, K.G., Foster, G.R., Weesies, G.A., & Porter, J.P. (1991). RUSLE: Revised universal soil loss equation. *Journal of Soil and Water Conservation, 46(1),* 30-33.

Renschler, C., Diekkruger, B., & Mannaerts, C. (1997). Regionalization in surface runoff and soil erosion risk evaluation, in regionalization of hydrology. *Proceedings of the International Conference on Regionalization in Hydrology,254*, 233-241.

Ritchie, J.C., Walling, D.E., & Peters, J. (2003). Application of geographical information systems and remote sensing for quantifying patterns of erosion and water quality. *Hydrological Processes, 17,*885-886.

Saha, A., Ghosh, P., & Mitra, B. (2018). GIS based soil erosion estimation using Rusle Model: A case study of Upper Kangsabati watershed, West Bengal, India. *International Journal of Environmental Sciences & Natural Resources, 13(5),* 119-126.

Sarkar, A. (2018). Accuracy assessment and analysis of land use land cover change using geoinformatics technique in Raniganj coal field area, India. *International Journal of Environmental Sciences & Natural Resources, 11(1),* 25-34.

Schumm, S.A. (1956). Evolution of drainage systems and slopes in badlands at Perth Amboy, New Jersey. *Geological Society of America Bulletin, 67,* 597–646.

Shamsi, U.M. (1996). Storm-water management implementation through modelling and GIS. *Journal of Planning* and *Management,122(2),* 114-127.

Sheikh, A.H., Palria, S., & Alam, A. (2011). Integration of GIS and Universal Soil Loss Equation (USLE) for soil loss estimation in a Himalayan watershed. *Recent Research in Science and Technology, 3(3),* 51-57.

Shin, G.J. (1999). The Analysis of Soil Erosion Analysis in the Watershed Using GIS. Ph.D. Thesis, Gang-won National University, Chuncheon, Korea,

Shinde, V., Tiwari, K.N., & Singh, M. (2010). Prioritization of micro watersheds on the basis of soil erosion hazard using remote sensing and geographic information system. *International Journal of Water Resources and Environmental Engineering, 2(3),*130-136.

Singh G., Rambabu, V.V., & Chandra, S. (1981). Soil loss prediction research in India, Bulletin of Central Soil & Water Conservation Research & Training Institute, T12/D9. Dehradun, India.

Singh, G., Babu, R., Narain, P., Bhusan, L.S., & Abrol, I.P. (1992). Soil erosion rates in India. *Journal of Soil and Water Conservation, 47(1),* 97-99.

Singh, M.C., Yousuf, A., & Prasad, V. (2021). Morphometric and principal component analysis-based prioritization of reservoir catchments using geospatial techniques for land and water conservation aspects in North-West India. *Arabian Journal of Geoscience, 14,*598, 4-22.

Singh, O., & Sarangi A. (2008). Hypsometric analysis of the lesser Himalayan watersheds using geographical information system. *Indian Journal of Soil Conservation, 36(3),* 148-154.

Strahler, A. (1964) Quantitative geomorphology of drainage basins and channel networks. In V. Chow (Eds.), *Handbook of Applied Hydrology*(pp. 439-476), McGraw Hill.

Sujatha, E.R., Selvakumar, R., Rajasimman, U.A.B., & Victor, R.G. (2013). Morphometric analysis of subwatershed in parts of Western Ghats, South India using ASTER DEM. *Geomatics, Natural Hazards and Risk, 6(4),* 326-341. https://doi.org/10.1080/ 19475705.2013.845114

Thapliyal, A., Panwar, A., & Kimothi, S. (2017). Prioritization based on morphometric analysis in Alaknanda basin. *Global Journal of Science Frontier Research: Environment & Earth Science, 17(3),* 28-34.

Tiruneh, G., & Ayalew, M. (2015). Soil loss estimation using geographic information system in Enfraz watershed for soil conservation planning in highlands of Ethiopia. *International Journal of Agricultural Research, Innovation and Technology, 5(2),* 21-30.

Vittala, S.S., Govindaiah, S., & Gowda, H.H. (2008). Prioritization of sub-watersheds for sustainable development and management of natural resources: An integrated approach using remote sensing, GIS and socio-economic data. *Current Science, 95(3),* 345-354.

Wijesundara, N.C., Abeysingha, N.S., & Dissanayake, D.M.S.L.B. (2018). GIS-based soil loss estimation using RUSLE model: A case of Kirindi Oya River basin, Sri Lanka. *Modeling Earth Systems and Environment, 4,* 251-262. https://doi.org/10.1007/ s40808-018-0419-z

Williams, J.R. (1975). Sediment-yield prediction with universal equation using runoff energy factor. In *Present and perspective technology for predicting sediment yield and sources* (pp.244-252), USDA.

Wischmeier, W.H., & Smith, D.D. (1965). Predicting rainfall-erosion losses from cropland east of the Rocky mountains: A guide for selecting practices for soil and water conservation. USDA,*Agricultural Handbook, 282***,** 47.

Wischmeier, W.H., & Smith, D.D. (1978). Predicting rainfall erosion losses-A guide to conservation planning. USDA, *Agricultural Handbook, 537.*

Wu, S., Li, J., & Huang, G.H. (2005). An evaluation of grid size uncertainty in empirical soil loss modeling with digital elevation models. *Environmental Modeling and Assessment, 10,* 33-42.

Yadav, R.P., Aggarwal, R.K., Arya, S.L., Singh, P., Prasad, R., Bhattacharya, P., Tiwari, A.K., & Yadav, M.K. (2005). Rainwater harvesting and recycling technology for sustainable production in small agricultural watershed- Johranpur. CSWCRTI Bulletin No. T-50/C-11. Central Soil and Water Conservation Research and Training Institute, Research Centre, Chandigarh, 165.

Yadav, R.P., Panwar, P., Arya, S.L., & Mishra, P.K. (2015). Revisit of Shivalik region in different States of North Western India. *Journal of Geological Society of India, 86,* 351-360.

Yadav, R.P., & Sachdev C.B. (2008). Assessment of soil erosion in Haryana State, *Journal of the Indian Society of Soil Science, 56,* 99-105.

Yesuph, A.Y., & Dagnew, A.B. (2019). Soil erosion mapping and severity analysis based on RUSLE model and local perception in the Beshillo catchment of the Blue Nile basin, Ethiopia. *Environmental Systems Research,8,* 17.

ABSTRACT

Title of Thesis	:	Priority Areas Assessment for Soil Erosion Control in Watershed using Geospatial Technology in Shivalik Foothills (Haryana)
Full Name of the Degree Holder	:	**Sundeep Kumar Antil**
Admission Number	:	2017AE4D
Title of the Degree	:	Doctorate of Philosophy
Name of Discipline	:	Soil and Water Engineering
Name and Address of Major Advisor	:	Dr. M. S. Sidhpuria Professor Department of Soil and Water Engineering CCS Haryana Agricultural University, Hisar-125004 (Haryana), India
Degree Awarding University	:	CCS Haryana Agricultural University Hisar-125 004 (Haryana), India
Year of Award of Degree	:	2022
Major Subject	:	Soil Science
Total Number of Pages in Thesis	:	92 + vii
Number of Words in Abstract	:	209

Key words: Satellite imaginary, Digital elevation model, Land use land cover, ArcGIS, watershed delineation, stream order, RUSLE, watershed prioritization, Morphometric parameters, soil loss estimation

(An abstract of the thesis submitted to CCS Haryana Agricultural University, Hisar, in partial fulfillment of the requirements for the degree of Master of Technology in Farm Machinery and Power Engineering)

Geospatial technologies are widely used for thematic mapping and information on status of land use land cover, morphometric analysis of watershed parameters, prediction of soil loss and several other information. The priority areas were assessed and delineated in the Shivalik foothill using the Sentinel 2A, SRTM, Erdas Imagine and ArcGIS 10.7.1 image processing software. The delineated watersheds were designated as WS1, WS2, WS3, WS4, WS5, WS6 WS7, WS8, WS9 and WS10 and further analysed for land use and land cover attributes, morphometric parameters i.e. basic parameters of watersheds, drainage network and geometry and drainage textural analysis of selected watersheds. Soil loss under different watersheds was estimated through integration of RUSLE with geospatial technology and all six parameters of the RUSLE were calculated. The 98.07% area of the selected watersheds was under 0-5 t $ha^{-1}yr^{-1}$ followed by 1.45% area with 5-10 t $ha^{-1}yr^{-1}$. The rest of the categories i.e. 10-20, 20-40 and more than 40 t $ha^{-1}yr^{-1}$ covered 0.26%, 0.13% and 0.08% of the total area, respectively. The estimated soil loss was reclassified in GIS environment in range of 0-5, 5-10, 10-20, 20-40 and >40 t $ha^{-1}yr^{-1}$ and assigned the severity class and priority class as slight, moderate, high, very high and severe and 5,4,3,2,1 respectively to the selected watershed.

MAJOR ADVISOR **SIGNATURE OF THE STUDENT**

HEAD OF DEPARTMENT

CURRICULUM VITAE

(a)	Name	:	Sundeep Kumar Antil
(b)	Date of Birth	:	09-12-1974
(c)	Place of Birth	:	Deepalpur, Sonepat
(d)	Mother's Name	:	Sarla Devi
(e)	Father's Name	:	Jai Bhagwan Antil
(f)	Permanent Address	:	Village & PO - Deepalpur, District - Sonepat, Haryana
(h)	Mobile	:	09466780360
(i)	E-mail	:	sundeepantil@gmail.com

(j) **Academic Qualification**

Degree	Univ./Board	Year of Passing	Percentage of marks/OGPA	Subjects
Ph. D	CCS HAU, Hisar	2022	7.94/10.00	Soil and Water Engineering
M. Tech.	CCS HAU, Hisar	2002	7.52/10.00	Agricultural Engineering with specialization in Soil and Water Engineering
B. Tech.	CCS HAU, Hisar	1997	2.20/4.00	Agricultural Engineering

(k) Co-Curricular Activities : -

(l) Medals/Honors received : -

(m) List of Publications : 01

- Antil, S.K., Sidhpuria, M.S., Kumar, M. Kumar S., and Bhardwaj N. (2022). Review on land use, land cover analysis and soil loss estimation through rusle and geospatial technologies. *Journal of Plant Development Sciences*. 14(7), 615-619.

I hereby, declare that all the information, given in resume is true to the best of my knowledge.

Dated:

Place: Hisar

Signature of Student

UNDERTAKING OF THE COPYRIGHT

I, **Sundeep Kumar Antil** Admn. No. **2017AE4D** undertakes that I give copy right to the CCS HAU, Hisar of my thesis entitled **"Priority Areas Assessment for Soil Erosion Control in Watershed using Geospatial Technology in Shivalik Foothills (Haryana)".**

I also undertake that, patent, if any, arising out of the research work conducted during the programme shall be filled by me only with due permission of the competent authority of CCSHAU, Hisar.

(Sundeep Kumar Antil)